

AD-A229 605

SSC-336

# LIQUID SLOSHING IN CARGO TANKS



DTIC  
ELECTE  
DEC 26 1990  
S B D  
Co

This document has been approved  
for public release and sale; its  
distribution is unlimited

## SHIP STRUCTURE COMMITTEE

### 1990

90 12 20 016

## SHIP STRUCTURE COMMITTEE

THE SHIP STRUCTURE COMMITTEE is constituted to prosecute a research program to improve the hull structure of ships and other marine structures by an extension of knowledge pertaining to design, materials and methods of construction.

RADM J. D. Sipes, USCG, (Chairman)  
Chief, Office of Marine Safety, Security  
and Environmental Protection  
U. S. Coast Guard

Mr. Alexander Malakhoff  
Director, Structural Integrity  
Subgroup (SEA 55Y)  
Naval Sea Systems Command

Dr. Donald Liu  
Senior Vice President  
American Bureau of Shipping

Mr. H. T. Hafler  
Associate Administrator for Ship-  
building and Ship Operations  
Maritime Administration

Mr. Thomas W. Allen  
Engineering Officer (N7)  
Military Sealift Command

CDR Michael K. Parmelee, USCG,  
Secretary, Ship Structure Committee  
U. S. Coast Guard

## CONTRACTING OFFICER TECHNICAL REPRESENTATIVES

Mr. William J. Siekierka  
SEA 55Y3  
Naval Sea Systems Command

Mr. Greg D. Woods  
SEA 55Y3  
Naval Sea Systems Command

## SHIP STRUCTURE SUBCOMMITTEE

THE SHIP STRUCTURE SUBCOMMITTEE acts for the Ship Structure Committee on technical matters by providing technical coordinating for the determination of goals and objectives of the program, and by evaluating and interpreting the results in terms of structural design, construction and operation.

### U. S. COAST GUARD

Dr. John S. Spencer (Chairman)  
CAPT T. E. Thompson  
CAPT Donald S. Jensen  
CDR Mark E. Noll

### NAVAL SEA SYSTEMS COMMAND

Mr. Robert A. Sielski  
Mr. Charles L. Null  
Mr. W. Thomas Packard  
Mr. Allen H. Engle

### MARITIME ADMINISTRATION

Mr. Frederick Seibold  
Mr. Norman O. Hammer  
Mr. Chao H. Lin  
Dr. Walter M. Maclean

### MILITARY SEALIFT COMMAND

Mr. Glenn M. Ashe  
Mr. Michael W. Touma  
Mr. Albert J. Attermeyer  
Mr. Jeffery E. Beach

### AMERICAN BUREAU OF SHIPPING

Mr. John F. Conlon  
Mr. Stephen G. Arntson  
Mr. William M. Hanzalek  
Mr. Philip G. Rynn

## SHIP STRUCTURE SUBCOMMITTEE LIAISON MEMBERS

### U. S. COAST GUARD ACADEMY

LT Bruce Mustain

### U. S. MERCHANT MARINE ACADEMY

Dr. C. B. Kim

### U. S. NAVAL ACADEMY

Dr. Ramswar Bhattacharyya

STATE UNIVERSITY OF NEW YORK  
MARITIME COLLEGE

Dr. W. R. Porter

### WELDING RESEARCH COUNCIL

Dr. Martin Prager

### NATIONAL ACADEMY OF SCIENCES MARINE BOARD

Mr. Alexander B. Stavovy

### NATIONAL ACADEMY OF SCIENCES COMMITTEE ON MARINE STRUCTURES

Mr. Stanley G. Stiansen

### SOCIETY OF NAVAL ARCHITECTS AND MARINE ENGINEERS- HYDRODYNAMICS COMMITTEE

Dr. William Sandberg

### AMERICAN IRON AND STEEL INSTITUTE

Mr. Alexander D. Wilson

Best Available Copy

**Member Agencies:**

*United States Coast Guard  
Naval Sea Systems Command  
Maritime Administration  
American Bureau of Shipping  
Military Sealift Command*



**Ship  
Structure  
Committee**

**An Interagency Advisory Committee  
Dedicated to the Improvement of Marine Structures**

**Address Correspondence to:**

**Secretary, Ship Structure Committee  
U.S. Coast Guard (G-MTH)  
2100 Second Street S.W.  
Washington, D.C. 20593-0001  
PH: (202) 267-0003  
FAX: (202) 267-0025**

**September 5, 1990**

**SSC-336  
SR-1284**

**LIQUID SLOSHING IN CARGO TANKS**

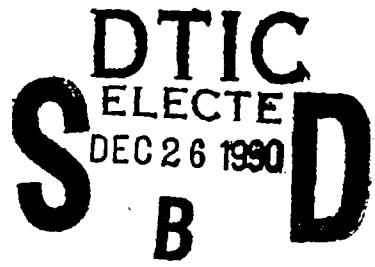
Sloshing liquids in partially filled cargo and ballast tanks have caused severe damage to ship structures. With ships being built with larger tanks, less internal structure, and more free surface area, the number of failures attributed to sloshing liquids have increased.

This report is based on twelve case studies of sloshing damage from several types of ships. Coefficients for sloshing forces, moments, and pressures were determined using model tests. These coefficients and a method to determine sloshing forces on a member using linear superposition calculations are included.

A handwritten signature in black ink, appearing to read 'J. D. SPES'.

**J. D. SPES  
Rear Admiral, U. S. Coast Guard  
Chairman, Ship Structure Committee**

①

1. Report No. SSC-336	2. Government Accession No.	3. Recipient's Catalog No.	
4. Title and Subtitle LIQUID SLOSH LOADING IN SLACK SHIP TANKS; FORCES ON INTERNAL STRUCTURE & PRESSURES		5. Report Date NOVEMBER 1986	
		6. Performing Organization Code	
7. Author(s) N.A. HAMLIN		8. Performing Organization Report No. G-179, SR-1284	
9. Performing Organization Name and Address WEBB INSTITUTE OF NAVAL ARCHITECTURE CRESCENT BEACH ROAD GLEN COVE, NEW YORK 11542		10. Work Unit No. (TRAIS)	
		11. Contract or Grant No. DTCG23-82-C-20016	
12. Sponsoring Agency Name and Address U.S. DEPARTMENT OF TRANSPORTATION UNITED STATES COAST GUARD OFFICE OF RESEARCH AND DEVELOPMENT WASHINGTON, DC 20590		13. Type of Report and Period Covered FINAL REPORT	
		14. Sponsoring Agency Code G-M	
15. Supplementary Notes			
16. Abstract <p>Based upon a survey of 12 cases of sloshing damage on 7 tankers and other ships of dry cargo, OBO, bulk and ore carrier types, 5 structural members were chosen for model testing to measure sloshing forces. Oscillating table tests were then run using partially filled tanks with realistic structure including the instrumented members. Sloshing force and moment coefficients are reported as well as sloshing pressure coefficients from pressure measurements on the tanks. A linear superposition calculation for sloshing force on one member is shown.</p> <div style="text-align: right;">  </div>			
17. Key Words Sloshing; Sloshing Forces; Impact Pressures; Oscillating Table; SHIPS; Sloshing Damage; Response Amplitude Operator; Seaway Spectrum, (TS)		18. Distribution Statement Document is available to the U.S. public through the National Technical Information Service, Springfield, Virginia 22161	
19. Security Classif. (of this report) UNCLASSIFIED	20. Security Classif. (of this page) UNCLASSIFIED	21. No. of Pages 113	22. Price

# METRIC CONVERSION FACTORS

Approximate Conversions from Metric Measures			
Symbol	When You Know	Multiply by	To Find
LENGTH			
mm	millimeters	0.04	inches
cm	centimeters	0.4	inches
m	meters	3.3	feet
m	meters	1.1	yards
km	kilometers	0.6	miles
AREA			
cm <sup>2</sup>	square centimeters	0.16	square inches
m <sup>2</sup>	square meters	1.2	square yards
km <sup>2</sup>	square kilometers	0.4	square miles
ha	hectares (10,000 m <sup>2</sup> )	2.5	acres
MASS (weight)			
g	grams	0.035	ounces
kg	kilograms	2.2	pounds
t	tonnes (1000 kg)	1.1	short tons
VOLUME			
ml	milliliters	0.03	fluid ounces
l	liters	2.1	pints
l	liters	1.06	quarts
l	liters	0.26	gallons
m <sup>3</sup>	cubic meters	36	cubic feet
m <sup>3</sup>	cubic meters	1.3	cubic yards
TEMPERATURE (exact)			
oC	Celsius temperature	9/5 (then add 32)	Fahrenheit temperature

Approximate Conversions to Metric Measures			
Symbol	When You Know	Multiply by	To Find
LENGTH			
in	inches	2.5	centimeters
ft	feet	30	centimeters
yd	yards	0.9	meters
mi	miles	1.6	kilometers
AREA			
in <sup>2</sup>	square inches	6.5	square centimeters
ft <sup>2</sup>	square feet	0.09	square meters
yd <sup>2</sup>	square yards	0.8	square meters
mi <sup>2</sup>	square miles	2.6	square kilometers
acres	acres	0.4	hectares
MASS (weight)			
oz	ounces	28	grams
lb	pounds	0.45	kilograms
	short tons (2000 lb)	0.9	tonnes
VOLUME			
ts	teaspoons	5	milliliters
fl oz	fluid ounces	16	milliliters
c	cups	30	milliliters
pt	pints	0.24	liters
qt	quarts	0.47	liters
gal	gallons	0.96	liters
ft <sup>3</sup>	cubic feet	3.8	liters
yd <sup>3</sup>	cubic yards	0.03	cubic meters
		0.76	cubic meters
TEMPERATURE (exact)			
oF	Fahrenheit temperature	5/9 (after subtracting 32)	Celsius temperature

1 in. = 2.54 cm (exactly). For other exact conversions and more detail tables see NBS Mon. Publ. 286, Units of Weight and Measures. Price \$2.25. SD Catalog No. C13 10 286.

## TABLE OF CONTENTS

<u>SECTION</u>	<u>PAGE</u>
I INTRODUCTION .....	1
II INDUSTRY SURVEY .....	3
III INSTRUMENTED STRUCTURAL MEMBERS AND PRESSURE TAP LOCATIONS .....	8
IV TEST TANK AND OSCILLATING TABLE FACILITY .....	14
V FORCE AND PRESSURE MEASURING SYSTEM .....	19
VI DATA ACQUISITION SYSTEM .....	20
VII TEST PARAMETERS .....	24
VIII PROCESSING OF FORCE MEASUREMENTS .....	27
IX PRESENTATION OF TEST DATA .....	28
X PRESSURE MEASUREMENTS .....	33
XI FORCES AND PRESSURES FOR SEPARATE TEST GROUPS .....	37
XII EXPERIMENTAL FORCES VERSUS THEORY .....	75
XIII APPLICATION TO DESIGN .....	78
XIV SUMMARY OF MAJOR RESULTS OF TESTS .....	84
XV RECOMMENDATIONS .....	87
XVI CONCLUDING REMARKS .....	90
XVII ACKNOWLEDGMENTS .....	91
XVIII REFERENCES AND BIBLIOGRAPHY .....	92
 APPENDIX A: DYNAMIC FORCE MEASUREMENT DEVICE FOR STRUCTURAL MEMBERS IN A SCALED-DOWN MODEL OF A SHIP TANK ..	 A-1
APPENDIX B: TANK DRIVE SYSTEM .....	B-1
APPENDIX C: REPRESENTATIVE SLOSHING FORCE GRAPHS .....	C-1



Availability Codes	
Dist	Avail and/or Special
A-1	

## I. INTRODUCTION

Sloshing of liquids in partially filled tanks may be thought of as the transfer of liquid from one side of the tank to the other in the form of a wave, which is excited by the periodic motion of the tank either angularly or in translation. Sloshing of liquids in ship tanks has undoubtedly been experienced as long as liquids have been carried. Only in perhaps the past 20 years has it been recognized as potentially troublesome. Reasons for the avoidance of sloshing problems on earlier ships can be attributed to the small size of tank compared with the size of ship and the presence of structure within the tank which characterized early vessels.

Three trends on certain present day types of vessels can be identified as contributing to the advent of sloshing as a serious problem:

- (1) Most tank vessels carrying crude oil or petroleum products nowadays generally do so with a smaller number of large tanks than in the past [Ref. (1)]. As a consequence, the natural period of waves at the free surface of the tank has been lengthened and tends to occur closer to the period with which ocean waves causing substantial ship motions are encountered. Furthermore, pressure changes for a given static angle of inclination are increased.
- (2) In order to minimize the pollution potential of petroleum carrying tankers, the structure inside the tanks of such vessels has been reduced and in some cases ("ecology" type vessels with double bottoms and double side walls) has been virtually eliminated. This substantially reduces the surfaces to which petroleum products will cling when the tank is pumped out; at the same time, the minimization of internal structure removes an important source of damping the motion of liquids in the tank when the tank is slack and sloshing occurs.
- (3) The development of high cubic capacity bulk carrying vessels has required the capability to use some of the cargo holds for water ballast or for liquid bulk cargoes. The hold internal surfaces are usually smooth to facilitate unloading of dry bulk cargoes. Therefore, when the hold is used

for water ballast or for liquid cargo, but is not completely full, sloshing in the hold may occur with the ship in a seaway. Such sloshing is not subject to the damping which would occur where there are significant amounts of structure within the hold.

This report is directed at ships which are obliged to operate with partially filled tanks of relatively large size compared with the size of ship. Measurements of forces on model structural elements and of pressures on the model tank during forced pitching, rolling and surging constitute the majority of the report. However, during the first phase of the project, an Industry Survey by the contractor's consultant on the project was made to identify actual ship cases where sloshing damage occurred.

Based upon the Industry Survey [Ref. (2)], a number of structural members were chosen for modeling, a model tank was designed and built, and model test measurements of sloshing forces and pressures were made. Prior to conducting the model tests, it was necessary to develop a system by which the sloshing forces on the structural members could be measured.

Later in the report it is shown how the results of the tests may be combined with ship motion predictions -- either theoretical or experimental -- together with linear superposition ship motion theory to find the root mean square of hydrodynamic force on the member and associated statistics.

The report concludes with recommendations for design guidance and for further work in this area.



## II. INDUSTRY SURVEY

At the start of the project, it was considered important to acquire a list of specific cases of sloshing in shipboard tanks which had resulted in damage to the ship's structure. These were believed necessary in order to allow an intelligent choice of structural elements and tank proportions to use in the model tests of sloshing forces which were to be run. To our knowledge, such a list did not exist. Therefore, the firm of M. Rosenblatt and Son was contracted to make a comprehensive survey of maritime organizations, ship operators, classification societies, salvage associations, etc. The results of this survey are given in Ref. (2). Liquefied natural gas carriers were specifically excluded from the survey. An additional task was to provide references and publications in the field of sloshing which were not available at Webb.

Finding cases of specific sloshing damage proved more difficult than anticipated in that a number of organizations which had found evidence of damage were unable to say that sloshing was the principal cause. Thus, poor welding, substandard scantlings, imprudent loading, structural notches and corrosion may so weaken a structure that normal in-service loadings result in damage. Nevertheless, nine specific cases of sloshing damage were identified by the Industry Survey. Three more cases were added as described in the open literature [Ref. (3)] giving a total of twelve. The basic elements of these twelve cases of sloshing damages are described below.

### Damage Cases

#### Case 1, Damage Report CA-1

This five-hold dry cargo ship experienced damage apparently from sloshing pressures on portable 'tween deck platforms in No. 3 hold when the hold below was ballasted with sea water and the platforms were in place -- depth of water in hold not reported, nor particulars of framing in hold, other than that transverse bulkheads were corrugated with vertical corrugations.

#### Case 2, Damage Report OBO-1

The No. 1 cargo hold of this ore-bulk-oil vessel experienced damage in way of the deck above and transverse bulkhead. Primary damage was in corners. The hold was ballasted with salt water to a depth of 30 to 40 percent.

#### Case 3, Damage Report BC-1

This seven-hold bulk carrier is fitted with upper and lower outboard corner ballast tanks giving an octagonal cross section shape to the cargo hold. Longitudinals are on the inboard or hold side of the upper corner tank sloping bulkheads. When the No. 4 hold was ballasted and 90 percent full of sea water, many of the longitudinals became severely twisted and distorted. There is a strong probability the ship was rolling at the time, although ship motions when damage occurred are not given.

#### Case 4, Damage Report T-1

This 240,000 tons displacement tanker is fitted with swash bulkheads at the 1/3 location in a 150 foot long center tank. The swash bulkheads take the form of deep transverse webs from the bottom and deck at the same frame location, each of depth about 26 percent of the depth of the tank. The tank is used alternately for crude oil and for ballast. After about two years service, the connection between the bottom longitudinal center girder and a vertical centerline girder from deck to bottom fractured on all four ships of the class. The vertical girder stiffens and supports the two swash bulkhead sections. Several repairs in the form of additional steel were made in sequence until the problem was solved.

When carrying oil, the tanks are 98 percent full; when ballasted with sea water, they are 60 percent to 90 percent full. It was believed that sloshing in those tanks when the ship was pitching in the ballast condition was the source of the fracture.

#### Case 5, Damage Report T-2

This 915 foot long crude carrier has a double bottom; the interior surface of the bottom of the tank is smooth. The 165 foot long No. 2 center tank has a smooth after transverse bulkhead except for centerline brackets. The forward bulkhead has three horizontal girders and a centerline vertical web and vertical stiffeners. Transverse webs at 15 feet spacing and longitudinals are fitted on the longitudinal bulkhead. No swash bulkheads are provided. The upper horizontal girder on the forward transverse bulkhead experienced buckling at the port end of the girder. This tank is run slack from time to time; damage to the girder was believed due to sloshing.

#### Case 6, Damage Report T-3

This is a sister ship of the vessel described in the Case 5 Damage Report T-2. Damage to the upper horizontal girder in the same tank occurred, the damage being a fracture and detachment of approximately  $15(\text{ft})^2$  of the port end of the girder plating, which fell away.

#### Case 7, Damage Report T-4

This 1092 foot tanker has the No. 3, 139 foot long center tank slightly aft of amidships; the tank was used for ballast. All three horizontal girders on the forward bulkhead were buckled and the transverse bulkhead was detached from the longitudinal bulkhead at the tank forward port corner for a distance of 65 feet and the transverse bulkhead pushed forward in way of the fracture to a maximum distance of 1.6 feet.

A swash bulkhead has been added to all center tanks as a remedial measure, the damage being attributed to sloshing.

#### Case 8, Damage Report T-5

This 830 foot long tanker experienced a 0.5 foot long fracture in a port longitudinal bulkhead in the No. 3 center tank about 33 feet above the bottom of the tank. The center tank was loaded with oil, about 60 percent full, some of which leaked into the adjoining ballast tank.

#### Case 9, Damage Report T-6

This 1050 foot long, 254,000 tons loaded displacement tanker experienced corrosion, wastage, fracturing and buckling of five transverse web frames in a 98 foot long wing tank on the inboard side of the tank at about amidships when the tank was ballasted with salt water, said to be 94 percent full. Similar damage was experienced by stiffeners (assumed to be longitudinals) above LS10, at approximately the 10 meter waterline.

Table I gives principal vessel and tank particulars of the foregoing nine cases of tank damage.

TABLE I

## Principal Vessel and Tank Particulars of Reported Tank Damages Due to Sloshing

Damage Case	Vessel Type	Ship Characteristics and Seaway Particulars at Time of Damage					Particulars of Tank Damaged					
		LBP	Beam	Approx. Draft Fwd/Aft	GM (Est.).	Speed, Heading	Sea State	Liquid Type	Depth	Length/Width/Depth	Distance from Amidships	Distance Off
1	CA-1	137 m	25 m	4.25 m/6.20 m	2.03 m	abt. 10 knots	6	seawater	100%	18 m/21 m/10.5 m	approx. 9 m fwd	center
2	OBO-1	787 ft	106 ft	43.4 ft even keel	...	...	...	seawater	30-40%	100 ft/106 ft/62 ft	12 m fwd	center
3	BC-1	218 m	32.2 m	7.57 m/8.08 m	4.5 m	abt. 15 knots	...	seawater	90%	25.4 m/32.2 m/16.2 m	202 ft fwd	center
4	T-1	1037 ft	160 ft	62.5 ft even keel	...	15.5 knots	...	{seawater} {crude oil}	60-90%	150 ft/74 ft/80 ft		center
5, 6	T-2, T-3	915 ft	166 ft	...	...	...	...	...	...	165 ft/78 ft/69 ft	112 ft 277 ft fwd	center
7	T-4	333 m	51 m	12.2 m/13.5 m	...	10.6 knots @ 127 deg	...	seawater	93%	42.5 m/20 m/27 m	10 m fwd	center
8	T-5	253.2 m	44.2 m	11.82 m even keel	...	...	...	crude oil	60%	40.5 m/12.0 m/25 m	52 m aft	15 m to port
9	T-6	320 m	52.4 m	26 ft/37 ft ballast condition	50.5 ft	abt. 10 knots	...	seawater	94%	30 m/17.4 m/24.6 m	13 m fwd	9 m off centerline

Several additional cases of sloshing damage are cited in Ref. (3), which is written by a principal surveyor for Det Norske Veritas. These are as follows:

Case 10, Ref. (3)

The damage occurred on horizontal stringers in the wide forepeak of a large oil tanker with no longitudinal bulkhead in the tank.

Two stringers, one at about mid depth and the other at 75 percent depth above the bottom, were severely damaged -- cracked and buckled plating and plating torn loose and hanging down.

Case 11, Ref. (3)

Cracked and buckled bulkhead plating was found at the lower corners of transverse bulkheads on an ocean ore carrier on which ballast water was being carried in the generally rectangular hold with the hold about 25 percent full.

Case 12, Ref. (3)

A 9000 deadweight ton ore, bulk, oil carrier with generally octagonal hold shape experienced major damage to the shell and side framing when the hold was 50 percent full of ballast water. The ship had experienced heavy rolling during the voyage. The damage consisted of plating and frames permanently deflected outwards, with a crack in the shell and frames, twisted and partly torn loose.

The above cases of sloshing damage were thus found on one dry cargo ship, one ocean ore carrier, two ore-bulk-oil ships, one bulk carrier, and seven tankers (the shortest of which was 830 feet long).

The damage resulted mostly from ballast water in the tank or hold. In a few cases, ballast water and crude oil had been carried on alternative voyages before the damage was discovered.

### III. INSTRUMENTED STRUCTURAL MEMBERS AND PRESSURE TAP LOCATIONS

An overall objective of the project is to provide guidance for the tank designer regarding hydrodynamic loads on tank internal structure induced by sloshing. To this end, six representative structural members were designed and built to model scale to fit within the tank described in Section IV. These members were designed to be supported by the force gages covered in Section V. The choice of structural members to so instrument was based upon the twelve specific cases of structural damage listed in Section II.

Table II lists the instrumented structural members. They are designed for realistic locations and are considered to represent typical structures on ships of the type found in the Industry Survey. Also shown are the representative dimensions of the members. However, in order to provide sufficient space for attachment of the force gages and to assure that forces of measurable magnitude would be developed when sloshing, the depth of some of the members normal to the tank walls is arbitrarily increased over that of typical ship members as a compromise with pure geometrical similarity between model and ship.

Dynamic sloshing pressures were to be measured in addition to measurements of sloshing forces. Accordingly, a number of locations were chosen for pressure tap installations on the walls of the tank. See Table III.

Table IV correlates the damage cases with the instrumented structural members chosen and the pressure taps which were used.

Figures 1 through 5 show details of the instrumented structural members including the location of the attached force gages. Lexan plastic, 1/8 inch thick, was used as the material from which the members were made. Stiffening was cemented to the members as seemed necessary to keep the natural frequency of vibration of the member well above that of tank oscillation. In the case of the swash bulkhead, Members FS-8, FS-9, FS-10, the natural frequency of the member, when excited by a concentrated force at the centroid of the member and held at the three force gage attachment points, was estimated to be of the order of 18 Hertz, which is well above the test frequency of tank oscillation of 1 Hertz or less.

TABLE II

## Structural Members Instrumented for Sloshing Force Tests

<u>NUMBER</u>	<u>TYPE MEMBER</u>	<u>MEMBER SIZE</u>	<u>FOR TESTING IN</u>
FS-1	Longitudinal stiffener on hold side of topside ballast tank sloping bulkhead	2" deep 1/2" stiffener 1/2" face plate	Bulk Carrier Hold
FS-3	Transverse web frame at side shell	2 1/2" deep 0.3" stiffener	Tanker Wing Tank
FS-4	Transverse web frame (alternative location)	2 1/2" deep 0.3 stiffener	Tanker Wing Tank
FS-5	Shell longitudinal	2 1/4" deep 1/4" face plate	Tanker Wing Tank
FS-6	Horizontal girder on transverse bulkhead	2 1/4" deep 3/4" face plate	Tanker Center Tank
FS-7	Horizontal girder on transverse bulkhead (alternative location)	2 1/4" deep 3/4" face plate	Tanker Center Tank
FS-8	Swash bulkhead at one third length (bottom section)	4 3/4" deep 1 1/4" face plate	Tanker Center Tank
FS-9	Swash bulkhead at mid length (bottom section)	4 3/4" deep 1 1/4" face plate	Tanker Center Tank
FS-10	Swash bulkhead at mid length (top section)	4 3/4" deep 1 1/4" face plate	Tanker Center Tank

TABLE III

## Pressure Tap Locations

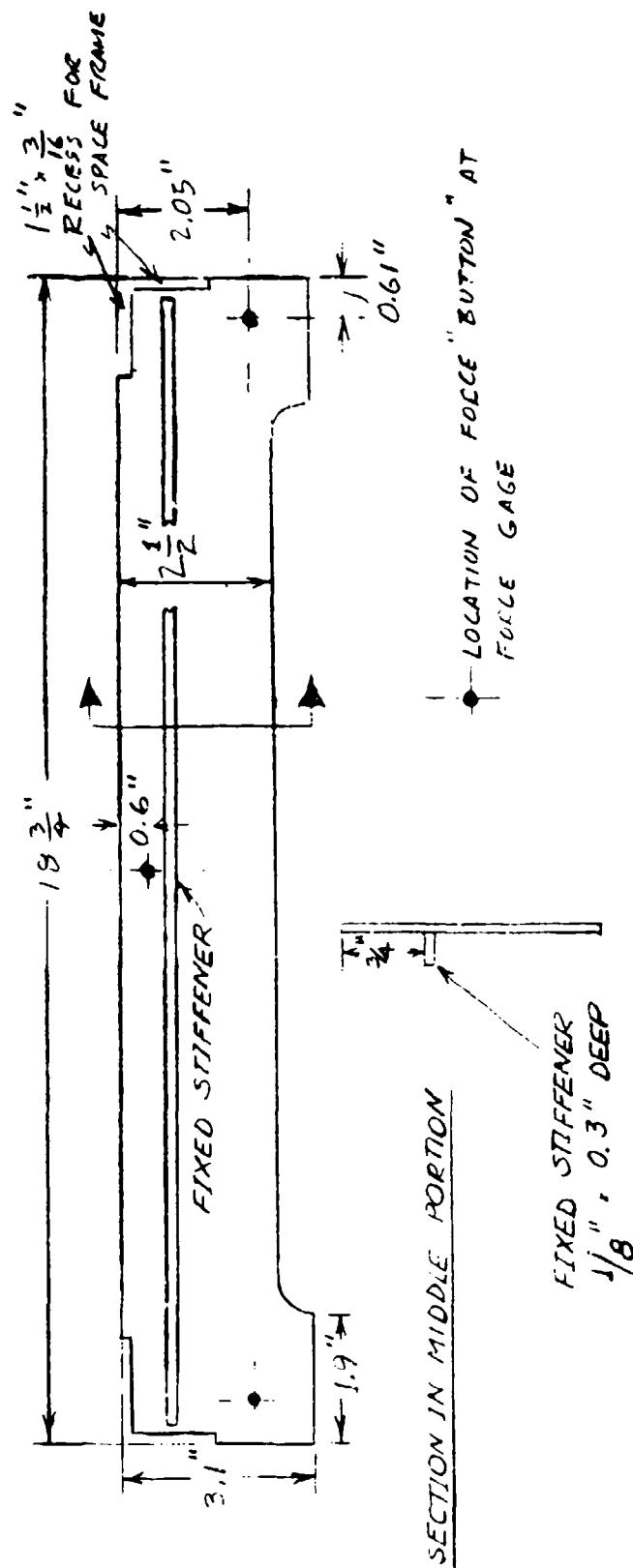
<u>LETTER</u>	<u>LOCATION</u>	<u>FOR TESTING IN</u>	<u>MOLDED DISTANCE FROM SIDE EDGE</u>	<u>MOLDED DISTANCE FROM TOP EDGE</u>
F	Middle of top at end	Tanker wing and center tanks	6"	0.44"
H	Corner of end bulkhead at mid-depth	Tanker wing and center tanks	2.5"	9.8"
I	Back from end corner on middle of top	Tanker wing tanks	6"	5.9"
J	Middle of top at end, structure end of tank	Tanker center tanks	6"	0.44"
K	Corner of tank top at end, smooth end of tank	Tanker wing and center tanks	0.31"	0.44"
L	Smooth end bulkhead in corner, one third depth down	Tanker center tanks	0.81"	5.3"
M	Smooth end bulkhead at middle of tank, two thirds depth down	Tanker center tanks	6"	14.1"



TABLE IV

**Correlation of Damage Cases with Instrumented Structural  
Members and Pressure Tap Locations**

<u>DAMAGE CASE</u>	<u>CORRESPONDING INSTRUMENTED STRUCTURAL MEMBER</u>	<u>PRESSURE TAP LOCATION</u>
1	FS-1	
2	FS-1	
3	FS-1	
4	FS-8, FS-9, FS-10	L, H, J, K, M
5	FS-6, FS-7	F, H, J, L, M
6	FS-6, FS-7	F, H, J, L, M
7	FS-6, FS-7	F, H, J, L, M
8	FS-5	F, K
9	FS-3, FS-4, FS-5	F, H, I, K
10	FS-5	F, K
11	FS-1	
12	FS-1	

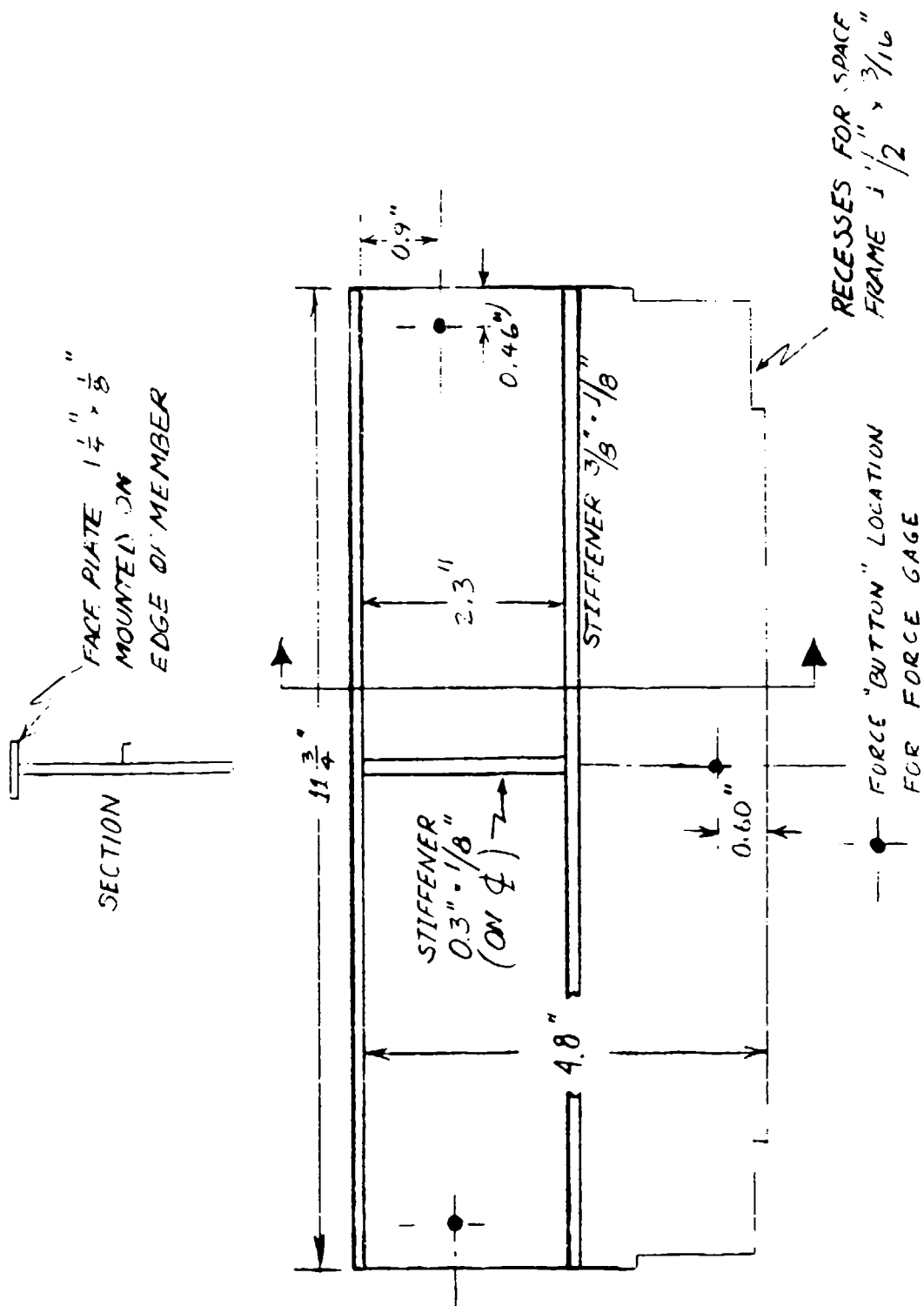


INSTRUMENTED STRUCTURAL  
MEMBERS PS-3 & PS-4

Figure 1







INSTRUMENTED STRUCTURAL  
MEMBERS FS-8, FS-9, FS-10

Figure 4

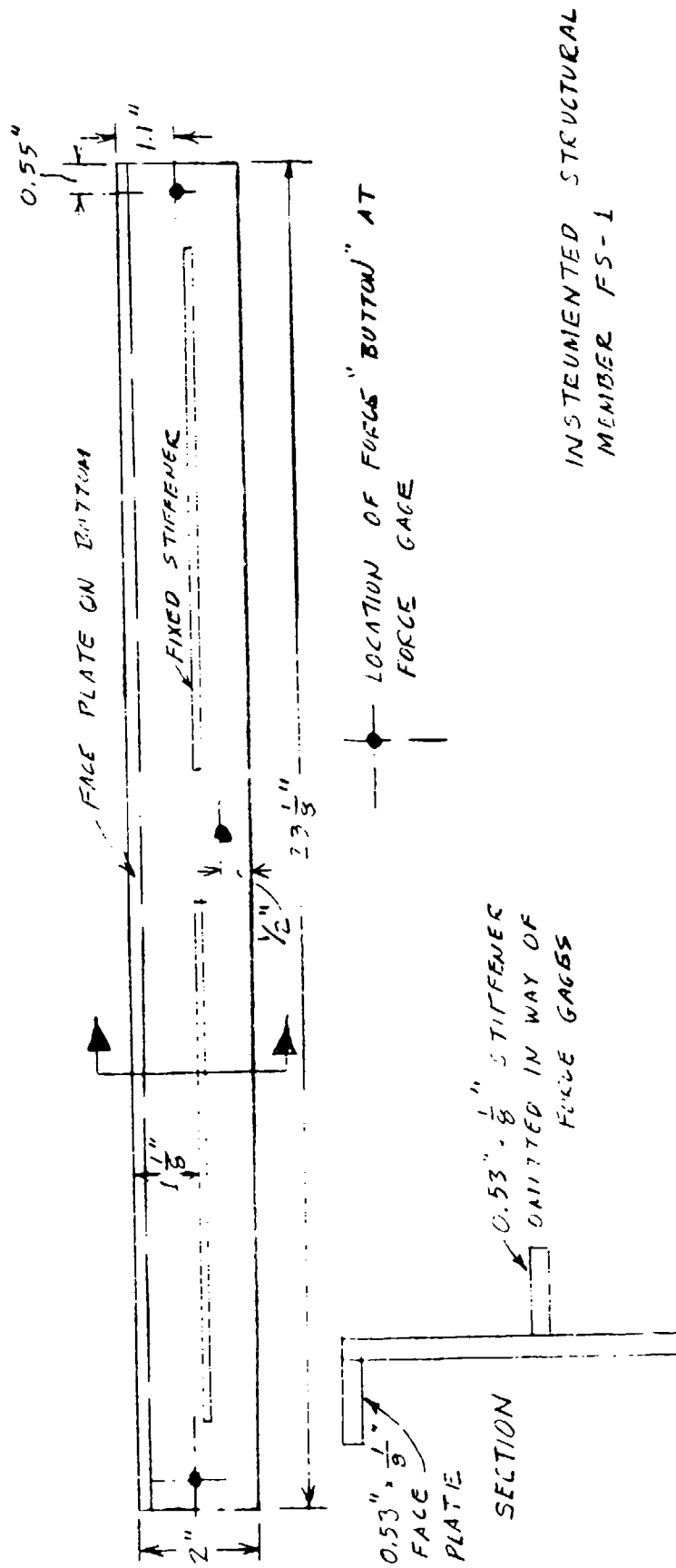


Figure 5

(THIS PAGE INTENTIONALLY LEFT BLANK)

#### IV. TEST TANK AND OSCILLATING TABLE FACILITY

A single rectangular test tank was fabricated to represent, by subdivision, three basic examples of ship tanks which had experienced sloshing damage according to the Industry Survey. These are described below:

- (1) The wing tank of a typical tanker with the tank oriented to represent pitching of the ship. The range of typical scale factors\* is from about 34 when representing a 50,000 DWT ship, to about 50 when representing a VLCC of 200,000 DWT. The wing tank proportions are achieved by fitting a watertight bulkhead on the longitudinal centerline of the basic tank in order to close off half of it and so reduce the breadth of the tank as modeled. The centerline bulkhead is fitted with a flange and watertight gasket and is supported by standoffs from the back (dry) side of the basic tank. Various internal structural members were then fitted.
- (2) The center tank of a tanker of about the same range of sizes as tank (1) and obtained by modifications only of the internal structure of (1). As in the case of (1), the tank was oriented to represent pitching on the ship.
- (3) The hold of a bulk carrier which is alternately used for dry cargo and for ballast water. The full basic tank was used and the model when oscillating represents rolling of the ship. A typical scale factor, ship to model, is 35. The ship represented would be of the order of 60,000 tons full-load displacement. The sloping bulkheads represent the upper and lower outboard corners of the hold, which typically are smooth on the hold side. However, for the case assumed, the upper sloping bulkheads are stiffened by longitudinals on the hold side inasmuch as bulk carriers built with this arrangement have experienced sloshing damage to the longitudinals. The sloping bulkheads are fitted firmly against adjoining surfaces, but corner openings allow free flooding outboard of the bulkheads, but within the confines of the basic tank.

---

\* Scale factor equals ratio of ship tank dimensions to corresponding model tank dimensions.



The basic tank is shown in isometric view in Figure 6. Inside dimensions within the tank's internal surface are 36 inches by 23 1/4 inches by 19 inches. It was decided to make all vertical surfaces and the watertight bulkhead -- to be omitted for tests with members FS-1 and FS-2 -- out of 3/8 inch thick transparent Lexan plastic. The top and bottom of the tank are fabricated of 1/4 inch thick aluminum.

The end and side windows are bolted to external welded aluminum frames. These panels are bolted to external vertical steel corner connecting angles and to the continuous bottom plate. The cover plates on top of the tank are in four sections to allow access to the top force gages for members FS-3, FS-4 and FS-10.

All bolts through the bottom, ends and sides are countersunk on the interior to allow a smooth surface for the flows which develop during sloshing and for insertion of non-instrumented structural members. The bolted configuration allows the tank to be completely disassembled and for other tanks to be fitted for future testing. Gaskets are provided at all flat surface connections.

The ten locations for instrumented members each require three force gage locations with a slot and four bolt holes for each or a total of 30 slots. Inactive slots are filled by blanks bolted through the force gage attachment holes. Pressure taps for thirteen pressure transducer locations are provided.

The watertight bulkhead is connected at bottom and ends by aluminum angles bolted through these surfaces; a heavier aluminum angle stiffens the top of the bulkhead and is connected to the cover plates by tapped holes and machine screws.

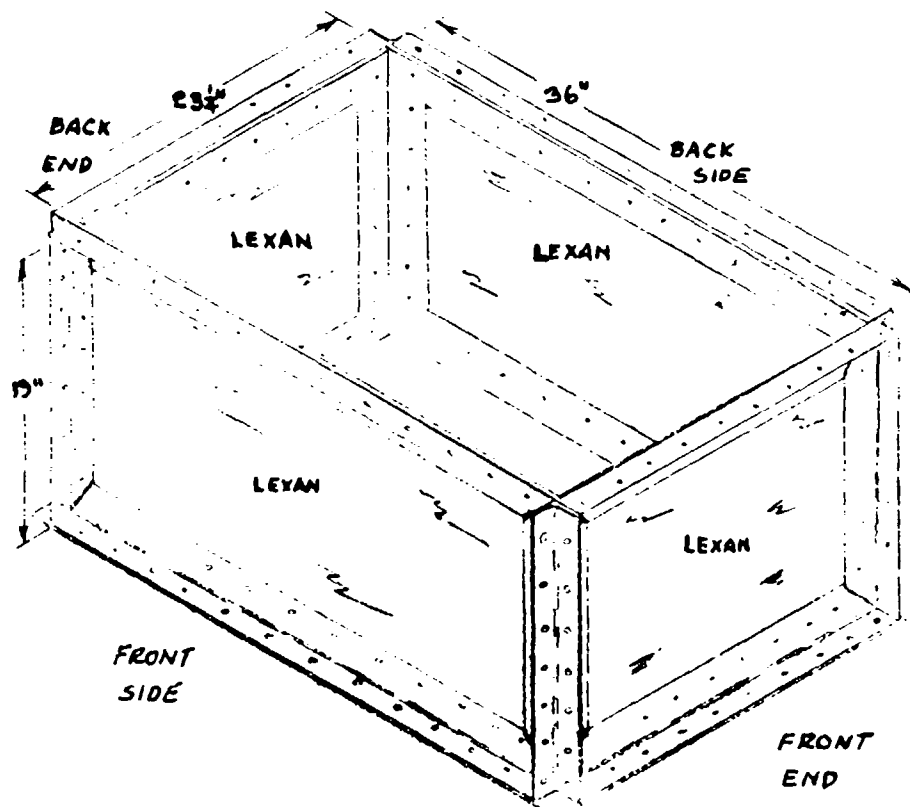
The watertight bulkhead has been located within the tank to provide a twelve inch inside width between the front side window and the bulkhead; this side is that portion of the tank in which measurements were made when representing a tanker wing tank or center tank.

Figure 7 is a photograph of the test tank showing the longitudinal bulkhead.

The Webb Oscillating Table Facility is shown in isometric view and as designed in Figure 8. However, for the present project, the tank was oscillated in the rotational mode by a lever and crank, connecting rod arrangement, driven by an eccentric connected to the output of a 15 to 1 speed reducer, which was in turn driven by a 2 horsepower "Vari-Drive" variable speed motor rather than by the hydraulic piston arrangement shown in Figure 8. When oscillating in the

translational mode, an hydraulic power pack and servo valve with feedback drive the carriage through the long hydraulic cylinder shown in Figure 8. The power pack consists of a 7.5 horsepower motor driving a Vickers in-line piston pump together with an accumulator.

The oscillating table, test tank, instrumented members and force gages were built in the Webb machine shop. Detail design and plans for the oscillating table had been furnished by Lehman Associates of Centerport, New York, under a National Science Foundation Grant, which also covered the cost of constructing the facility.



Isometric View of Open Tank with Cover Plates Removed,  
No Structure or Bulkhead is Installed

Figure 6 Basic Tank Assembled

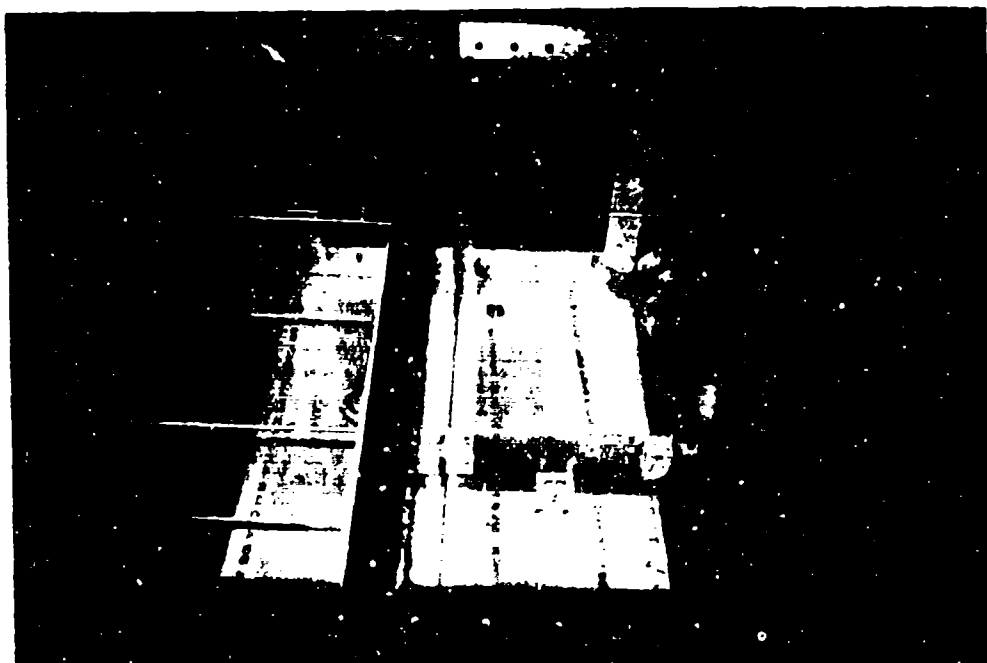
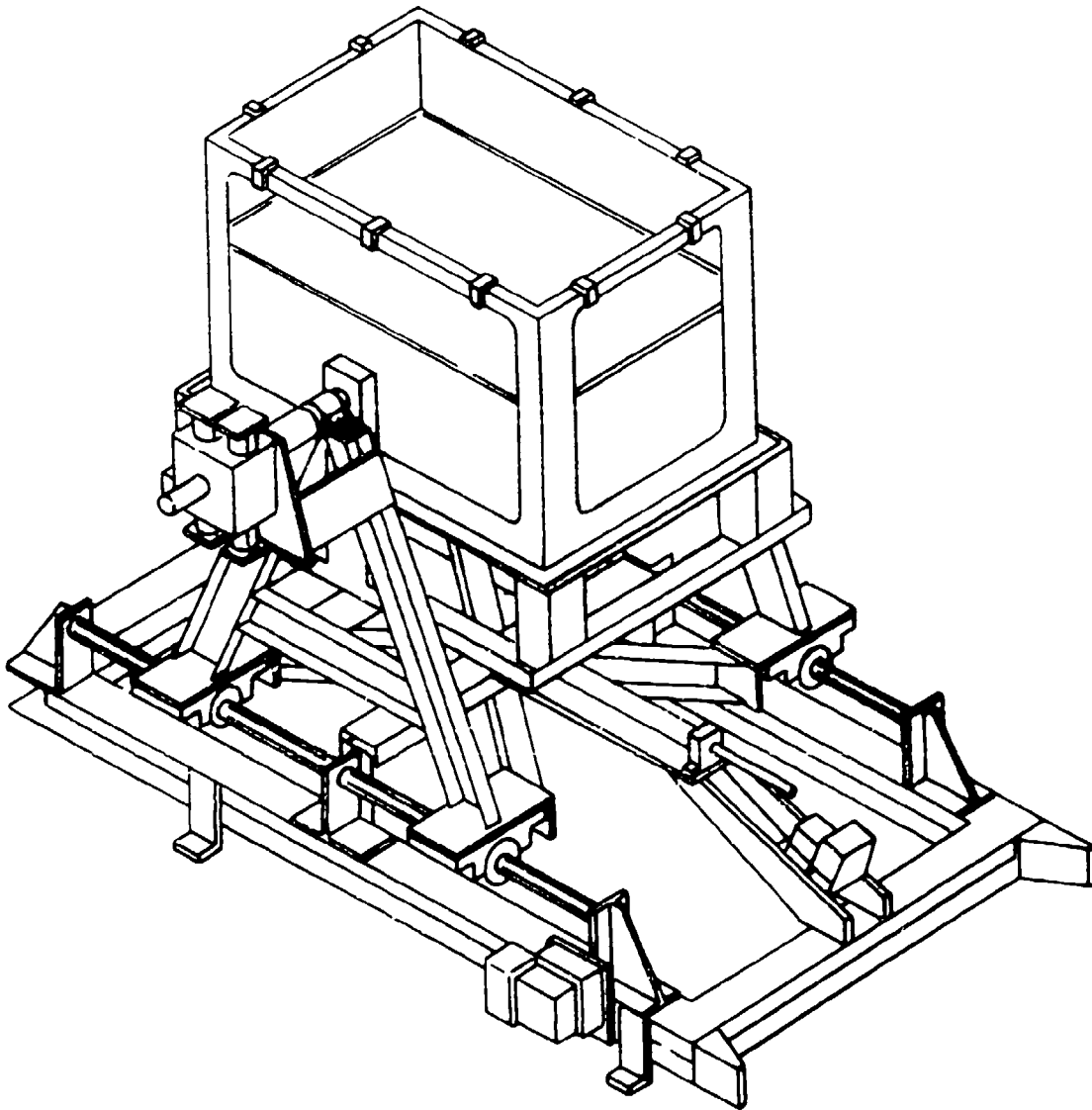


Figure 7 Test Tank Showing Longitudinal Bulkhead

Figure 8

Isometric View of Oscillating Table Facility as Designed



## V. FORCE AND PRESSURE MEASURING SYSTEM

The method adopted for measuring sloshing forces makes use of small strain gaged cantilever beams which pass through slots in the wall of the tank and support the structural member of interest at three points -- generally each end and the middle of the member -- and measure forces developed normal to the plane of the member. The force gages are described and illustrated in Appendix A.

Each of the three cantilevers is milled from an aluminum I beam section. The base of the cantilever then forms the outside of a free-flooding support housing, which is screwed to the outside of the Lexan tank window in way of the instrumented structural member. Forces are transmitted to each cantilever by an attachment housing, screwed to the structural member, which presses against a ball or button at the end of the cantilever. Since the lever arm formed by the cantilever is thus fixed, it is possible to calibrate the cantilever by applying known loads at the force button. The spherical shape of the button restricts the loading experienced by the cantilever to a force at a specific location on the cantilever -- that is, a spurious moment cannot be transmitted by the force button.

Calibration of the three force gages was accomplished by suspending known weights from the force button on the cantilever with the support housing clamped outside the tank. The resulting voltages of the Wheatstone bridge, which is unbalanced by the change in resistance of the strain gage as the cantilever bends, were recorded. All calibrations showed linear readings with load. The gains in the signal conditioning circuit were then set so that one volt equalled one pound force at the force button.

The strain gages attached to the cantilevers are Model EA-13-250PD-350, procured from Measurements Group, Inc., installed in pairs on both surfaces of the cantilevers. Full temperature compensation is thereby obtained.

Sloshing pressures were measured by two Endevco Model 8506 peizo-resistive pressure transducers, one rated for 2 psi and the other 5 psi. Their calibration was checked by pressurizing statically with a manometer, which showed the rated output was being achieved.

## VI. DATA ACQUISITION SYSTEM

It was decided to acquire the force and pressure test data on an available Apple IIe computer for later display and printing out as graphs or as recorded (digitized), thereby avoiding the need for recording on stripcharts. To this end, a data acquisition program was developed which records 10 seconds worth of data at the rate of 100 times a second on 6 channels, i.e., 3 force gages, 2 pressure gages and 1 timing signal.

The timing signal in the case of pitch or roll tests was obtained by the momentary closing of a micro switch arranged to be tripped at the start of each cycle by one end of the swinging table as it reached its limit of travel. However, in the case of combined pitch and surge runs, the timing signal was taken as the feedback signal generated by a pinion gear connected to a potentiometer which moved with the carriage as it surged and was rotated by a rack fixed to the surge rails of the oscillating table facility.

Force gage and pressure transducer signals were received and amplified by a Measurements Group 2100 signal conditioner/amplifier. This instrument has high stability and can receive signals with frequencies up to 5 KHz.

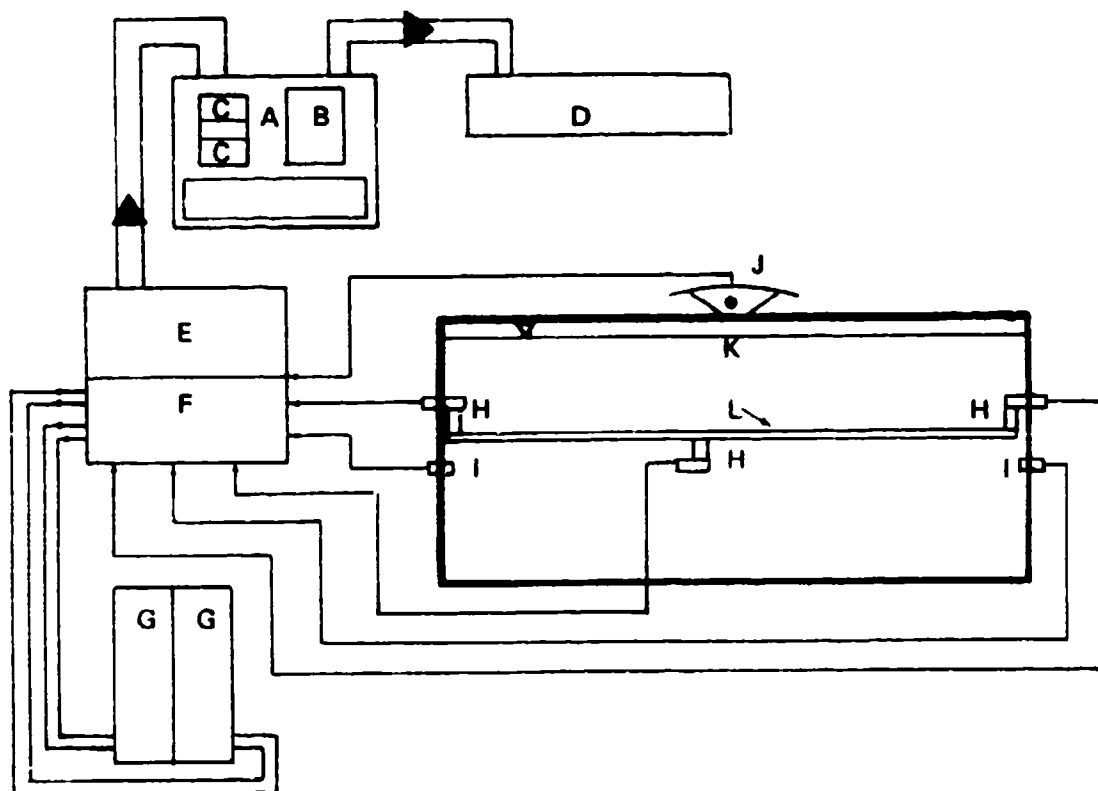
The amplified signals were digitized by an ADALAB data acquisition system which was obtained through Interactive Microware, Inc. The system permits conversion of the Apple computer into a data acquisition device through the insertion of an interface card in the computer.

Figure 9 is a schematic diagram of the data acquisition system.

Pitch and roll amplitudes were set manually by changing the degree of eccentricity on the mechanical eccentric which is driven by the output shaft of the speed reducer. Pitch and roll amplitudes were then read visually by a printer which passed a scale of degrees on the carriage of the oscillating table. These data were written down at the time of the test.

In the case of pure surge tests or combined pitch and surge tests, the surge amplitude was recorded from the visual travel of the carriage past a fixed scale. Surge amplitude can be controlled by either the hydraulic pressure of the Vickers hydraulic piston pump or by an amplitude potentiometer which changes the magnitude of the command potentiometer signal driven by the speed reducer output shaft. Generally, the amplitude potentiometer was used to change surge amplitude. See Appendix B.

**Instrumentation Schematic Wiring Diagram Indicating Location, Type, Number  
and Nature of Data to be Acquired in Each Test Run**



A APPLE IIe COMPUTER WITH ADALAB INTERFACE CARD  
B CATHODE RAY TUBE  
C DISK DRIVE  
D EPSON HARD COPY PRINTER  
E ADALAB (DATA ACQUISITION SYSTEM)  
F SIGNAL CONDITIONING  
G STRIP CHART RECORDER(OPTIONAL)  
H FORCE TRANSDUCERS  
I PRESSURE TRANSDUCERS  
J ANGULAR DISPLACEMENT SWITCH  
K TANK MODEL  
L INSTRUMENTED STRUCTURAL MEMBER  
INSIDE TANK

Oscillating periods were controlled by the manual control of the Vari-Drive system. Later study of timing signals versus a time scale can give precise values of period. Figure 10 is a calibration curve of Vari-Drive setting versus oscillating table period.



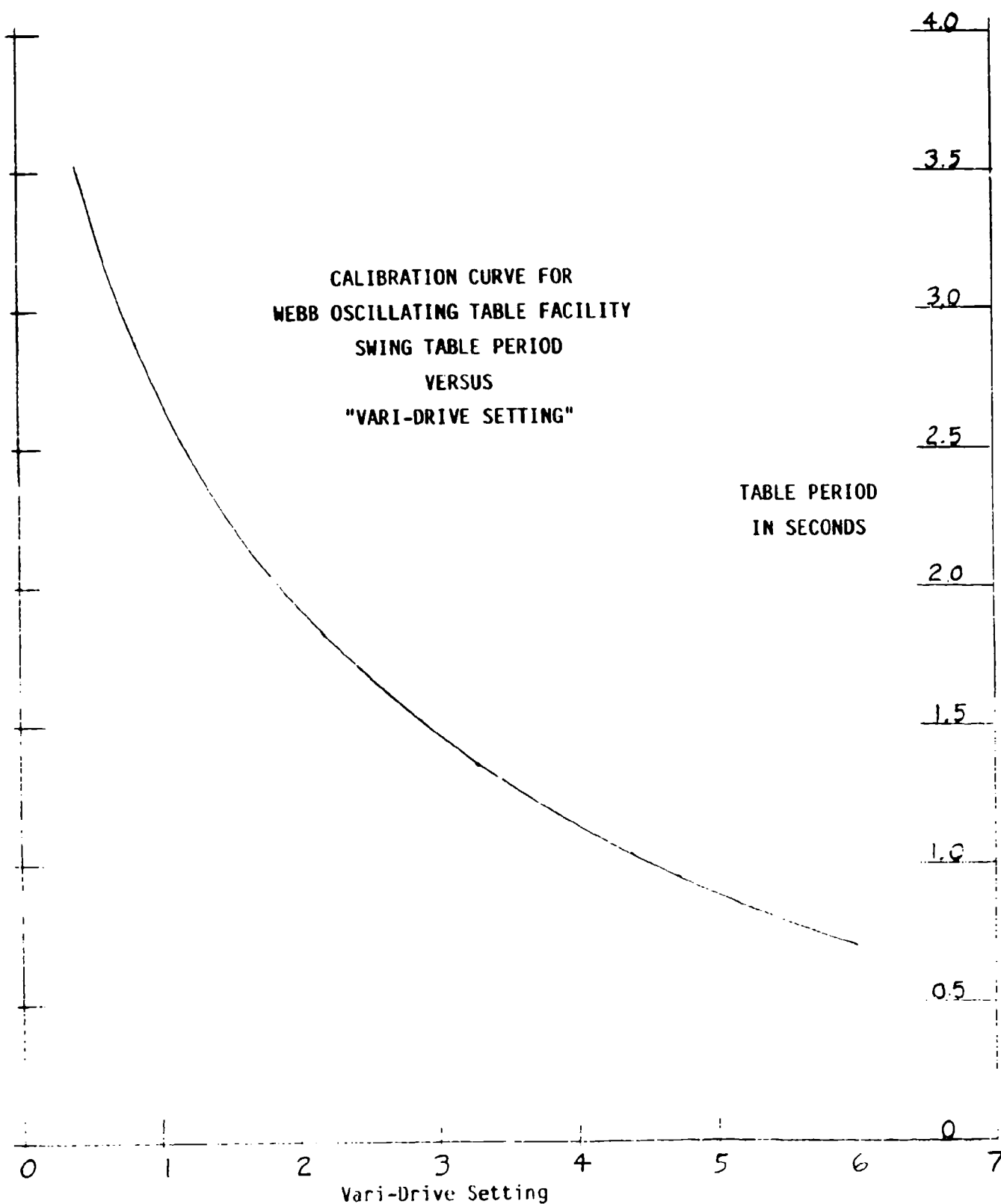


Figure 10

## VII. TEST PARAMETERS

In view of the great number of possible combinations of type of tank, type of member, fill depth, period of oscillation, amplitude of oscillation, type of motion (rotational or translational) and presence of additional structure in the tank, it was necessary to limit the number of test runs to a minimum for any one combination in order to maximize the generality and usefulness of the test data. In addition, the sponsoring agency was interested in a broad range of liquid specific gravities and consideration of enroute service viscosities. To this end, the various combinations were broken down into test groups which, in general, covered test runs with a single instrumented member. Table V lists all Test Groups accomplished together with relevant data.

In order to account for the frequency at which large sloshing would occur, non-dimensionalized pitch and roll were first estimated for the typical ships being considered as a function of period of encounter based upon the Series 60 model test results in waves [Ref. (4)]. A rough approximation to tank sloshing over the range of ship periods of encounter giving substantial ship response was then made by the assumption that the sloshing response in the tank can be represented by a linear spring, mass damper system. This gave limits of tank model periods beyond which it was unnecessary to test. When the tests were run, the apparent resonant point fell within these limits.

### Visual Impression of Flows in Tank

The test program concentrated on periods of excitation which appeared to give maximum wave activity in the tank for a given amplitude of oscillation (or pitch). In pitching, this period was invariably longer than the natural period of a smooth rectangular tank with no structure as determined from Figure 11. This indicates substantial hydrodynamic damping is provided by the structure in the tank.

TABLE V

## Test Groups and Conditions

TEST GROUP	MODE OF MOTION	STRUCTURAL MEMBER FOR FORCE MEASUREMENTS	TYPE OF TANK	PRESSURE TAPS USED	PERCENT OF FILL	OSCILLATION AMPLITUDES	STRUCTURE IN TANK	TYPE OF TEST	REMARKS
I	Pitch	FS-3 transverse web at side shell	Wing	I	40, 65, 90	4°, 8°	Transverse webs both sides	Force and Pressure	
II and IIA	Pitch	FS-4 transverse web at tank mid length	Wing	H	40, 65, 90	4°, 8°	Transverse webs both sides	Force and Pressure	Some runs with webs removed one side
III	Pitch	FS-5 shell longitudinal	Wing	F, K	65, 78, 90	4°, 8°	End girders, longitudinals one side, webs other side	Force and Pressure	
IV	Pitch	FS-6 horizontal end girder on transverse bulkhead	Center	F, J	65, 90	4°, 8°	End girders	Force and Pressure	Some runs without face plate on Member FS-6
V	Pitch	FS-7 end girder at lower height	Center	H, F, M	40, 65	4°, 8°	End girders	Force and Pressure	Some runs without face plate on Member FS-7
VI	Pitch	FS-8 swash bulkhead at 1/3 length, bottom	Center	L, M, H J, K	40, 65, 90	4°, 8°	1/3 bottom swash bulkheads, end girders, 1/3 top swash bulkheads	Force and Pressure	Some runs without face plate on Member FS-8; some runs with 1/3 top swash bulkheads removed
VII	Pitch	FS-9 swash bulkhead at mid length, bottom	Center	L, M, H J, K	40, 65, 90	4°, 8°	End girders	Force and Pressure	Some runs without face plate on Member FS-9; some runs without end girders
VIII	Pitch	FS-10 swash bulkhead at mid length, top	Center	L, K	90	4°, 8°	End girders	Force and Pressure	Some runs without face plate on Member FS-10
IX	Roll	FS-1 hold side longitudinal on sloping bulkhead	Cargo Hold		40, 65, 90	4°, 7.5°, 15°, 29.5°	Longitudinals on sloping bulkheads	Force	
XII	Pitch	FS-4 transverse web at tank mid length	Center		40, 65	4.5°, 7.8°, 8°	Transverse webs both sides	Force	Center of tank 4 ft. forward of pitch axis
XIII and XIII A	Pitch	FS-4 transverse web at tank mid length	Center		65		Transverse webs both sides	Force	CaCl <sub>2</sub> brine, s.g. = 1.13 to 1.31, temperature 60°F to 146°F; fresh water, temperature 36°F to 90°F
XV	Pitch and Surge	FS-4 transverse web at tank mid length	Center		40	1.5", 3" surge; 4°, 6° pitch	Transverse webs both sides	Force	Surge from pitch phase angles 0°, + 90°, + 180°; some runs surge only; some runs pitch only

The period of oscillation was varied from the longest period available to the shortest for one set of visual observations and different modes of wave motion observed, as follows:

With very long periods, the surface of the water remained virtually horizontal.

As the period shortened, waves began to build up and became a maximum at an apparent resonant period.

With further reduction in period, the wave activity in the tank virtually ceased and the water closely followed the tank.

With the shortest period, wave activity in the tank again became evident.

These observations are consistent with Ref. (5) in which the shortest period wave above is referred to as a second mode.

During most runs, vorticity was evident at the wave surface in way of the tank internal structure. In particular during test groups I and II, it was seen that deep vortices with surface depressions up to an inch formed at the inboard edges of the five webs on each side of the tank during each cycle.

Observations were made of the path of discrete particles of foreign materials -- small pieces of paper, cigarette ash, etc. -- dropped in the tank during test group II when the two sets of transverse webs were fitted. With substantial wave activity, the movement of the particles was erratic and non repeatable; at times, a particle might move from one side of the tank to the other while nearby particles hardly moved in the wave cycle. These movements emphasized the vorticity which develops along the inboard edges of the web frames. Thus, the resonant flow patterns were highly turbulent.

In the case of higher frequency, shorter period runs, such particles moved little with respect to the tank, further emphasizing that at these short periods, there is little noticeable wave activity.

## VIII. PROCESSING OF FORCE MEASUREMENTS

In order to provide useful sloshing force test data, it is necessary to account for the forces resulting only from the motion in space of the instrumented members in any oscillatory cycle. These represent a combination of static and dynamic forces and do not contribute to the hydrodynamic forces being experienced. However, these forces are present when the tank is filled with water and being oscillated. Thus, the measured force is a gross force and includes both the hydrodynamic force and the inertia and gravity of the instrumented member and attachment assembly. In order to separate out these latter forces -- which are tare forces -- additional test runs were made with the instrumented member in place and supported by the force gages but with the tank emptied of water. These runs are known as "dynamic tare" runs and were run at the same amplitudes and periods as the measuring runs.

Dynamic tare forces were subtracted from the gross forces on the computer after adjusting the two force records to the same phase in the cycle. This was accomplished by lining up the micro switch signals -- or feedback signals in the case of tests with surge -- on the computer scope.

## IX. PRESENTATION OF TEST DATA

Each run provided the sloshing force at the three force gages. In the case of many runs, dynamic pressure was also measured at two locations. These data were digitized by the computer when acquired. They were, in general, first displayed for checking on the computer scope for the ten second measuring period to assure consistency before storing on disk. Subtraction of tare force readings was accomplished after the test phase.

Various alternative presentation modes are available:

- (a) The gross minus tare force data may be printed out as graphs of the individual force gage traces against time.
- (b) The maximum to minimum individual gage gross minus tare forces, and the pressures, may be determined from the computer displays of the computer point count representing these quantities and may be tabulated.
- (c) The maximum to minimum of the average (or mean) gross minus tare force measurements from the three force gages being used in any one run may be similarly tabulated. This is the same as one third of the maximum vector sum of the forces at the three gages. This has the advantage compared with taking the sum of three gages as in (b) that a true maximum force on the member may be found when there is a significant phase difference in the cycle of the peak force at any one gage compared with the other two gages.
- (d) Force centroids may be computed by finding the moments of the forces at any two gages about the third gage using the force gage attachment locations.
- (e) Force and pressure coefficients  $C_F$  and  $C_P$  may be computed and plotted against period of oscillation or against other parameters at a fixed period of oscillation, such as amplitude of oscillation, tank location and tank Reynolds Number.

To accomplish alternative (a) for all the test runs (approximately 700 individual force and pressure records) is considered a prohibitively large task. For this report, a combination of the above procedures has been used. However, the recorded computer disks are on file at Webb Institute in the event further processing is needed.

Interpretation of force and pressure data for cases when impacts occurred is limited in general to values which alternate at frequencies of less than 100 Hertz, which is the sampling rate. Therefore, there is a chance even higher frequencies were present, although this is considered unlikely. A few exploratory runs were made using twice the sampling rate over one half the elapsed time. These showed no significant increase in maximum forces or pressures.

In the case of dynamic pressures, some "drift" of the zero motion pressure was observed on some of the runs but could not be corrected, for example Figure 11. In computing the pressure coefficients, therefore, one half the peak to peak pressure differences are used when the recorded pressure trace does not show evidence of impacts. When impacts do occur, however, the impact pressure is estimated from the graphed trace above a generally steady state or mean value. It may be noted that large negative pressures are not uncommonly recorded at a number of the pressure taps.

### Force, Moment and Pressure Coefficients

In order to make the measured sloshing forces and pressures useful for design purposes, they are converted into dimensionless coefficients and plotted against dimensionless periods.

Sloshing force amplitude  $F$  is non-dimensionalized by dividing by the quantity (for pitch oscillation),  $\rho g A \lambda \phi_a$  where:

$\rho$  = mass density of sloshing liquid

$g$  = acceleration of gravity

$A$  = projected area of instrumented member

$\lambda$  = length of tank normal to axis of oscillation

$\phi_a$  = amplitude of tank oscillation (pitch), radians

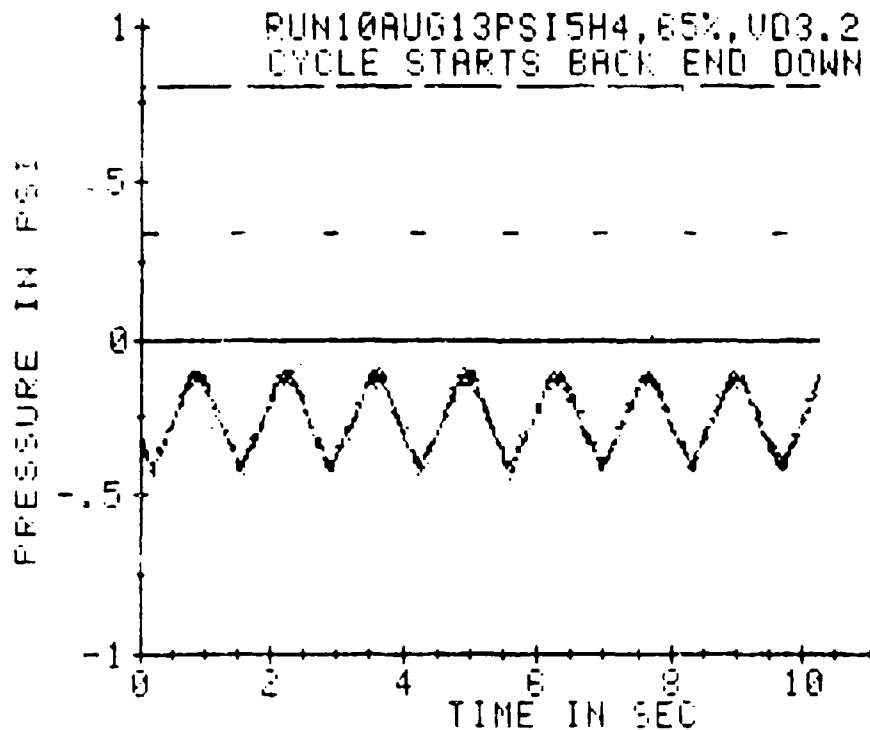


Figure 11: Example of "Drift" of Pressure Measurements

Then the sloshing force coefficient  $C_F$  is:

$$C_F = F / \rho g A \ell \theta_a$$

In the denominator of  $C_F$ , the factor  $\ell \theta_a$  is proportional to the rise of liquid at the end of the tank resulting from tank motion only.

In the case of sloshing pressure amplitude  $P$ , the denominator (for pitch) is taken as:

$$\rho g \ell \theta_a$$

Thus, the sloshing pressure coefficient  $C_p$  is:

$$C_p = P / \rho g \ell \theta_a$$



For members in which the sloshing forces are approximately 180 degrees out of phase at one end compared with the other, sloshing moment is considered more useful than sloshing force. Member FS-5, test group III, the shell longitudinal is of this type. Sloshing moment coefficient  $C_M$ , reported for this member, is defined as:

$$C_M = M / \rho g A x^2 \theta_a$$

where:  $M$  = sloshing moment amplitude computed from the three force gage readings about an axis through the member at its midpoint parallel to the axis of oscillation.

Assuming the model test curve is entered at the same Froude number as the ship,  $C_F$ ,  $C_M$  and  $C_p$  should apply both to ship and model when  $\theta_a$  is the same on model and ship. The same Froude number is achieved if  $T_s/T_m = \sqrt{L_s/L_m}$ , where the subscripts s and m apply to ship and model.

The dimensionless period used as a base against which  $C_F$ ,  $C_M$  and  $C_p$  are plotted is  $T_n/T$  where:

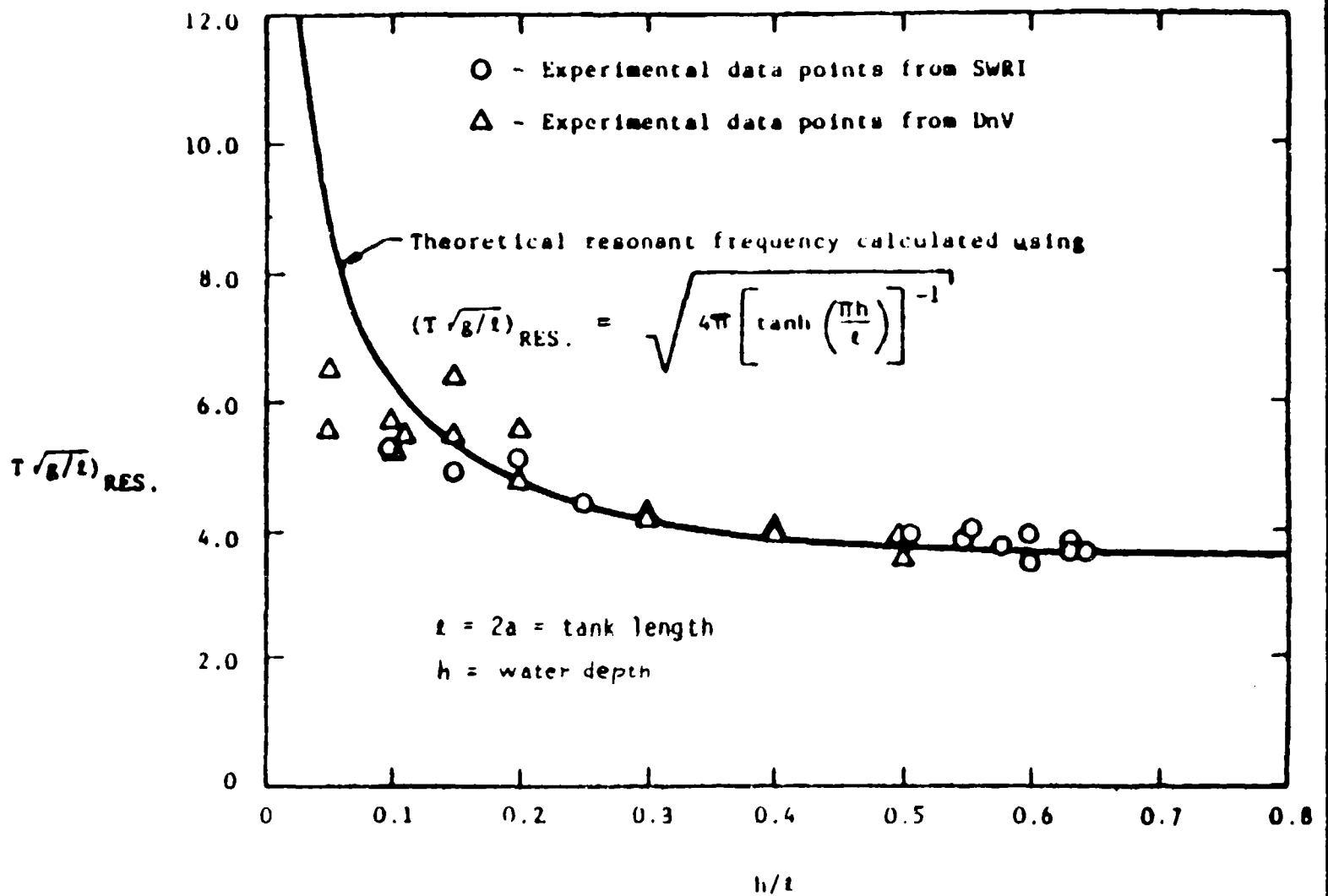
$T_n$  = natural period of sloshing according to Figure 12

$T$  = period of oscillation of tank

This abscissa is chosen to assist in extrapolating  $C_F$ ,  $C_M$  and  $C_p$  to higher and lower periods, it being recognized that sloshing is a vibratory phenomenon with damping and a resonant period. Were there sufficient test values for each combination to extend the experimental data on each side of the resonant period without extrapolation, a simpler dimensionless period not involving  $T_n$  could be used. Where the measured force, pressure and moment curves showed significant asymmetry in each motion cycle with one loop of the curve larger than the other, the height of the larger loop was taken as the amplitude.

Figure 12

Natural Sloshing Period of a Rectangular Tank  
[From Ref. (7)]



## X. PRESSURE MEASUREMENTS

Figures 17, 21, 23, 25, 27 and 29 show sloshing pressure coefficients from measurements in eight of the test groups. In general, it can be said that impact pressures were substantially higher than non-impact pressures. The highest non-impact pressure coefficients  $C_p$  were about 2.0.  $C_p$  ranged from 2 to 20 when impacts occurred.

Almost all impact pressures were measured in the roof or top of the tank and with a fill depth of 90 percent. There was considerable variability in these high impact  $C_p$  values. Small differences in the period of oscillation appeared to cause large differences in  $C_p$ . In some cases, the 8 degrees impact  $C_p$  values exceeded those for 4 degrees; in other cases, this trend was reversed.

More consistency is apparent in the 4 degrees, 8 degrees non-impact  $C_p$  values, when  $C_p$  for 8 degrees invariably was less than  $C_p$  for 4 degrees (for the same fill depth and period ratio  $T_n/T$ ). See also Section XI, M, Page 72.

The highest pressures measured were in the top of the tank for test group VII.

Higher non-impact pressures were measured when a significant part of the internal tank structure was removed -- (SB) points on Figure 17.

Figures 13, 14 and 15 are representative examples of pressure time histories as printed from the computer record disks.

The run identification at the top of each graph in general consists of the following data in sequence:

Run number; date; pressure transducer (5 psi or 2 psi); pressure tap location; amplitude of swing; percent fill; vari-drive setting.

Swing table position at which the timing switch is closed is shown on the next line.

Figure 13

Representative Sloshing Pressure Time History, Test Groups I and II

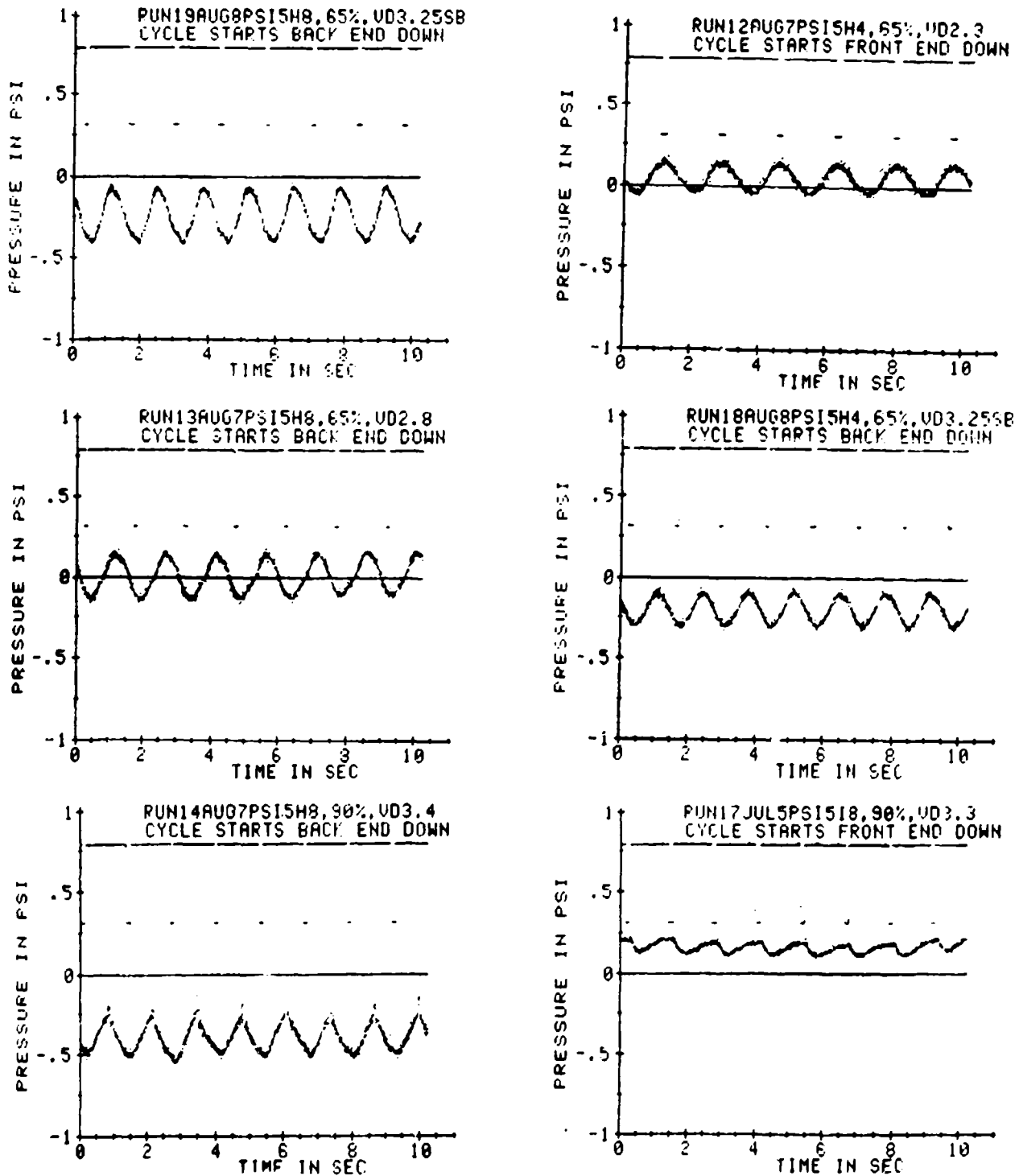


Figure 14

Representative Sloshing Pressure Time History, Test Groups IV and V

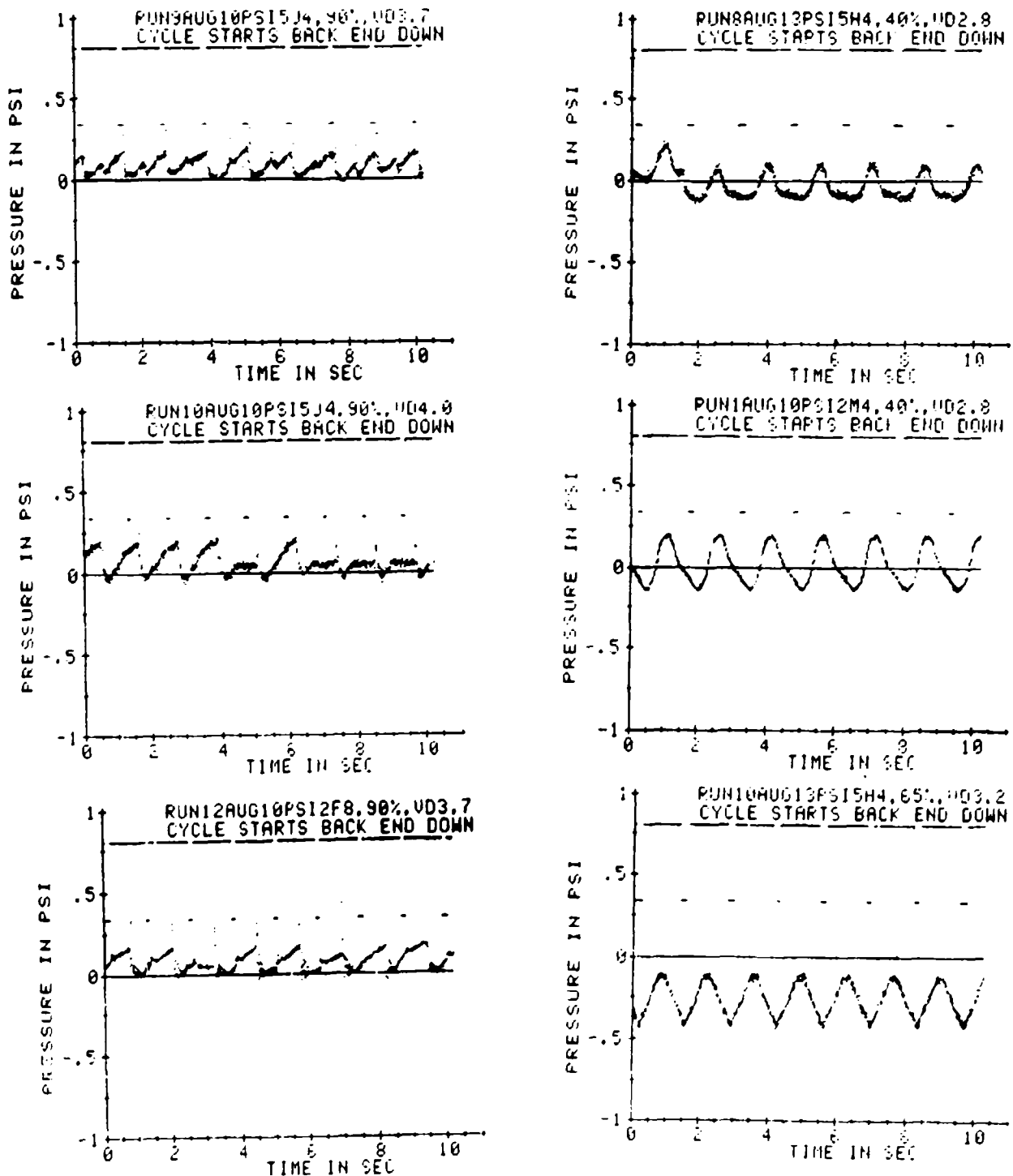
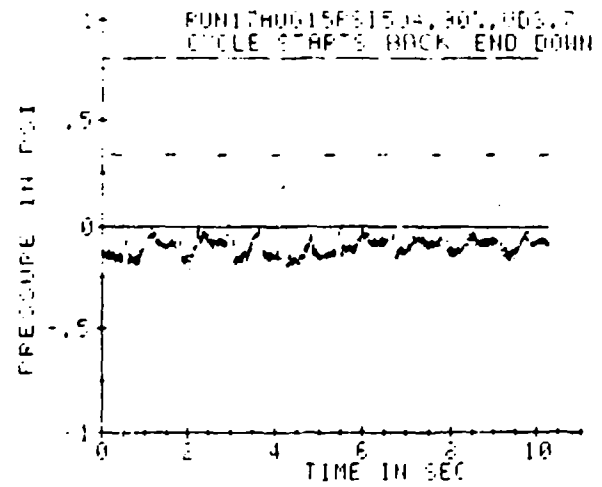
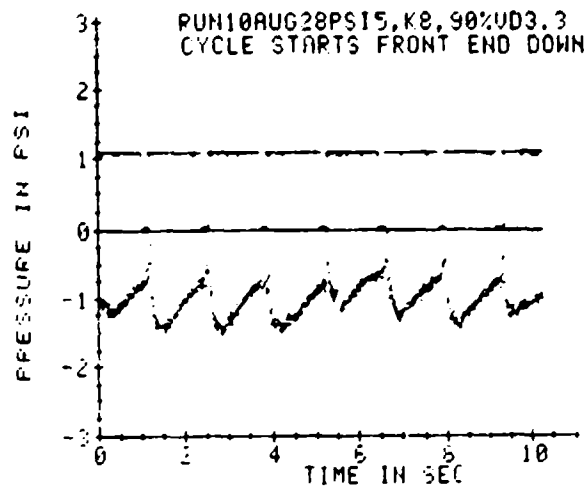
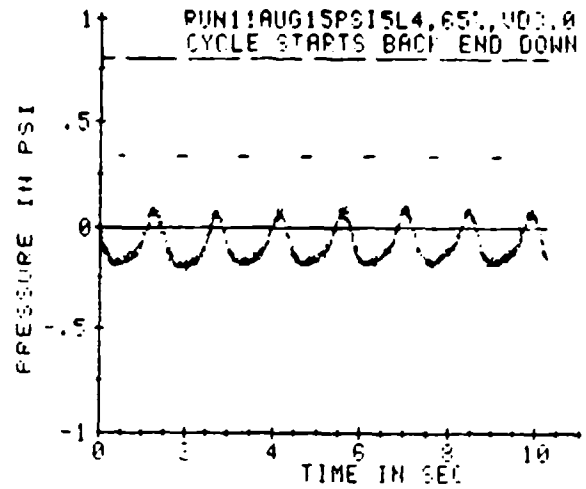
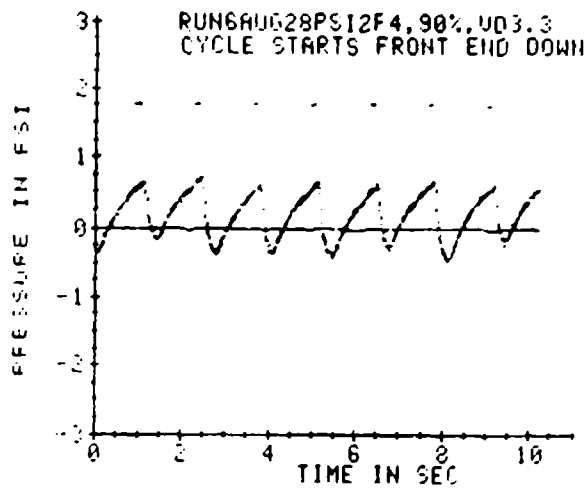
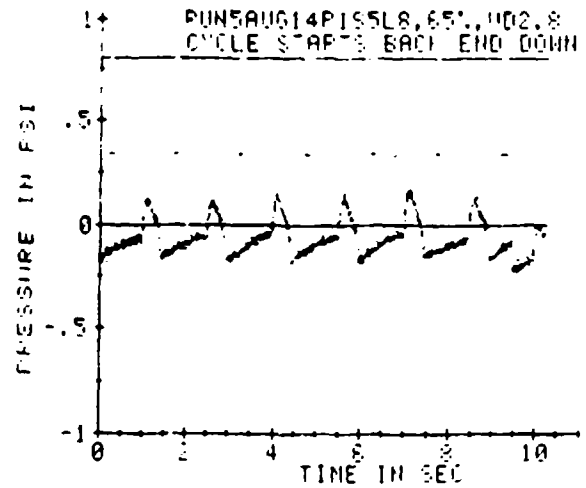
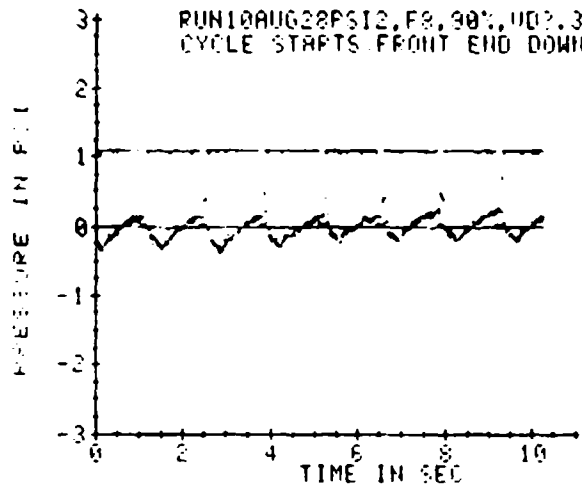


Figure 15

Representative Sloshing Pressure Time History, Test Groups III and VI



Test Group III

TEST GROUP VI

## XI. FORCES AND PRESSURES FOR SEPARATE TEST GROUPS

### A. Test Group I

Figures 16 and 17 show  $C_F$  and  $C_p$  for instrumented member FS-3, the transverse web at the end of a tanker wing tank. It is of interest that the highest  $C_F$  value, about 0.18, occurs with the middle fill depth tested, 65 percent. Based upon the force test data at 65 percent fill depth, there appears to be a resonance at about  $T_n/T = 0.85$ .  $C_p$  values at Location H are relatively low, being somewhat higher for the 90 percent fill case. As noted in Section X, Figure 17 shows a higher  $C_p$  on the end of the tank at about mid depth when the structure was removed from one side of the tank. At that time, non-symmetrical surface waves were observed running generally in a diagonal direction across the tank.

### B. Test Group II

The  $C_F$  values, Figure 18, are slightly higher than for test group I indicating larger sloshing loads on the transverse web when amidships than when at the tank end. The resonance at about  $T_n/T = 0.85$  is followed by a dropping off of sloshing force as  $T_n/T$  increases. The highest  $C_F$  found was with 90 percent fill depth when  $C_F = 0.22$  at  $T_n/T = 1.28$ , which probably occurs with such a short period to be of little concern to most ships.

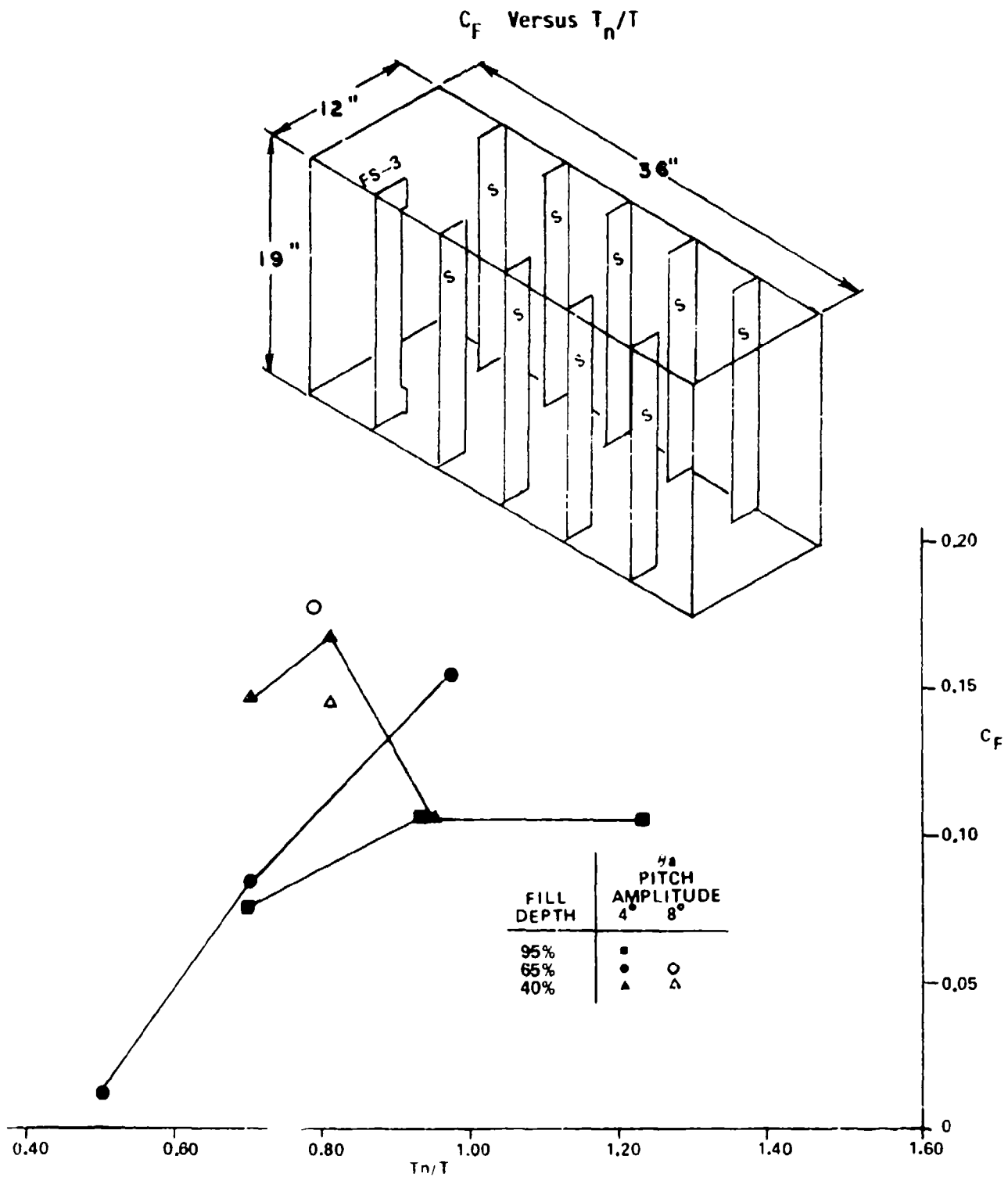
### C. Test Group IIA

Figure 19 shows  $C_F$  values on member FS-4, but run to determine with more precision the variation of  $C_F$  with period of oscillation  $T$ . Only one oscillating amplitude -- 4 degrees -- was used and one fill depth -- 65 percent. The resonance at  $T_n/T = 0.85$  is clearly shown, followed by a dropping off at  $T_n/T = 1.10$ , beyond which  $C_F$  rises again as  $T_n/T$  increases. These observations are entirely consistent with those in Ref. (5) which refer to the wave activity at higher  $T_n/T$  as a second mode. Visual observations of the surface waves in the tank showed very little relative motion at  $T_n/T = 1.02$  and 1.22. However, at the shortest period tested -- with  $T_n/T = 1.58$  -- short waves were seen in the tank.

TEST GROUP I

Figure 16

Force Tests, Member FS-3





## TEST GROUPS I AND II

## PRESSURE TESTS

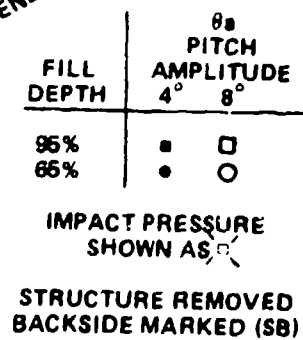


Figure 18

TEST GROUP II

$C_F$  Versus  $T_n/T$

Force Tests, Member FS-4

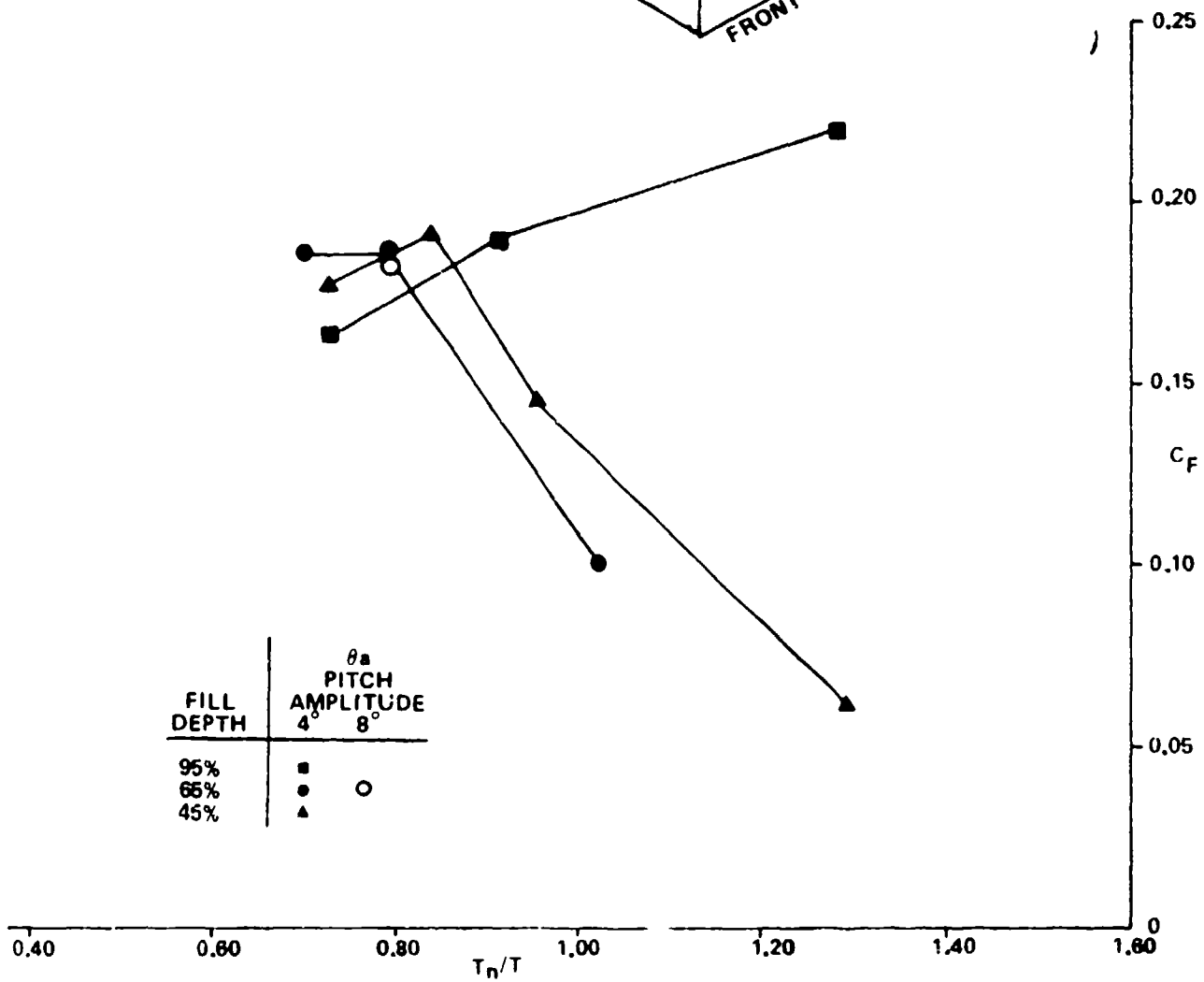
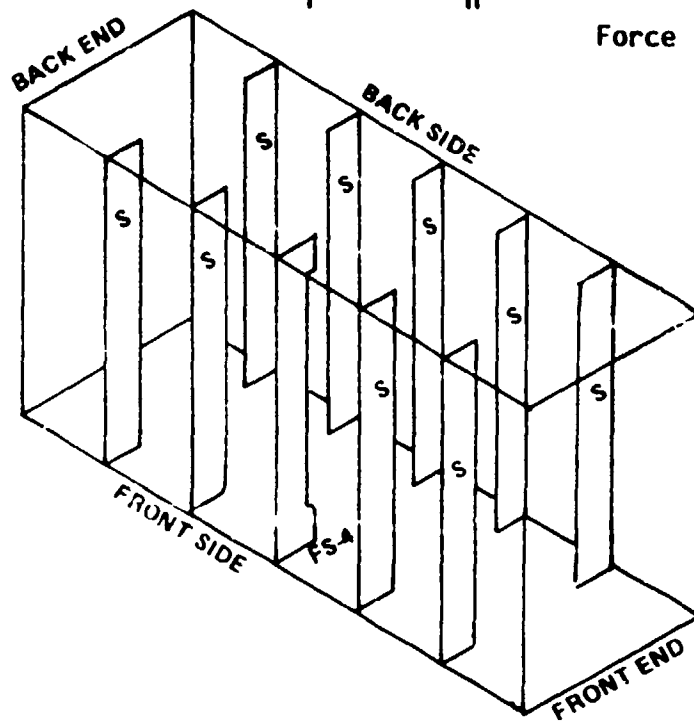
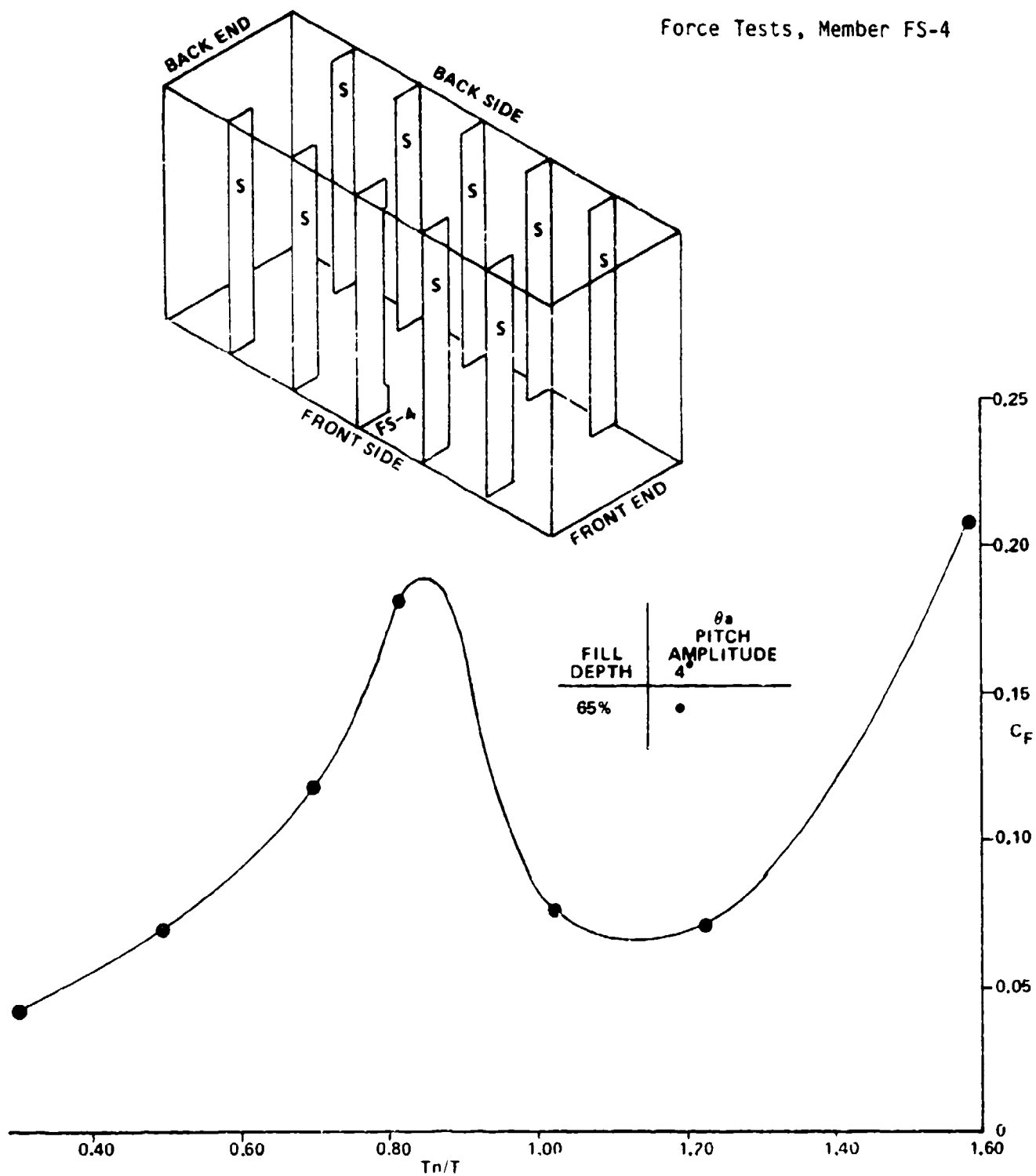


Figure 19

$C_F$  Versus  $T_n/T$

TEST GROUP IIA

Force Tests, Member FS-4



The resonant  $C_F$  value is about 0.19, but as with test group II,  $C_F$  at the highest  $T_n/T$  tested is about 0.21.

#### D. Test Group III

This group is the only one for which a sloshing moment is reported rather than a sloshing force. Figure 20 shows that the highest  $C_M$  value -- about 0.11 -- occurred when the tank was filled about to the level at which the instrumented member, the shell longitudinal FS-5, was located. There is a notable resonance in the sloshing moment curve at slightly less than  $T_n/T = 0.80$  with the 78 percent fill depth. With a 90 percent fill depth, the resonant  $T_n/T$  value increases to around 0.9.

Quite high impact pressures were measured in the top of the tank at its end with an oscillating amplitude of 8 degrees, as shown in Figure 21. It is of interest that impacts in the corner where  $C_p = 8.5$  substantially exceeded those at the middle of the tank end. The confinement of flow in three dimensions, rather than two, may be responsible for such a corner effect.

#### E. Test Groups IV and V

The instrumented members represented horizontal end girders at the end of a tanker center tank with three such girders in it. Figure 22 shows the measured  $C_F$  values; Figure 23 shows pressures measured at four points in the tank. The sloshing force coefficient  $C_F$  were all higher than for the transverse webs.  $C_F$  values were much higher when impacts occurred, the direction of the impact force always being upward as the rising wave surface contacted the lower face of the girder. The highest  $C_F$  value -- 1.7 -- occurred when the tank was 65 percent full and an 8 degrees amplitude of pitch was used, the sloshing force being developed in the end girder in the upper position. Some increase in sloshing force seems indicated when a face plate is fitted on the instrumented member.

As shown by Figure 23, impact pressures in the top of the tank -- maximum  $C_p$  value = 6.7 -- exceeded non-impact pressures in the end of the tank. The use of a face plate on the top end girder led to a reduction in impact pressure at the top of the structural end of the tank midway across the tank. Impact pressures were higher at the top of the structured end than the smooth end.

Figure 20

TEST GROUP III

$C_M$  Versus  $T_n/T$

Moment Tests, Member FS-5

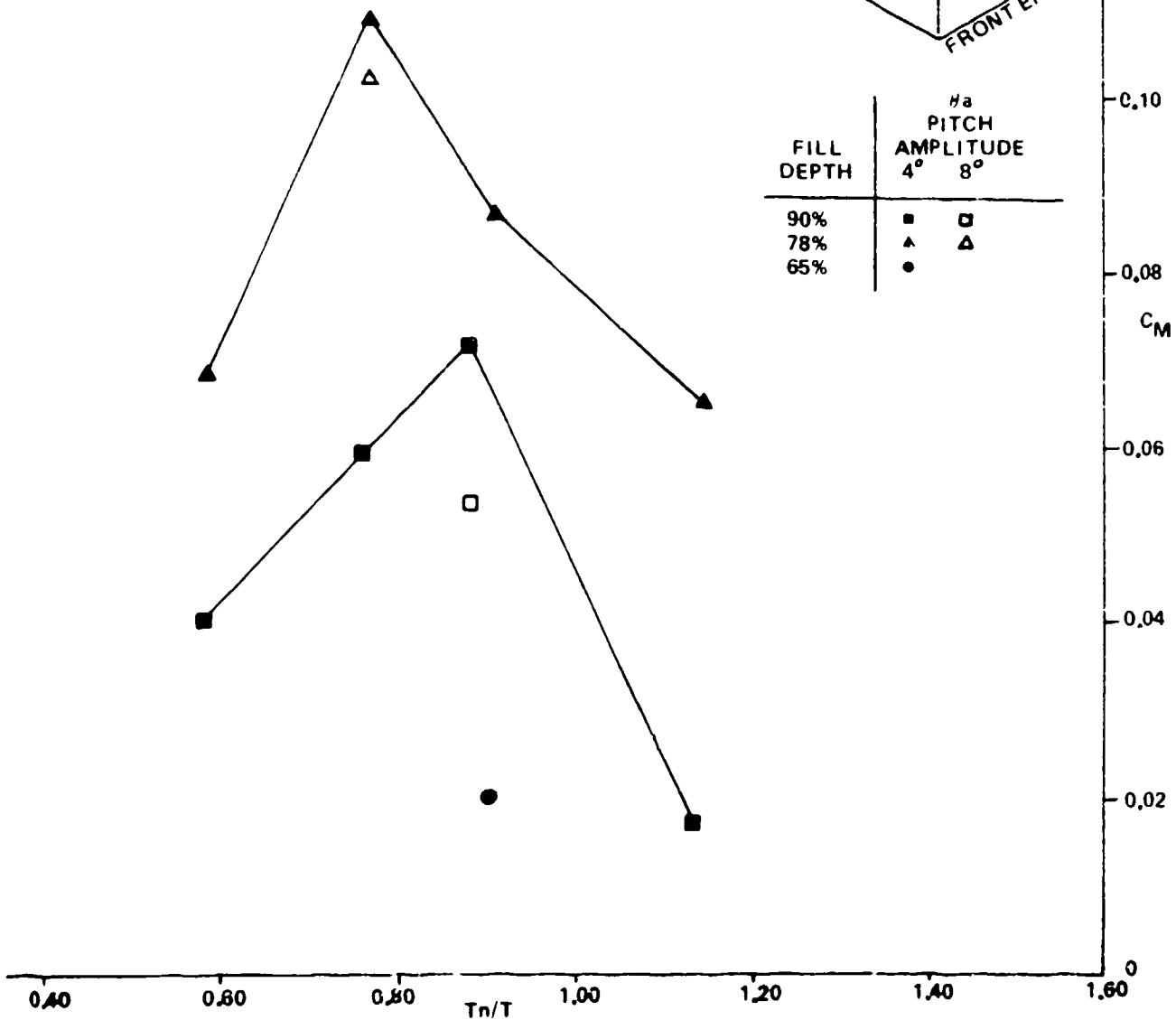
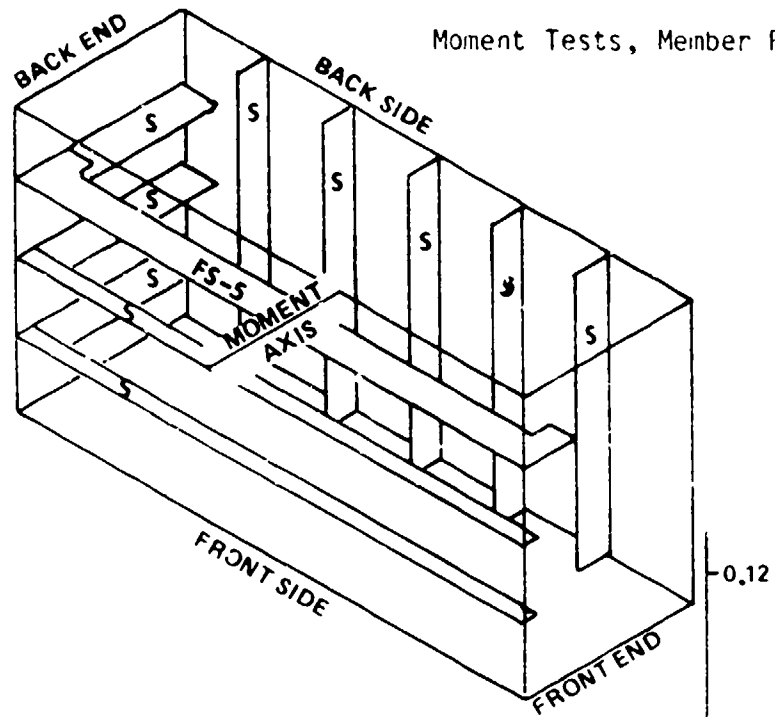


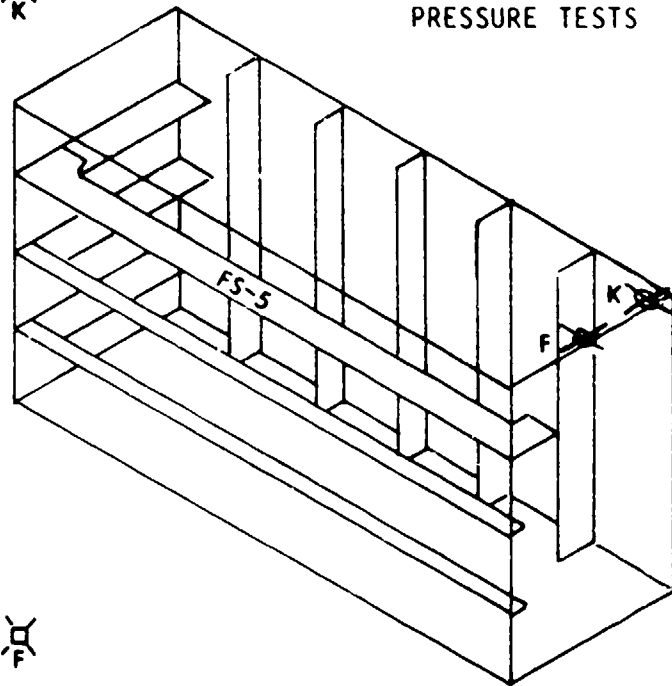
Figure 21

TEST GROUP III

$C_p$  Versus  $T_n/T$



PRESSURE TESTS



FILL DEPTH	$\theta_a$ PITCH AMPLITUDE	
	4°	8°
90%	■	□

IMPACT PRESSURE  
SHOWN AS

■ F  
■ K

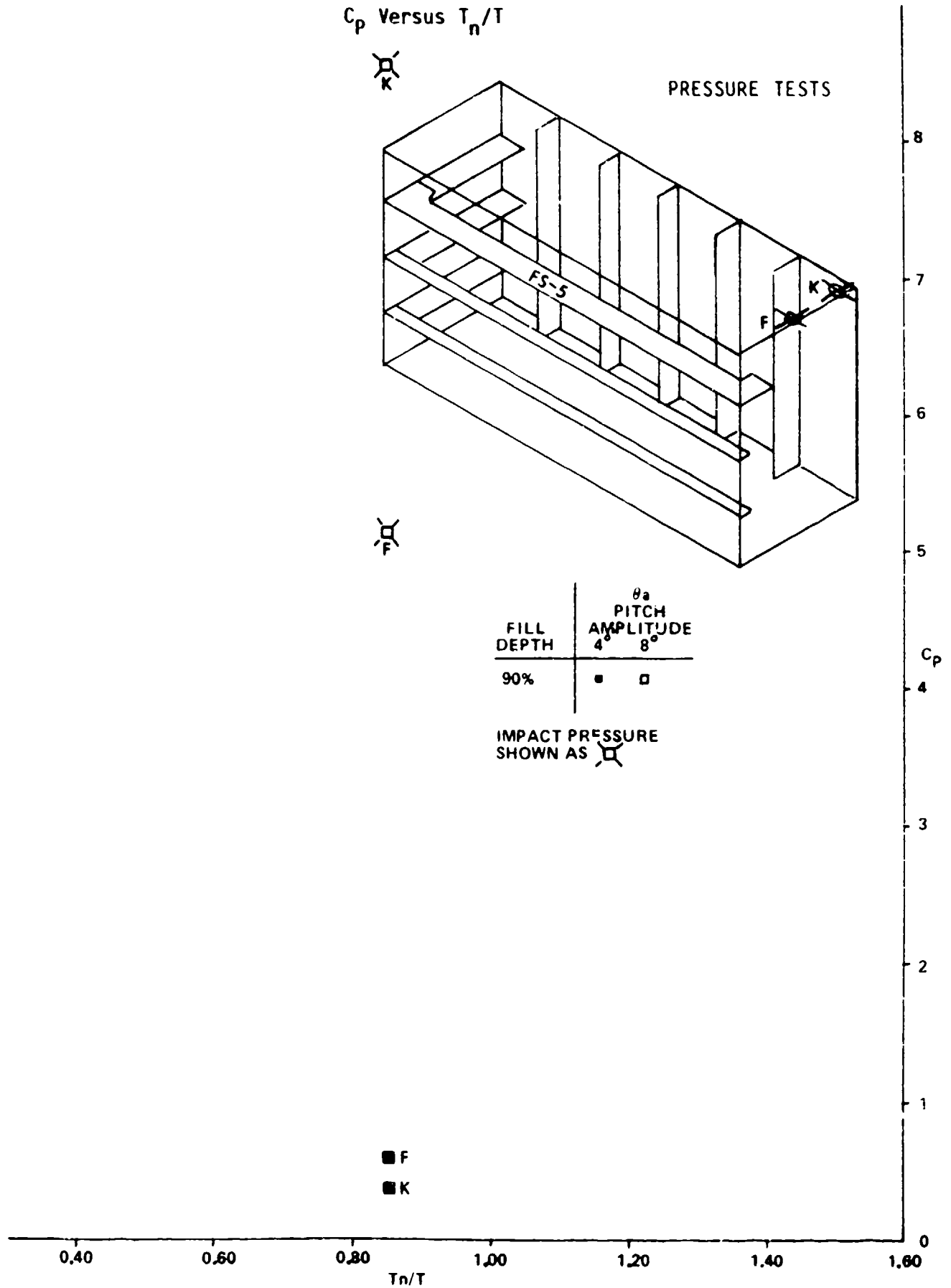


Figure 22

TEST GROUPS IV AND V

 $C_F$  Versus  $T_n/T$ 

Ø 6

Force Tests, Members FS-6 and FS-7

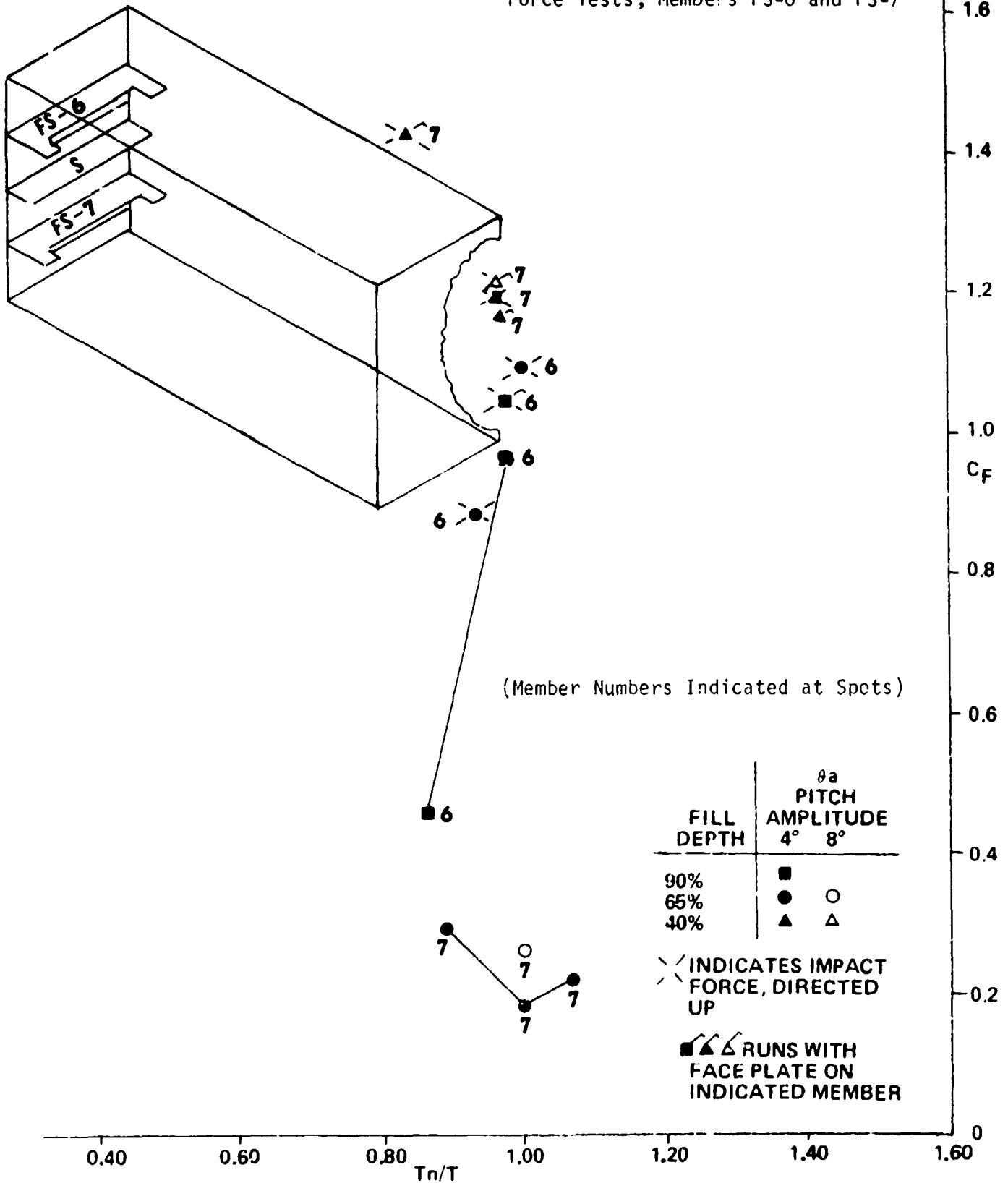
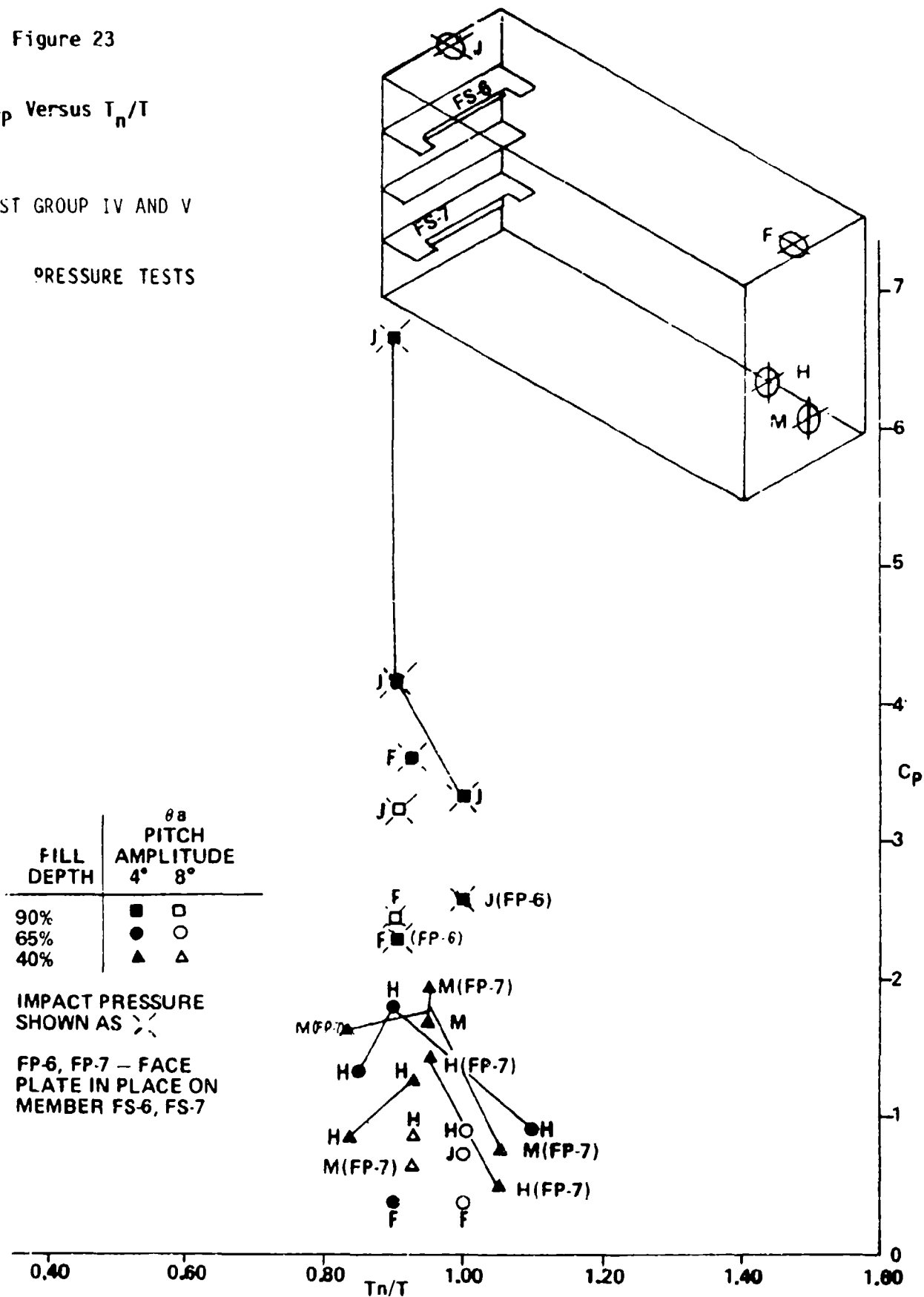


Figure 23

$C_p$  Versus  $T_n/T$

TEST GROUP IV AND V

PRESSURE TESTS





## F. Test Group VI

Figures 24 and 25 show  $C_F$  and  $C_p$  values for this case. The instrumented member, FS-8, is a swash bulkhead at the 1/3 length location on the bottom of a tanker center tank. The highest  $C_F$  value -- 0.76 -- was found in the 65 percent fill case and when a face plate was fitted on the member. The presence of the face plate increased the sloshing force by 30 percent at one condition. Bulkhead end girders were fitted for all runs.

With regard to the  $C_p$  values on Figure 25, the presence of a face plate on one lower swash bulkhead resulted in a slight reduction in the impact pressures at the smooth end top corner, pressure tap K, when the top swash bulkheads were not in place. The presence of the top swash bulkhead eliminated impacts at location K with 90 percent fill depth. With 40 percent fill depth, the lower swash bulkhead face plate had little effect on end bulkhead sloshing pressures at location M.

With a long excitation period,  $T_n/T = 0.60$ , and 65 percent fill depth, the end bulkhead pressures below the still waterline were more than the pressures slightly above the waterline, locations H and L. With a shorter period, near that for maximum wave activity,  $T_n/T = 0.81$ ,  $C_p$  was virtually the same at the two locations.

As with test groups IV and V, Figure 23, impact pressures at the structured end of the tank exceeded those at the smooth end, locations J and F, respectively.

Non-impact  $C_p$  values were in all cases less than 2.0.

## G. Test Group VII

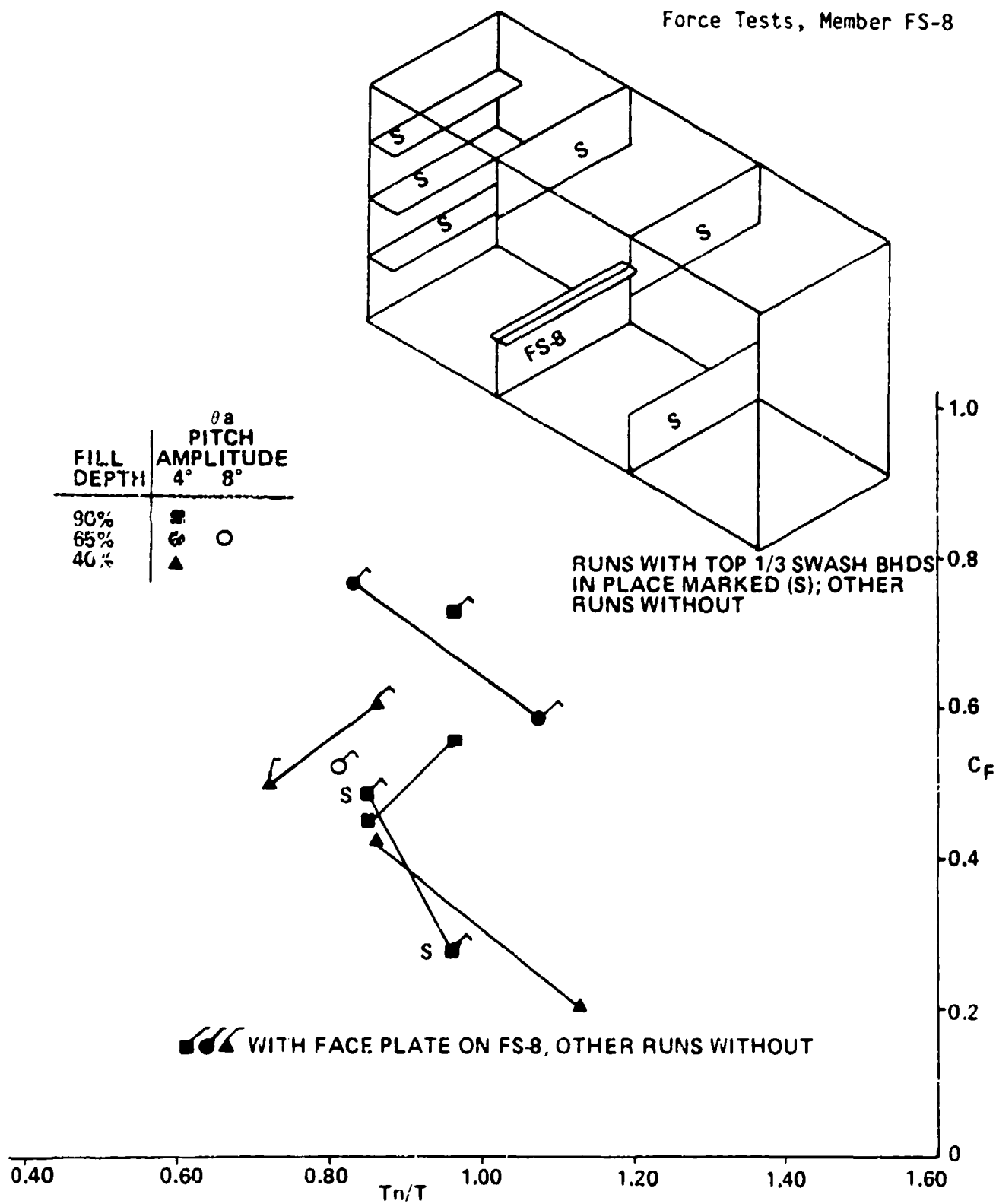
The test conditions were similar to those for test group VI except a single swash bulkhead was fitted on the bottom of the tank, rather than two at the 1/3 location. This member -- FS-9 -- was tested both with and without a face plate. Figures 26 and 27 show  $C_F$  and  $C_p$  respectively. There appears to be a resonance in the vicinity of  $T_n/T = 0.80$  -- 0.85. The presence of the face plate increased  $C_F$  by about 18 percent for one condition. The highest  $C_F$  measured was 0.66 with 65 percent fill depth.

Figure 24

Test Group VI

$C_F$  Versus  $T_n/T$

Force Tests, Member FS-8



TEST GROUP VI

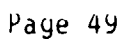


Figure 26

TEST GROUP VII

$C_F$  Versus  $T_n/T$

Force Tests, Member FS-9

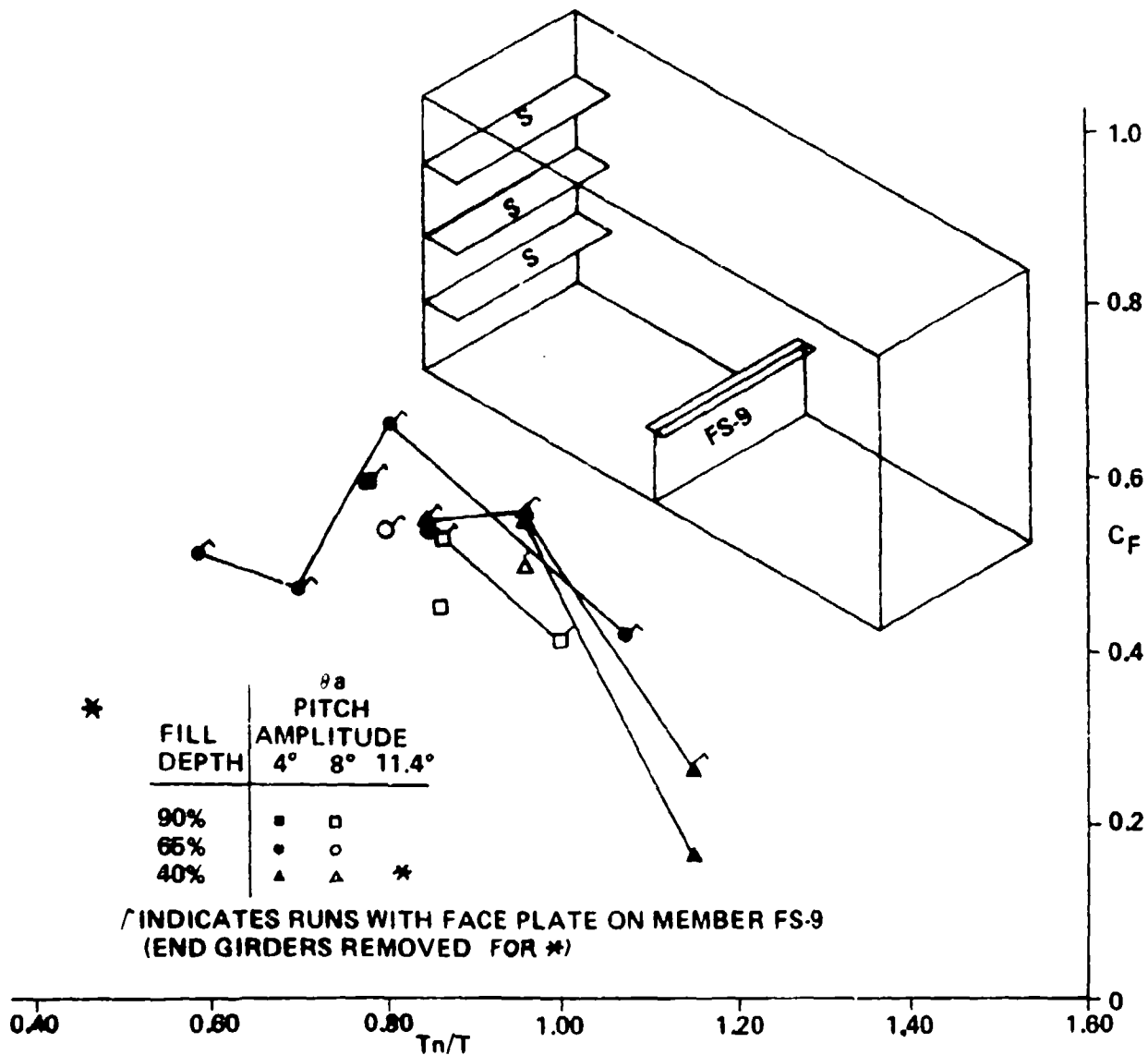
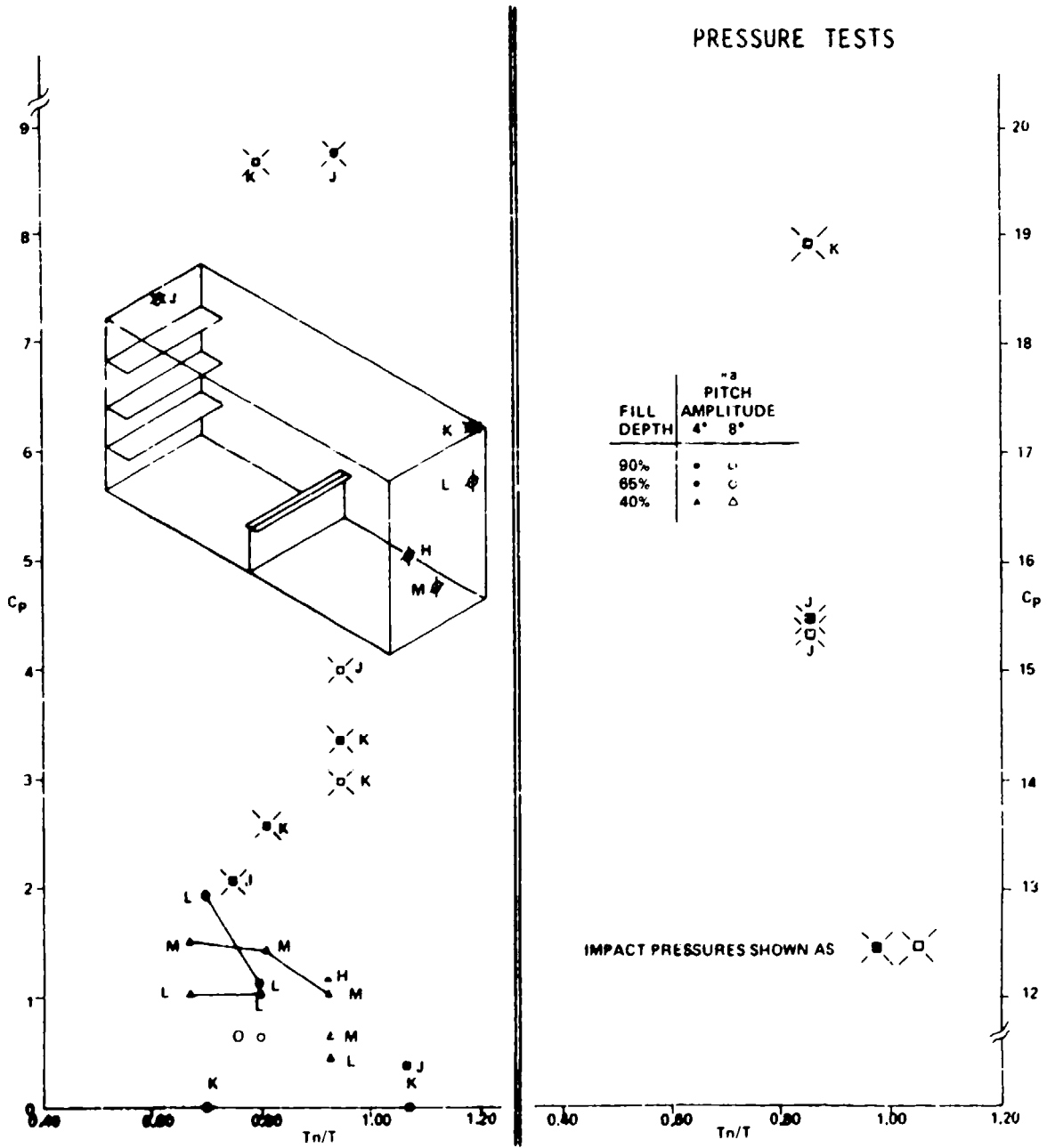


Figure 27

TEST GROUP VII

$C_p$  Versus  $T_n/T$



High impact  $C_p$  values were measured at the end of the tank. The highest  $C_p$  was almost 19, measured at the corner of the smooth end of the tank, Location K with an 8 degree amplitude, 90 percent fill depth at  $T_n/T = 0.81$ . Non-impact  $C_p$  values at the lower elevations were of the order of 2 or less.

Based upon the  $C_p$  values found with test group III, Figure 21, one would expect a higher  $C_p$  in the corner compared with that midway across the end of the tank, although such measurements were not made at the smooth end.

#### H. Test Group VIII

A limited number of sloshing force measurements and several pressure measurements were made with a swash bulkhead at the top of the tanker center tank model, instrumented member FS-10. Figures 28 and 29 show  $C_F$  and  $C_p$  which resulted. All runs were made with 90 percent fill depth. It is of interest that the highest  $C_F$  value -- 0.21 -- was measured at a  $T_n/T = 1.18$ . Sloshing pressure coefficients were higher on the smooth end corner of the top, Location K, than on the bulkhead end, Location L. The highest  $C_p$  -- 5.5 -- resulted from impact and occurred with 8 pitch degrees amplitude, when  $T_n/T = 0.83$ , and when a face plate was fitted on member FS-10. No impact pressures were measured with 4 degrees amplitude.

#### I. Test Group IX

Sloshing forces were measured on a hold-side longitudinal on the upper sloping bulkhead of a bulk carrier hold. For this test group, the longitudinal bulkhead was removed from the tank and sloping bulkheads at the upper and lower corners of the hold were fitted such that the fore and aft length of the model hold occupied the full 2 foot breadth of the tank. The spaces behind these sloping bulkheads were free flooding, but there was virtually no flow from the hold side to and from these spaces in any oscillating cycle. Three longitudinals were fitted on the hold side of each upper sloping bulkhead. The lowest of these on one bulkhead was instrumented member FS-1.

Figure 28

TEST GROUP VIII

$C_F$  Versus  $T_n/T$

Force Tests, Member FS-10

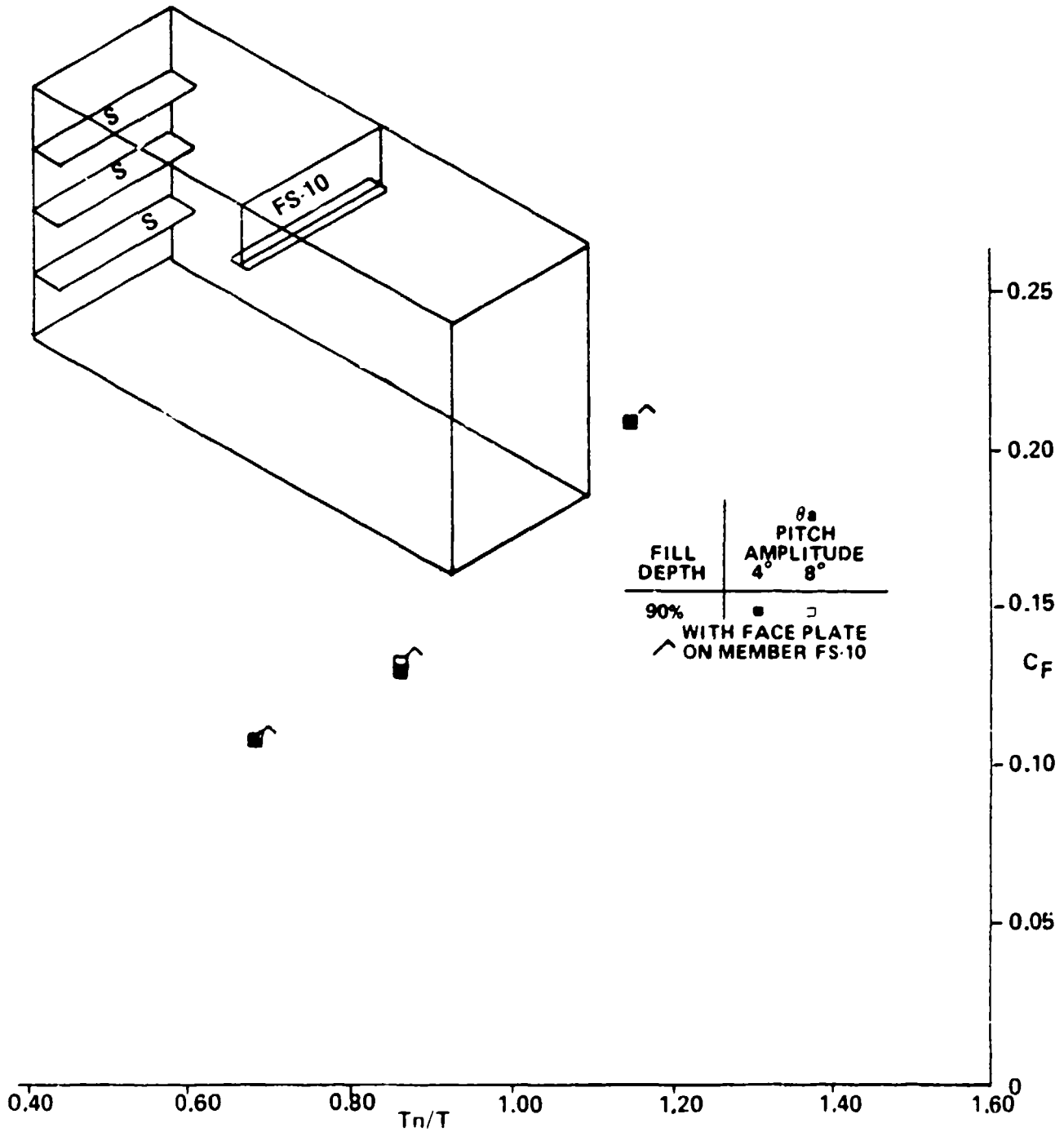
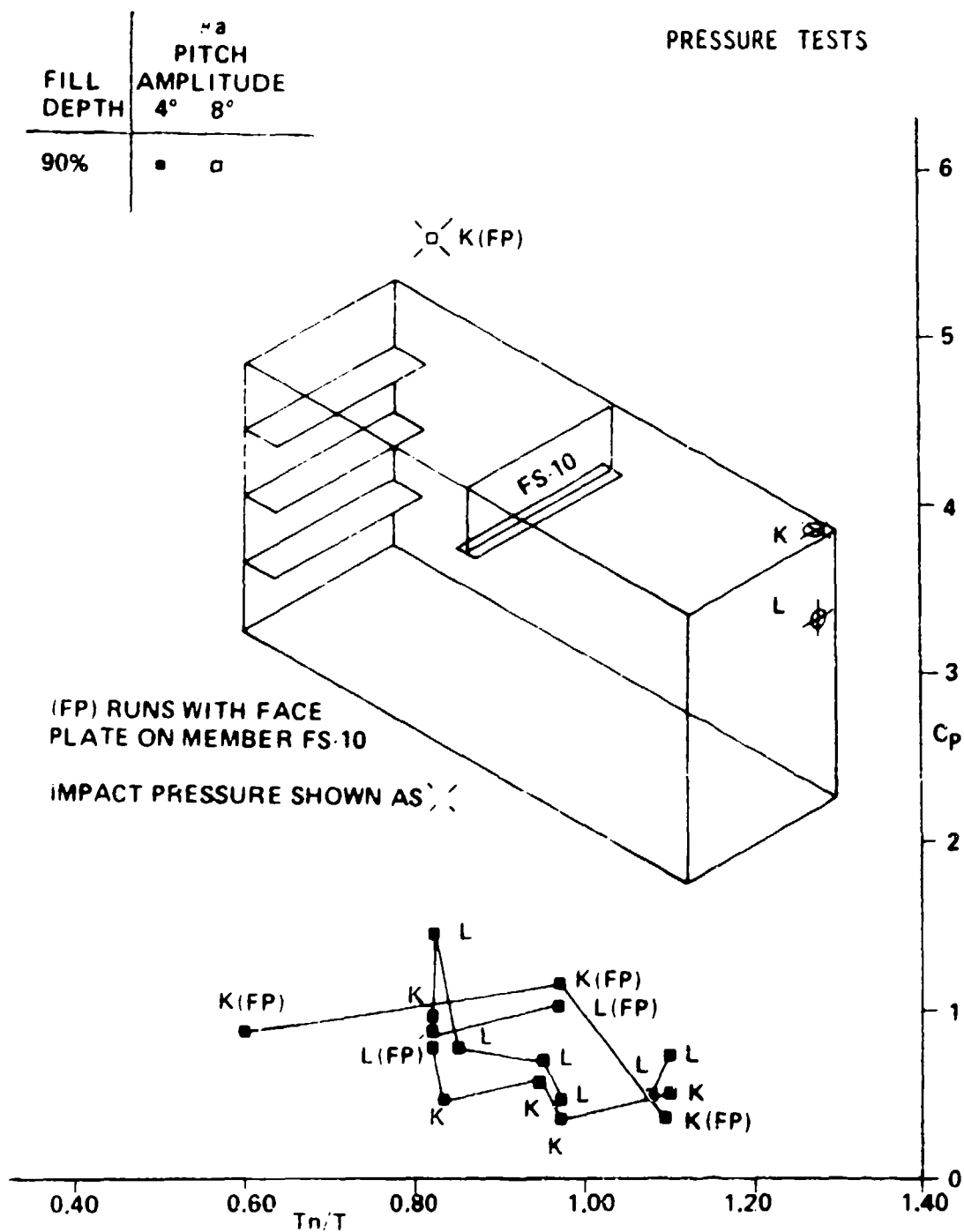


Figure 29

TEST GROUP VIII

$C_p$  Versus  $T_n/T$





As installed on the oscillating table, the tank was oriented to represent rolling of the ship. Tests were run with four amplitudes of roll. Figure 30 shows the sloshing force coefficients  $C_F$  which resulted. It was noted that the resonant motion of water in the tank was highly tuned indicating little damping, especially in the 40 percent fill depth condition.

A relatively large number of cycles were required after the tank was started in order for the wave motion to build up to a steady state condition.

The highest  $C_F$  -- 4.9 -- was found at  $T_n/T = 1.06$  with 40 percent fill depth,  $\phi_a = 7.5$  degrees. All  $C_F$  values in the vicinity of resonance were impact type, the impact force being directed upward as the water surface rising from below hit member FS-1.

The magnitude of impact sloshing forces developed on this test group were in excess of that for which the instrumentation was normally adjusted, and it was necessary to reduce the gain of the signal amplifier to 1/4 of the normal setting used on other test groups in order to prevent the recorded force going off scale.

A reflection of the rising wave surface at the side of the tank occurred as the wave contacted the horizontal shelf below the top corner tanks. This caused a secondary wave across the free surface of the tank and is believed to be the reason that  $C_F$  for  $\phi_a = 29.5$  degrees with 65 percent fill depth at  $T_n/T = 0.88$  is less than half  $C_F$  for 15 degrees, other parameters unchanged. That is, at the higher amplitude of roll, the secondary wave was sufficient to reduce the sloshing force on the member below that measured with  $\phi_a = 15$  degrees. Although no pressure measurements were made, it is clear that high pressures were developed at these times on the horizontal shelf and nearby shell surfaces.

Removal of the three longitudinals on one side of the tank had little effect on the sloshing forces experienced by member FS-1 on the other side.

## J. Test Group XII, Effect of Tank Location

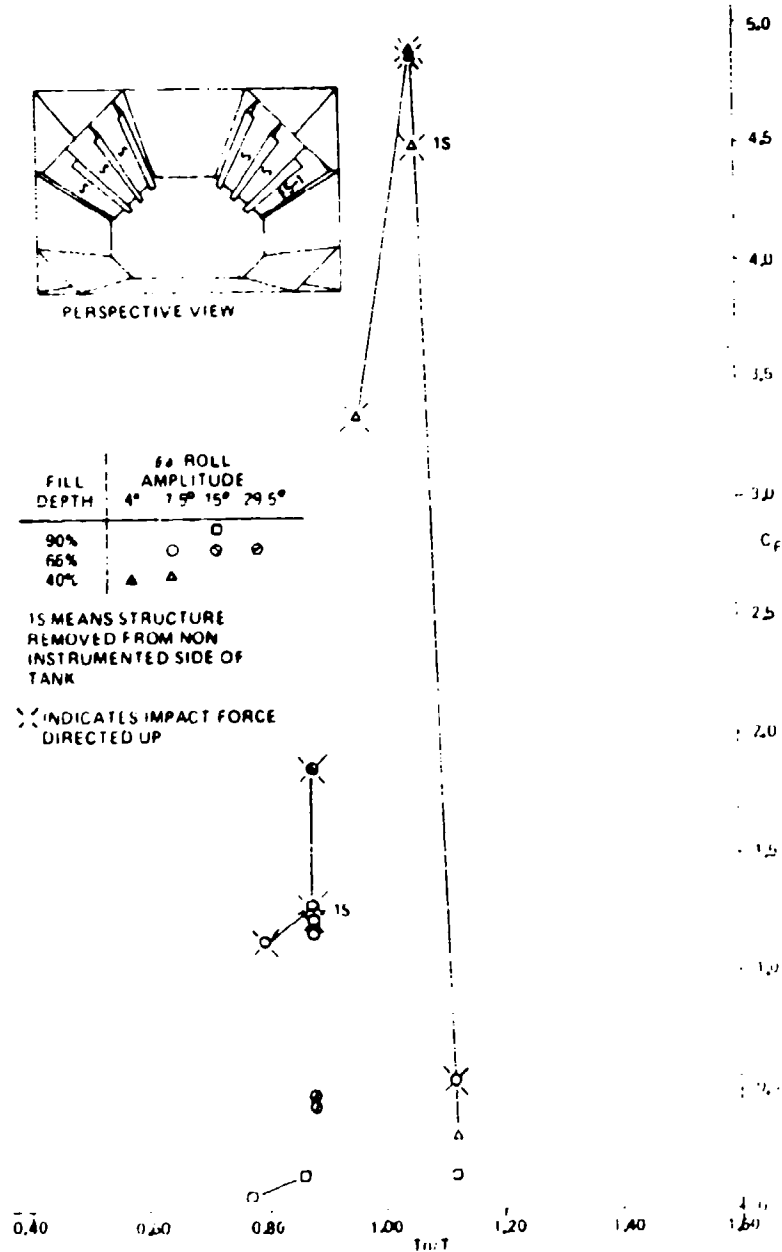
Figure 31 compares the sloshing force coefficient  $C_F$  for member FS-4 when the tank is centered at the oscillating table swing axis, and when it is centered 4 feet forward of the axis, as applied in test group XII. Adaptation of the test facility was accomplished by extending the swinging table with a stiffened truss.

Figure 30

TEST GROUP IX

$C_F$  Versus  $T_n/T$

Force Tests, Member FS-1

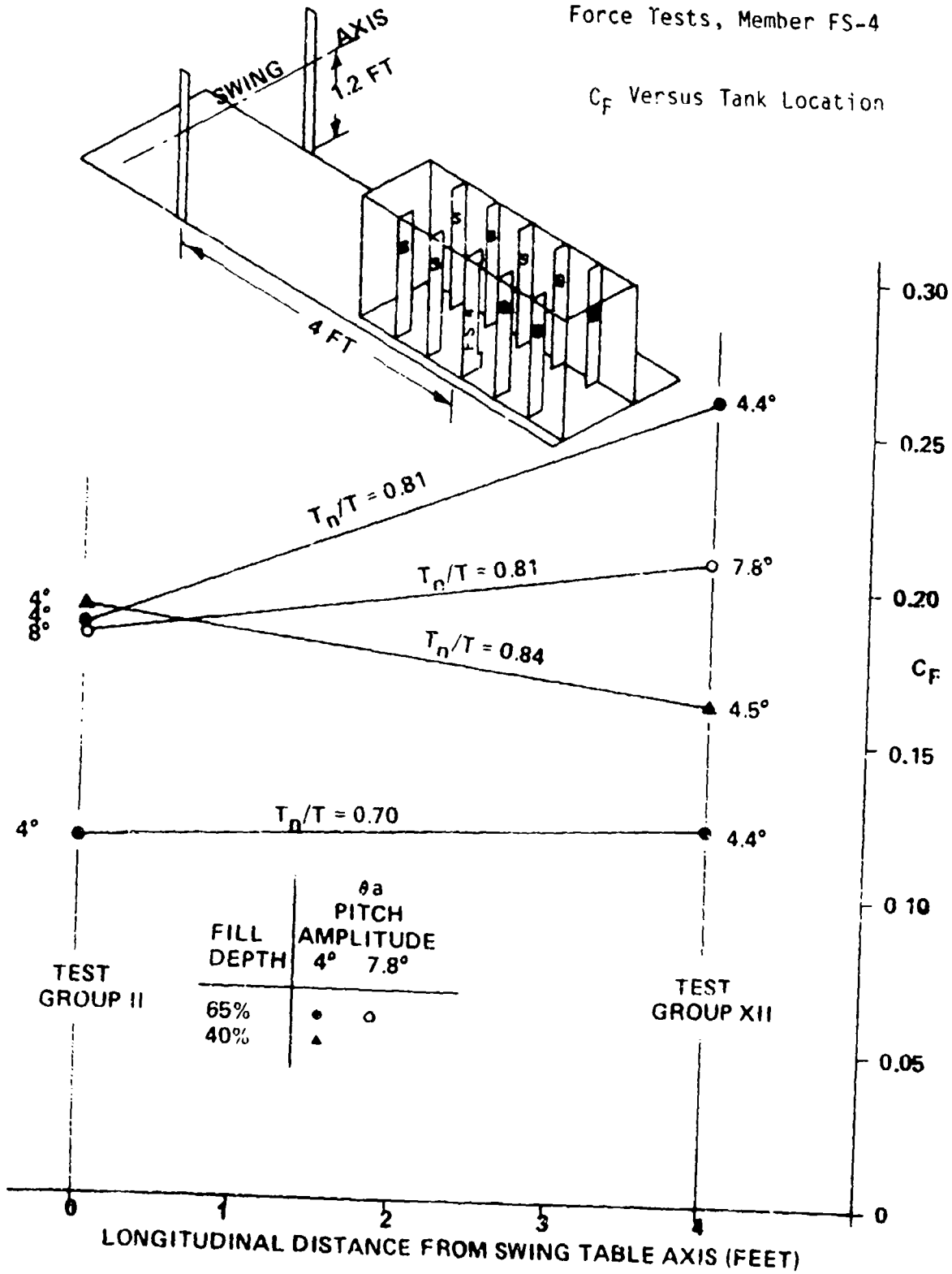


# TEST GROUPS II AND XII

Figure 31

Force Tests, Member FS-4

$C_F$  Versus Tank Location



The end of the extension was counterbalanced by a tensioned spring, rope, pulley arrangement rigged from above and applying an upward force. Although starting this system for a run gave erratic motions, once up to speed it worked satisfactorily and enabled consistent data to be obtained.

Of the four cases for which comparisons may be made, as shown in Figure 31, three showed an increase in sloshing force (maximum increase 40 percent -- average increase 20 percent) while one case, for a 40 percent fill depth and  $T_n/T = 0.84$ , showed a decrease of 15 percent as a result of moving the tank 4 feet off the swing axis.

The period ratios,  $T_n/T$ , used in test group XII corresponded with those in test group II when the tank was centered on the swing axis. These periods appeared to give approximately maximum  $C_F$  in the latter runs.

#### K. Test Groups XIII and XIII A, Effect of Liquid Density and Viscosity

Some liquids carried as bulk shipboard cargoes are significantly different both in density and viscosity from water. Although none of the damage cases found in the Industry Survey had shown damage in tanks carrying liquids other than oil or water, it was considered important to try to find by experiment what effect these variables have on sloshing forces. Accordingly, test group XIII was planned to determine sloshing forces on member FS-4, the centrally located transverse web in a tanker wing tank. Some degree of variation of viscosity was achieved by both icing the water to reduce temperatures to 36-37 degrees Fahrenheit and by using heated water at 86-90 degrees Fahrenheit. Upon the advice of oil well drilling authorities, calcium chloride ( $\text{CaCl}_2$ ) brines were chosen to provide increases in specific gravity.

Calcium chloride as a brine is virtually colorless, easily mixed from dry pellets and could be readily disposed of by ocean dumping in Long Island Sound. When mixing, substantial heat is liberated. Physical characteristics are given in Ref. (6). Viscosity increases with concentration at constant temperature.

In order to keep the brine viscosity in the range of that of water, the first brine was mixed directly in the test tank giving a specific gravity of about 1.3 with a temperature of 140-146 degrees Fahrenheit at the time the test runs were made. The brine was then thinned and additional runs made at a lower temperature. The brine was then temporarily saved.

On cleaning the tank after the  $\text{CaCl}_2$  runs in test group XIII, it was discovered that undissolved  $\text{CaCl}_2$  pellets had hardened in the support housing for the bottom force gage thereby restricting deflection of the force gage cantilever. Since test readings at this gage showed unexpectedly low forces, it was decided to repeat these runs. It was also found necessary to replace the strain gages on the cantilever of this force gage owing to the tenacity of the hardened  $\text{CaCl}_2$ .

Test Group XIII A repeated the prior test conditions with  $\text{CaCl}_2$  brines, except that the brine temperature was now 60 degrees Fahrenheit which substantially increased the viscosity of the liquid.

In the analysis of the test group XIII runs with hot  $\text{CaCl}_2$  brine, it was found that top gage forces were generally proportional to liquid density when compared with comparable runs using water. The kinematic viscosity  $\nu$  of the hot brine was close to that of cold water.

However, the test group XIII A runs showed reduced total force coefficients  $C_F$  compared with water. Figure 32 plots all  $C_F$  values for water and ambient temperature  $\text{CaCl}_2$  obtained in test groups XIII and XIII A. In order to analyze these differences, a tank Reynolds Number,  $R_e$ , was computed for each run, where:

$$\text{Tank } R_e = 2\pi d \theta_a / \nu T,$$

$\nu$  = kinematic viscosity of liquid,

$T$  = period of oscillation,

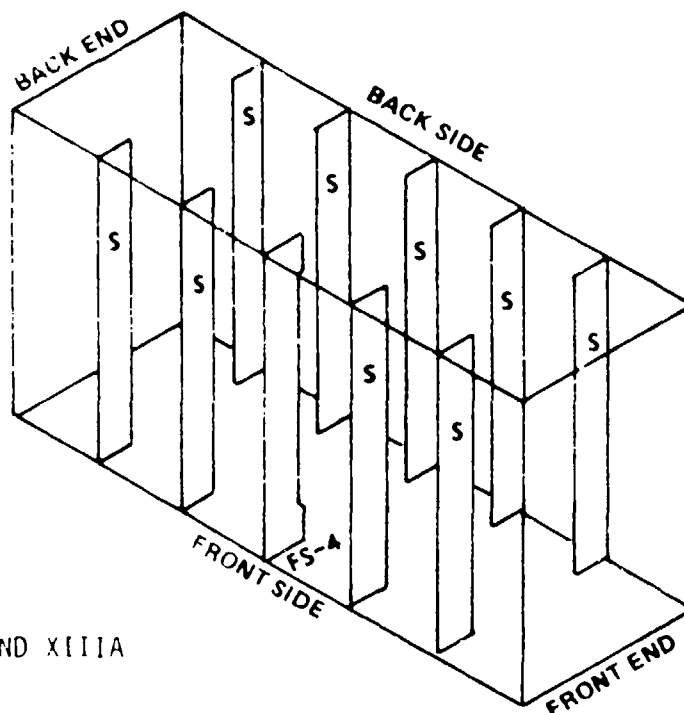
$d$  = minimum dimension of member normal to force.

Other symbols are as previously defined.

Figure 33 plots  $C_F$  versus tank  $R_e$  for the three period ratios  $T_n/T$  available. It is apparent that the level of  $\text{CaCl}_2$  values of  $C_F$  are below those of water. This seeming anomaly may perhaps be explained by the following considerations.

Figure 32

$C_F$  for Different Liquids



TEST GROUPS XIII AND XIII A

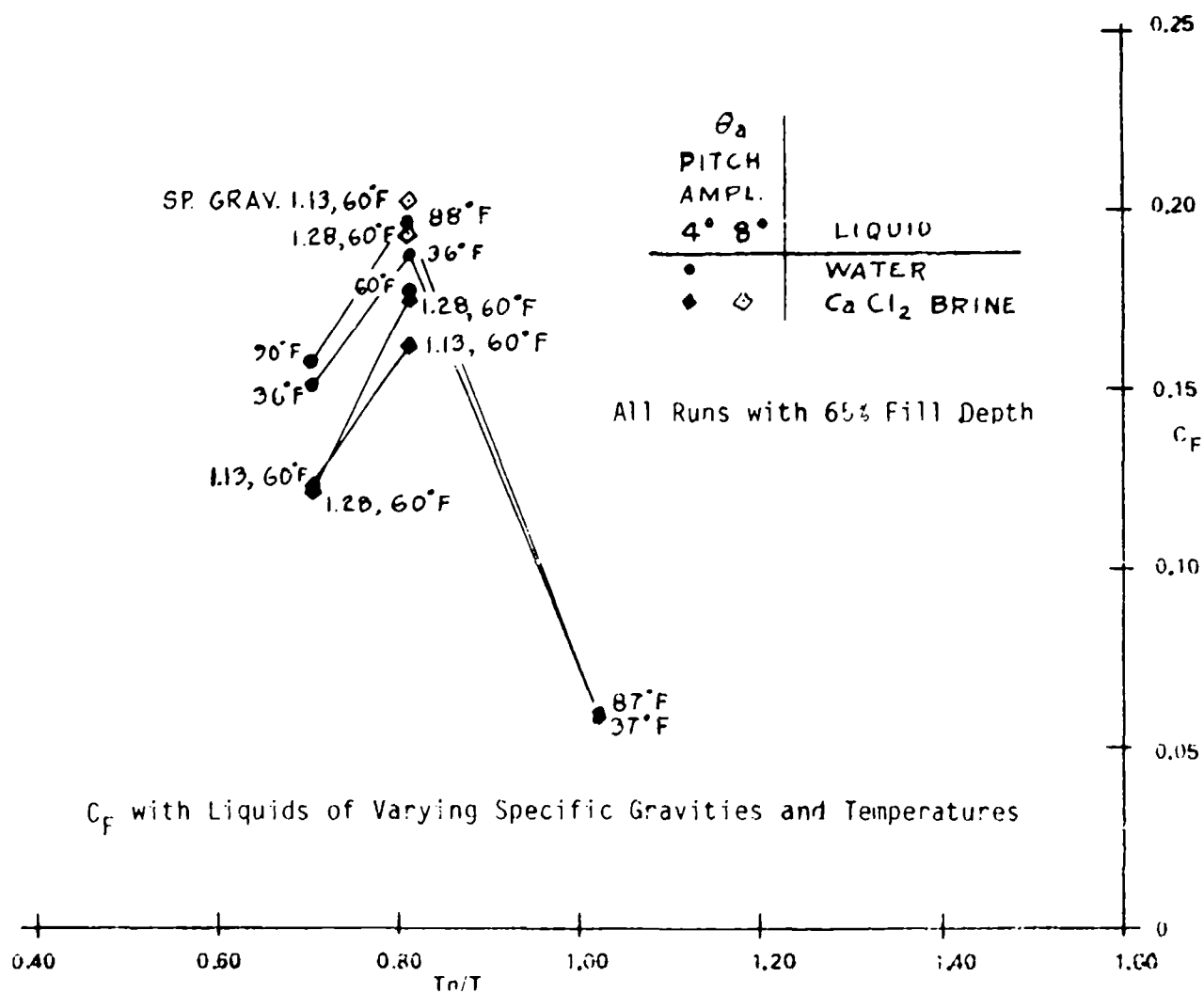
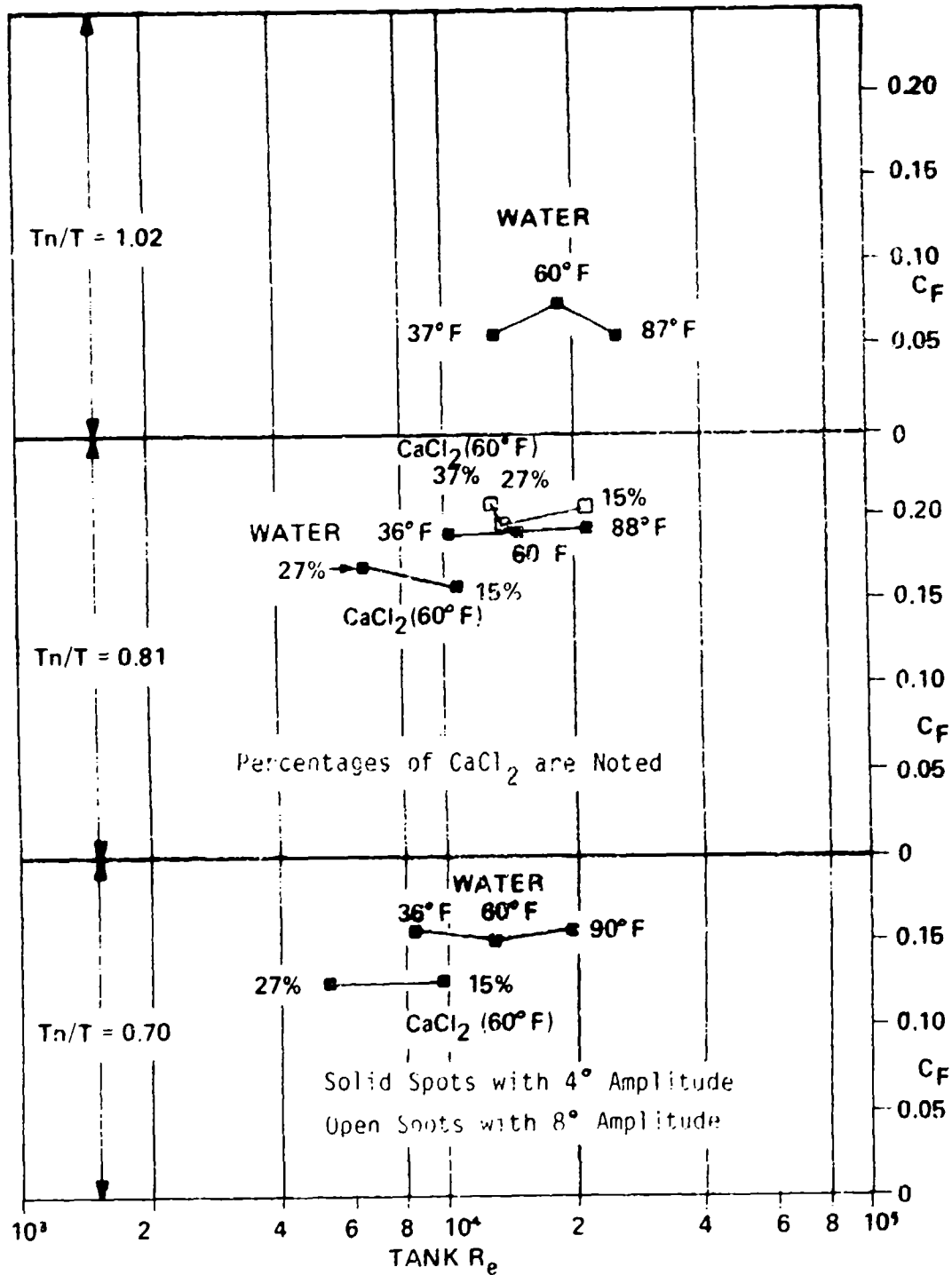


Figure 33

$C_F$  Versus Tank Reynolds Number



Both the sloshing force coefficient  $C_F$  and tank Reynolds Number  $R_e$  are based on the amplitude of motion, and of motion velocity of the tank itself -- not the velocities of liquid in the tank, which are not easily determined and for which a characteristic or representative value may be difficult to define. However, sloshing forces on the member are undoubtedly strongly influenced by the liquid velocities in the tank as the liquid passes the member, which are, in turn, a direct result of wave activity in the tank. Correspondingly, a realistic Reynolds Number ought to be based upon such velocities rather than on tank velocity. It seems likely that the higher viscosity of the  $\text{CaCl}_2$  ambient temperature brines leads to some reduction of wave amplitude in the tank for a given period and amplitude of tank excitation, due to greater frictional drag of the liquid past the tank walls and internal structure. The reduced wave activity would of itself reduce the forces and hence the dimensionless force coefficient  $C_F$  based upon tank amplitude  $\phi_a$ . Therefore, if  $C_F$  were to be based upon liquid velocity, then  $C_F$  for the  $\text{CaCl}_2$  brines would be increased compared with water. In addition, were it possible to base  $R_e$  upon liquid velocity, then the  $\text{CaCl}_2$ ,  $R_e$  would be further reduced compared with water.

Both of the foregoing effects would tend to bring the  $\text{CaCl}_2$  brine values in Figure 33 more in line with those for water.

In general, one cannot conclude that there is any reduction of  $C_F$  with increasing tank  $R_e$  -- say up to ship scale values of the order of  $10^6$  or more for water. If anything, the prior reasoning would indicate some possible increase in  $C_F$  with increasing tank  $R_e$  since both of these parameters are based upon tank motion rather than liquid motion.

As one example of the range of tank  $R_e$  for a ship carrying a liquid cargo (neither water nor petroleum), consider molten sulfur. This commodity is carried in tanks of relatively large size in contrast with many chemical cargoes which tend to be carried in a larger number of smaller tanks. Assume a tank length of 100 ft. and that the ship is pitching with an amplitude of 4 degrees. The kinematic viscosity of molten gas free sulfur at 265 degrees Fahrenheit =  $5.2 \times 10^{-5}$  ft<sup>2</sup>/sec, based on Ref. (8). This temperature is that mentioned in Ref. (9). Assume the width of web frame is 6 ft. and the ship is pitching at a 9 second period.

$$\text{Tank } R_e = 2 \pi \times 100 \times 6 \times 4 / (5.2 \times 10^{-5} \times 9 \times 57.3) = 5.6 \times 10^5 \text{ (molten sulfur)}$$



Since the viscosity of this molten sulfur is about 4.5 times that of water, it is apparent that a comparable tank  $R_e$  for a water ballast cargo, other parameters unchanged, is about

$$\text{Tank } R_e = 2.5 \times 10^6 \text{ (water).}$$

Inspection of Figure 33 will show the degree to which the model test  $C_F$  values must be extrapolated from the model test range to that of the ship when either liquid is being considered.

#### **L. Test Group XV, Combined Pitch and Surge**

The Webb Oscillating Table Facility was designed to be oscillated both in rotation and translation; hydraulic actuators and servo valves were procured to accomplish this. However, for test group XV, the hydraulic rotary actuator was not used, satisfactory operation being obtainable from the mechanically driven eccentric, connecting rod system. Rotation of the speed reducer output shaft connected to a rotating potentiometer provided a command signal to the hydraulic translation (surge) actuator and assured that the two motions were of identical period. The translation feedback potentiometer, geared to the carriage, provided a sine wave signal for comparison with the command signal and also gave a record of carriage position.

The test group XV runs were made using a longer period of oscillation than used for other test groups with instrumented member FS-4, in recognition of there having been few reported problems from surging in the past, but evidence of pronounced surging on some ships only in relatively long waves from astern [Ref. (10)]. Correspondingly, a fill depth of 40 percent was chosen in order to lengthen the natural surging period  $T_n$ . A 3 inch surge amplitude was chosen in association with 6 degrees of pitch amplitude; these separate motions were expected to give the same order of magnitude of sloshing wave force on the member. Runs were made with the surge and pitch motions in phase, 180 degrees out of phase and with surge to pitch phase angles of +90 degrees and -90 degrees. Phase conventions adopted are as follows:

Zero degrees pitch phase is with the forward end of the tank down

Zero degrees surge phase is with the carriage fully forward

A positive surge to pitch phase angle indicates that maximum surge is experienced earlier in time in the motion cycle than maximum pitch.

The pitch motion when in phase and 180 degrees out of phase was approximately sinusoidal as were the pitch motions with no surge present, it being recognized that rotational motion induced by a crank, connecting rod mechanism is only an approximate sinusoid. In the case of runs with pitch motion  $\pm 90$  degrees out of phase with surge, the kinematics of the mechanism lead to noticeable aberrations in the pitch motion cycle. However, the measured forces on the instrumented member do not appear to be significantly distorted, as shown by Figure 34, which shows graphs of the time history of sloshing force after deduction of tares.

Figure 35 shows the sloshing force coefficients for test group XV plotted against phase angle.

Runs were also made with the tank oscillating in surge and pitch separately. Figure 36 shows the sloshing force time history curves for these two runs as graphed by the computer after subtraction of dynamic tares (mean of three force gages). The surge force trace is slightly distorted because of a tendency for the carriage to vibrate at the back end of the stroke. This is believed to result from slight lost motion in the feedback circuit. The surge feedback signal wave, set to maximum at the forward end of the stroke, is included. The microswitch signal, in the case of pitch, with the forward end of the tank down, is also included.

The availability of separate surge and pitch sloshing force signals enables these signals to be combined in the computer, taking account of phase, in order to synthesize a combined surge plus pitch force for the four cases for which the combined forces were measured. Figure 37, 38, 39 and 40 compare the synthesized combined forces with the measured combined forces.

It is seen that the shapes of the comparable signals are quite similar. The poorest comparison is in the case of 180 degrees phase difference when both synthesized and measured signals are relatively small, Figure 38. In the case of in phase and  $\pm 90$  degrees out of phase force, the synthesized force amplitudes are of the order of 20 percent less than those measured.

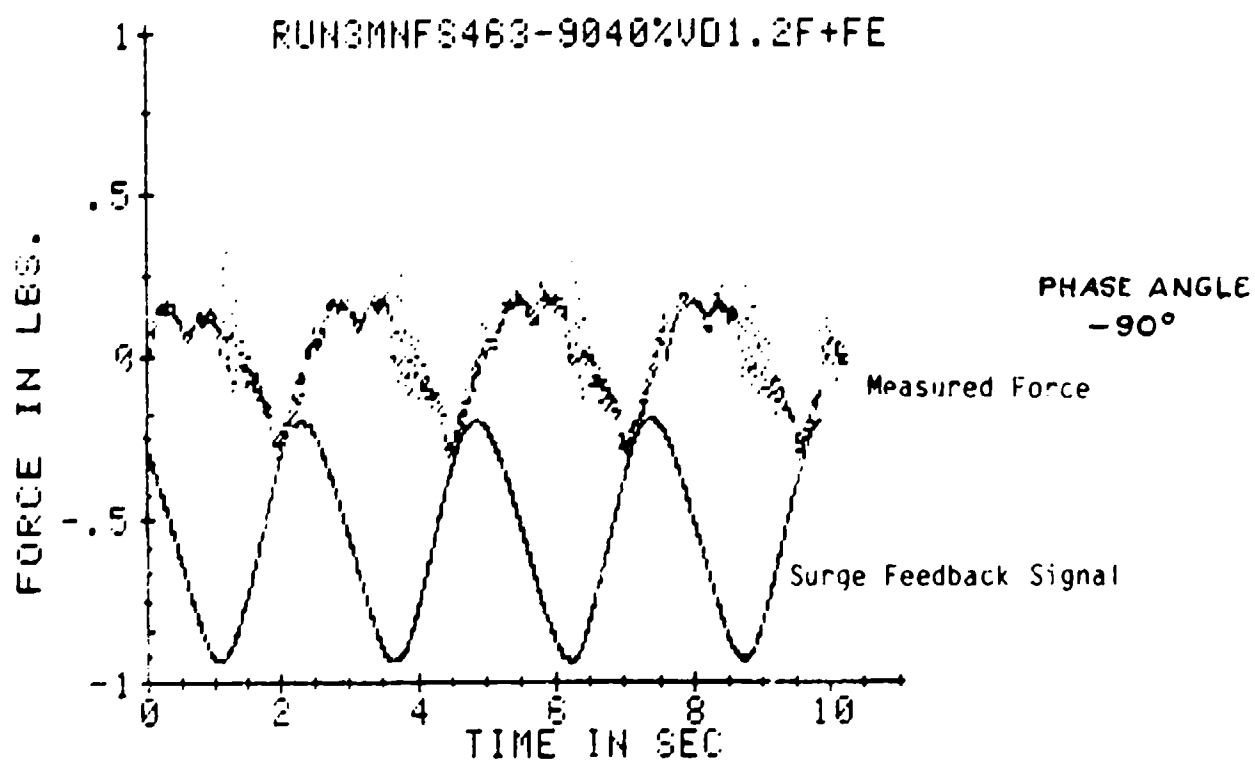
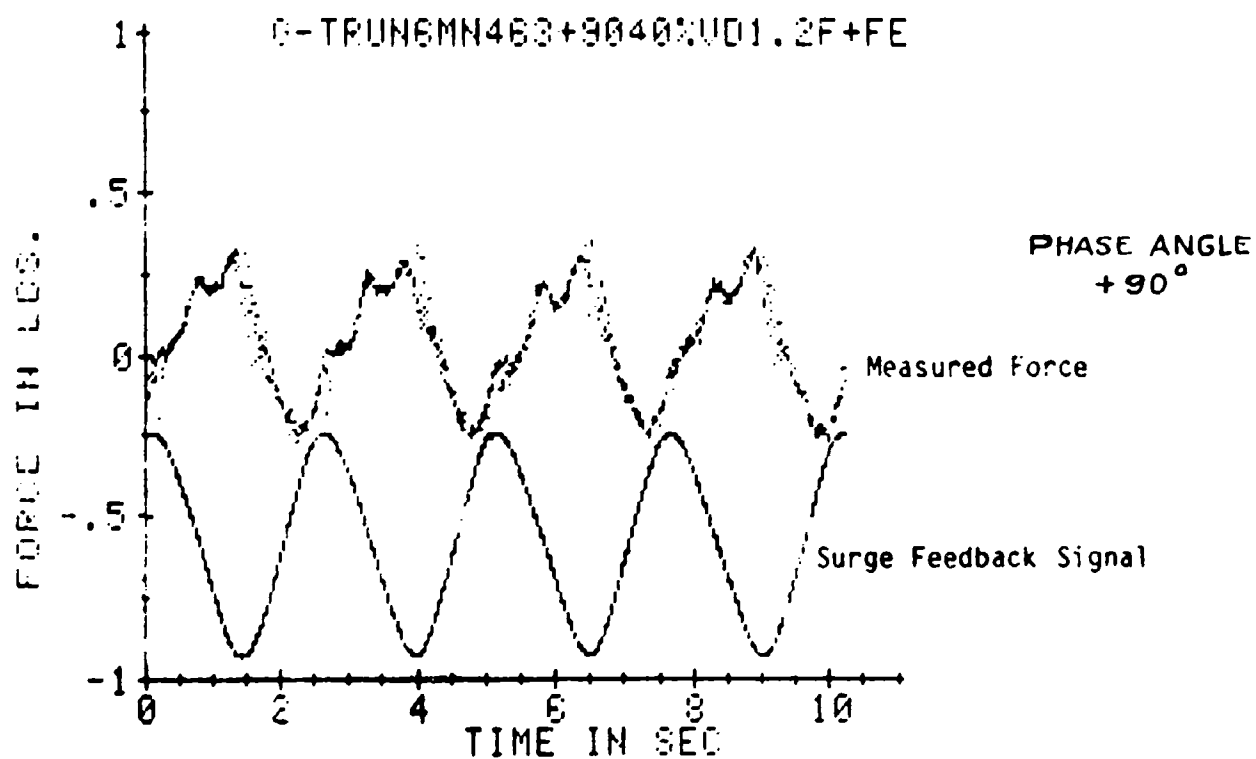
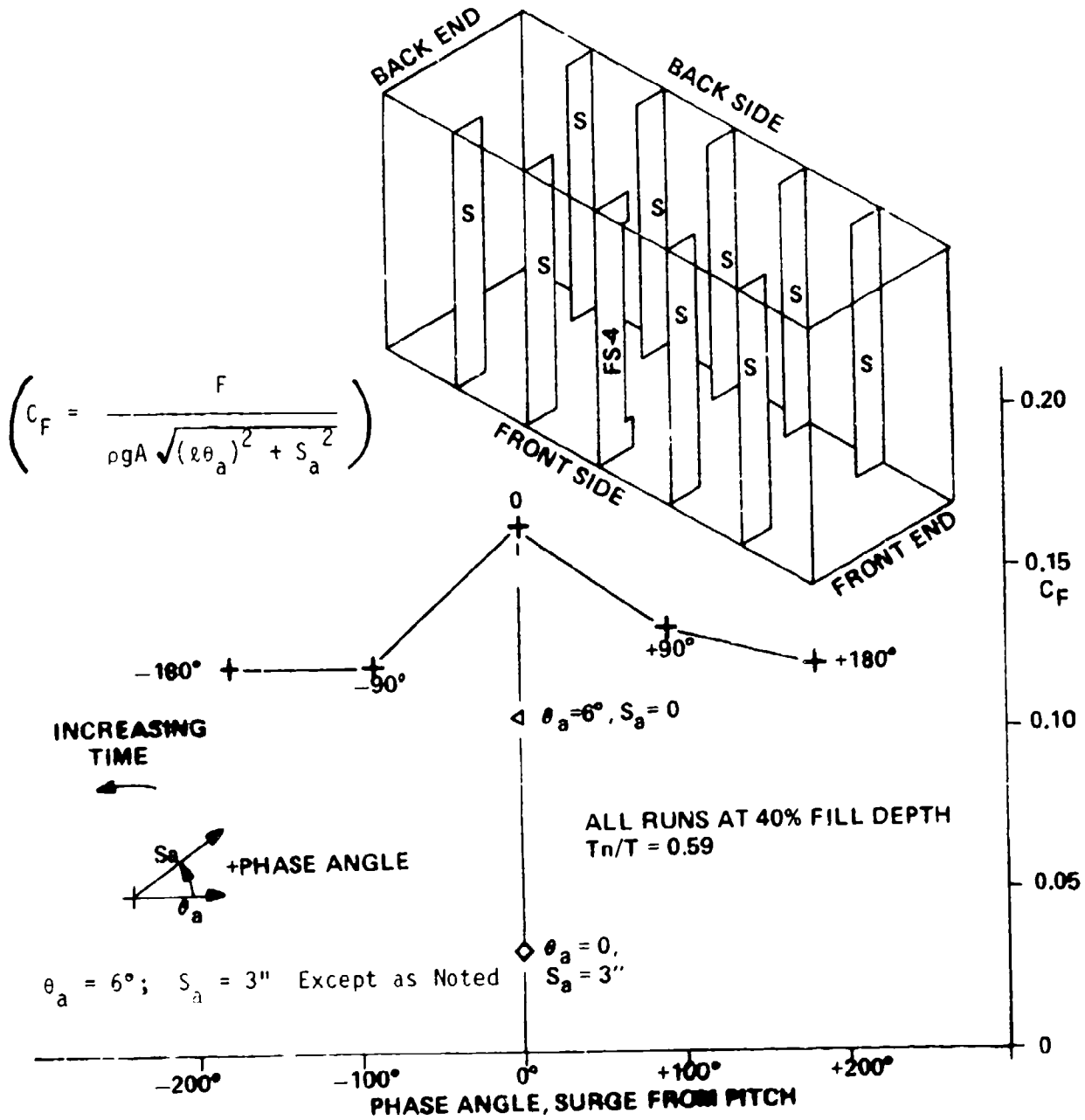


Figure 34 Time History, Mean Gross Minus Tare Sloshing Force, Combined Pitch and Surge, +90 Degrees and -90 Degrees Phase Angles

# TEST GROUP XV

Figure 35  $C_F$  for All Angles, Combined Pitch and Surge, Test Group XV

Force Tests, Member FS-4



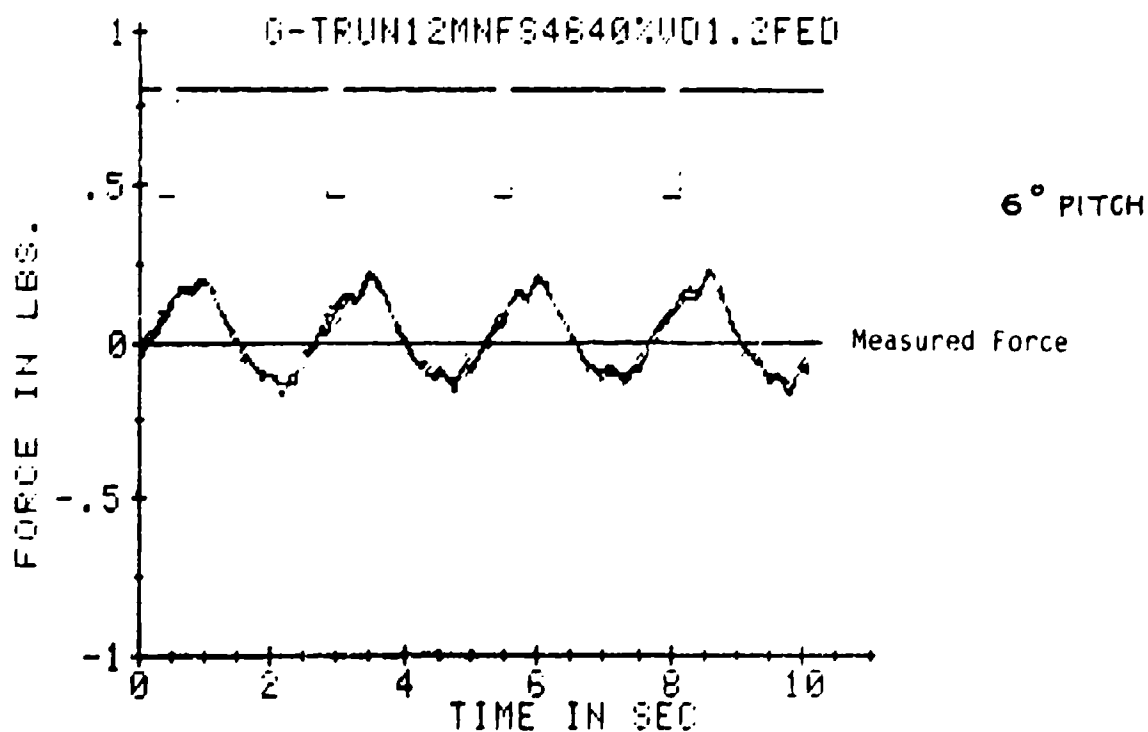
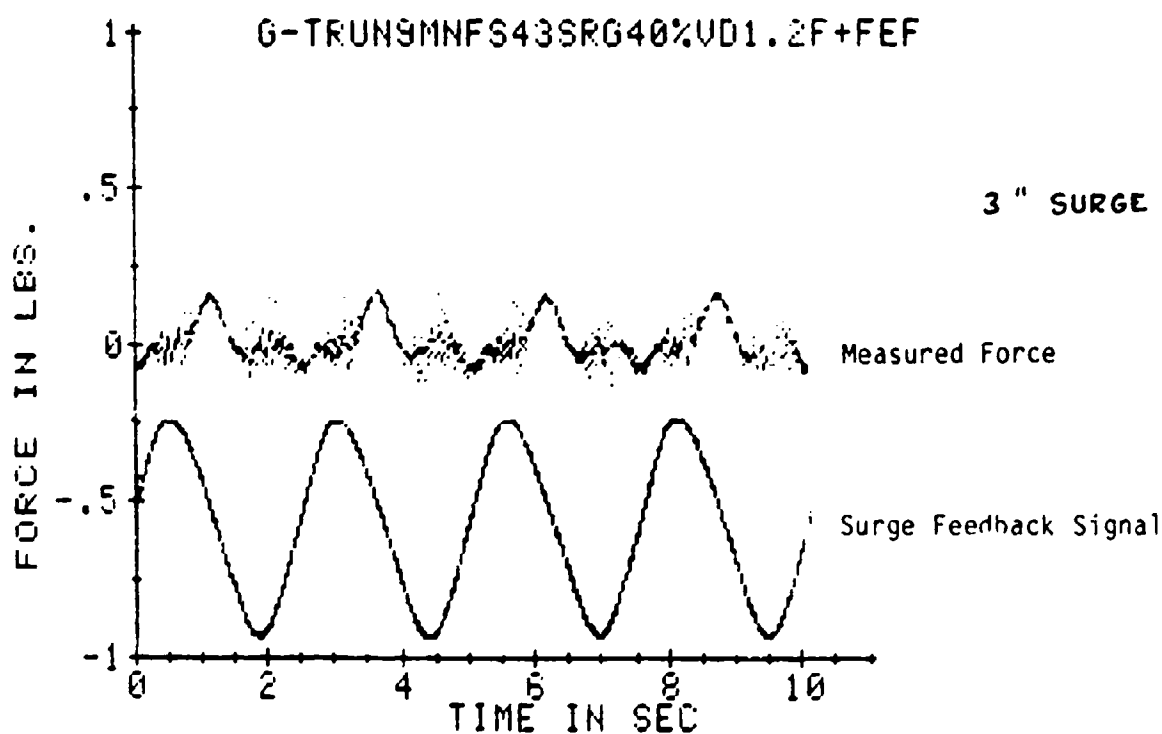


Figure 36 Time History, Mean Gross Minus Tare Sloshing Force, Separate Surge and Pitch

# COMB PITCH AND SURGE RUNS

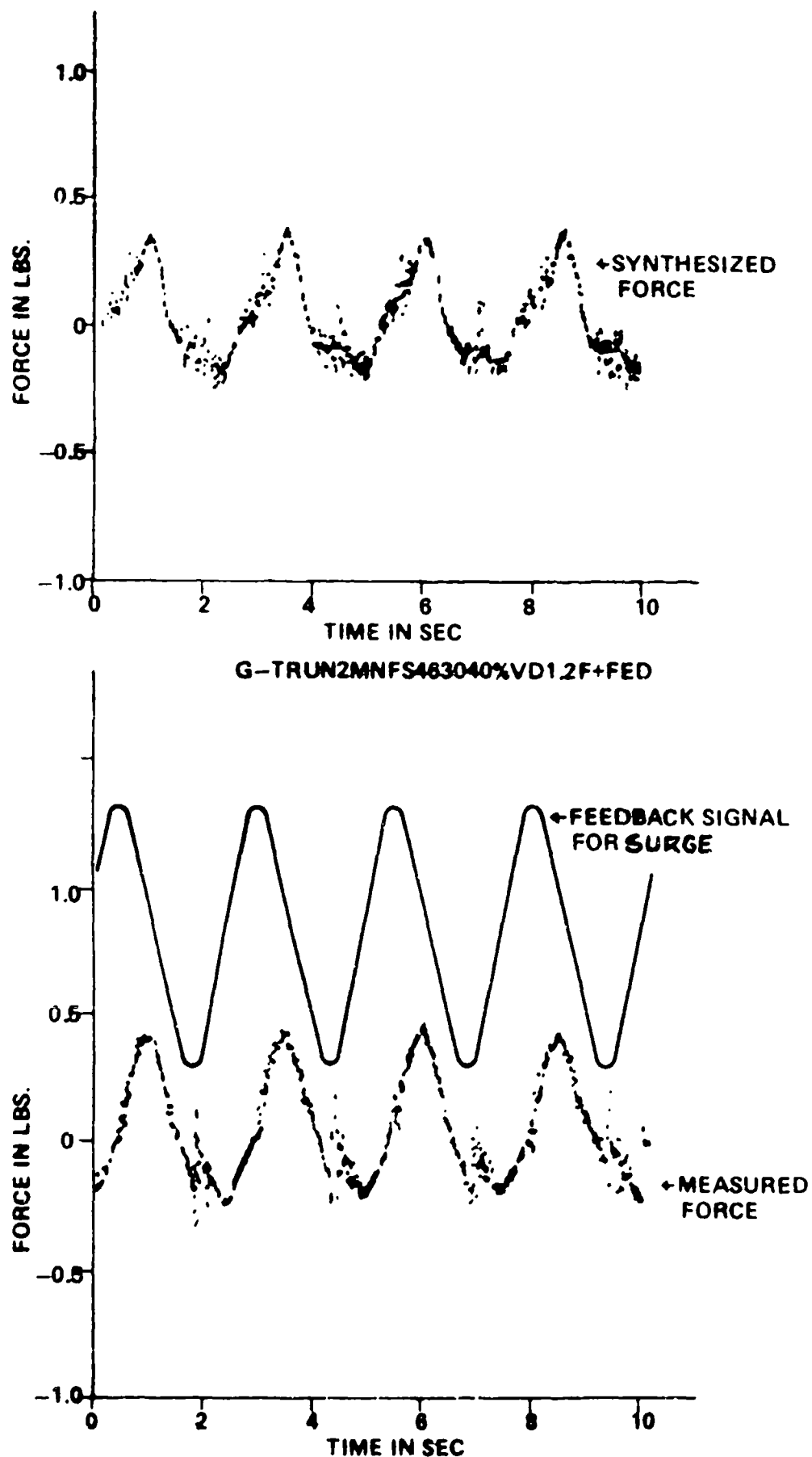


Figure 37 Time History, Mean Gross Minus Tare Sloshing Force, Surge and Pitch in Phase, Synthesized and Measured

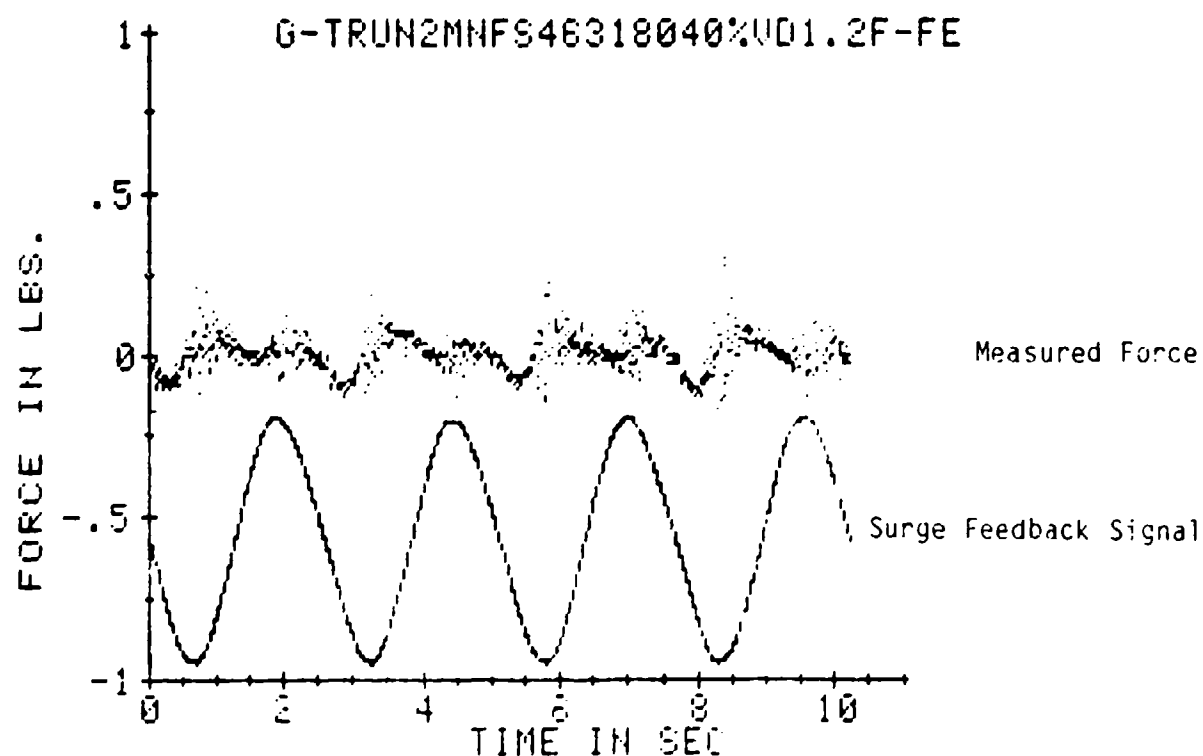
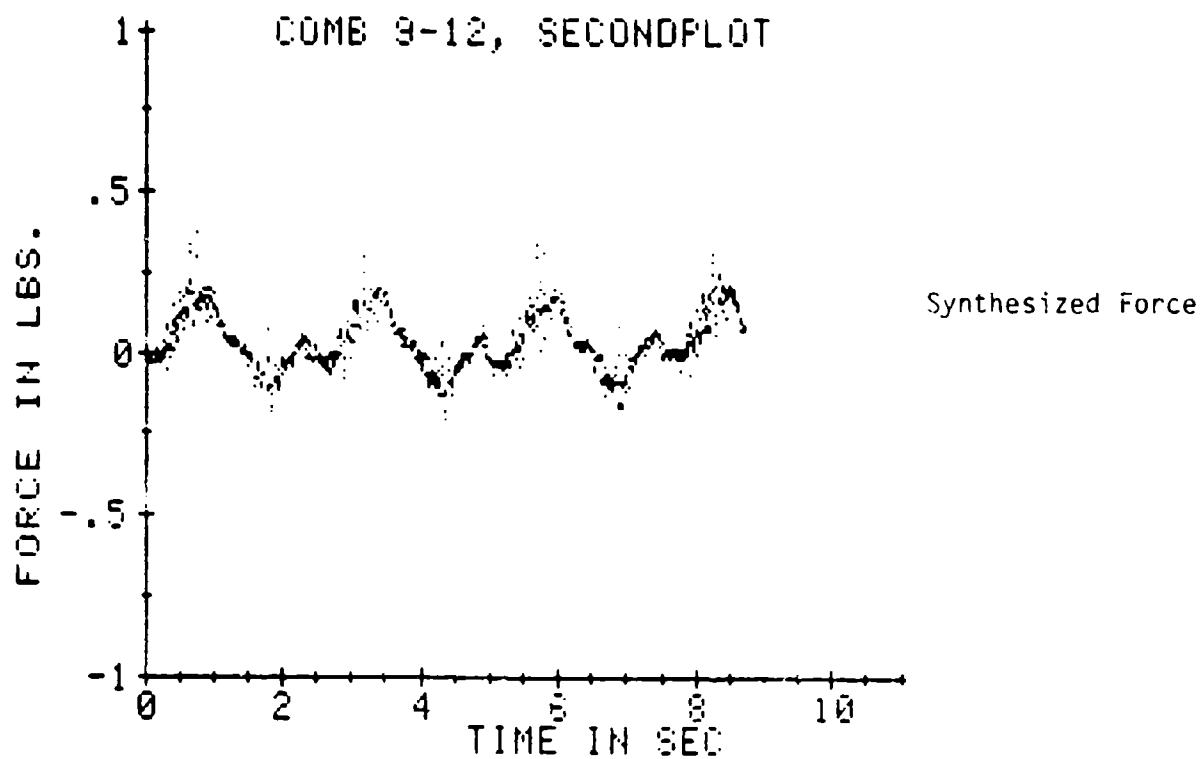


Figure 38 Time History, Mean Gross Minus Tare Sloshing Force, 180 Degrees Phase Angle,  
Synthesized and Measured Surge Plus Pitch

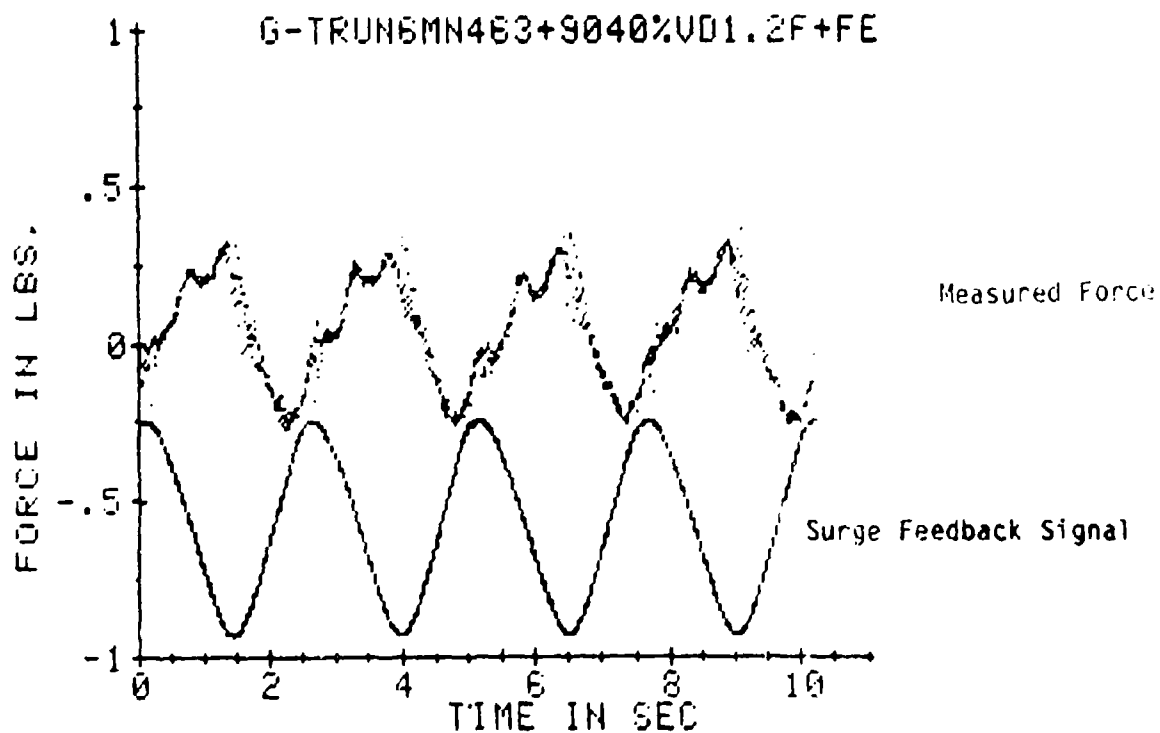
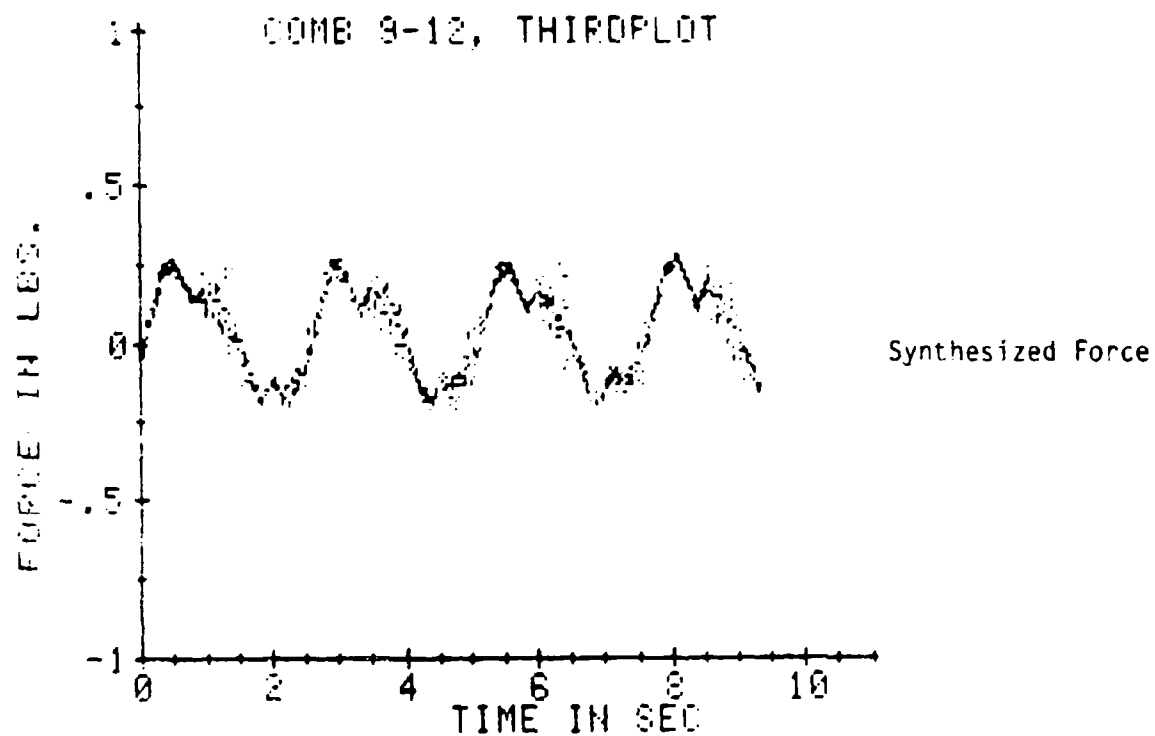


Figure 39 Time History, Mean Gross Minus Tare Sloshing Force, +90 Degrees Phase Angle, Synthesized and Measured Surge Plus Pitch



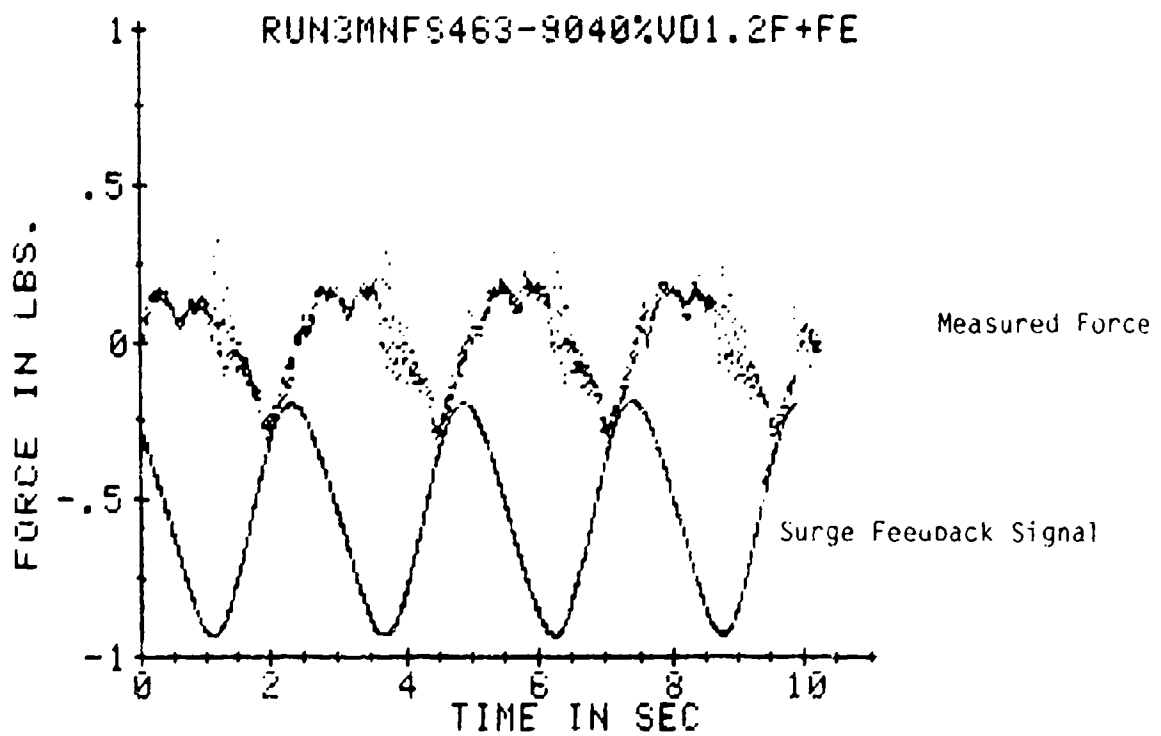
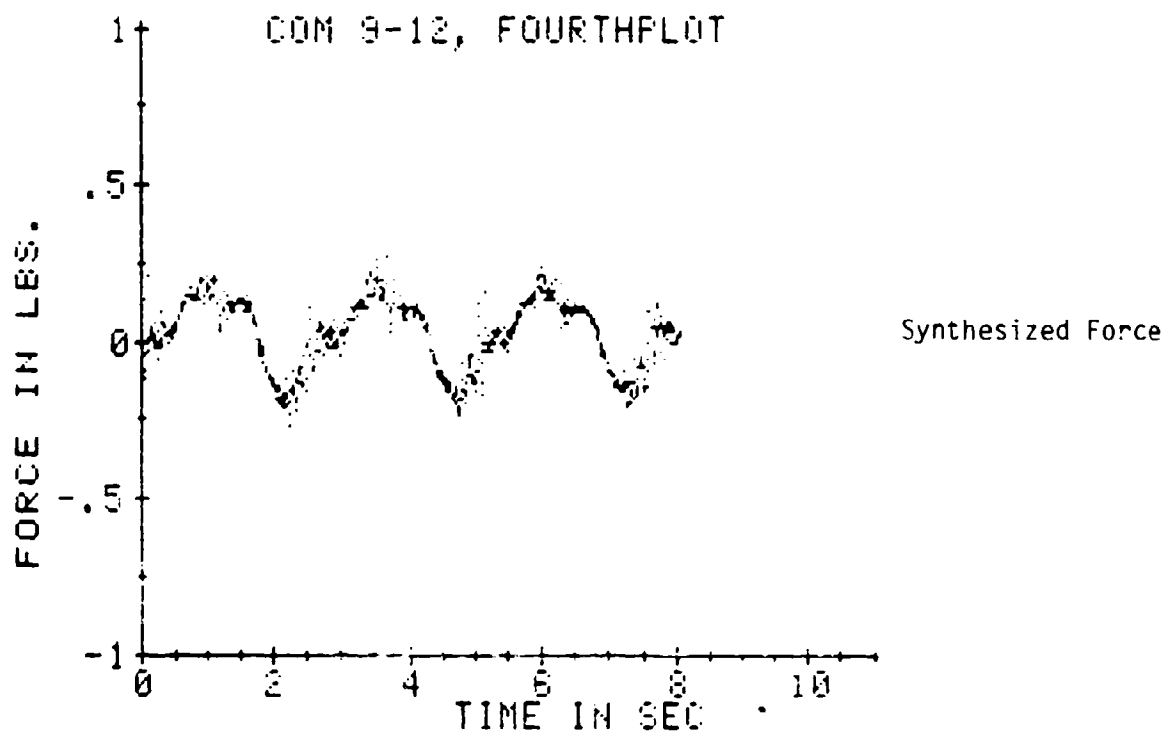


Figure 40 Time History, Mean Gross Minus Tare Sloshing Force, -90 Degrees Phase Angle, Synthesized and Measured Surge Plus Pitch

This may be a useful finding inasmuch as testing effort can be saved in the future if one can combine by computer the separately measured forces from surge and pitch respectively at the appropriate phase angles rather than having to run many cases of combined motions at a series of phase angles to suit the particular motion characteristics of the ship and tank in question.

#### M. Linearity of Measured Forces and Pressures

The force, moment and pressure coefficients  $C_F$ ,  $C_M$  and  $C_p$  all contain the amplitude of the exciting pitch, roll or surge motions,  $\theta_a$ ,  $\phi_a$ ,  $S_a$  in the denominator, it being assumed the measured quantities would tend to be linear with excitation.

In a number of instances, the tests were run with two excitations, typically  $\theta_a = 4$  degrees and 8 degrees, thereby allowing linearity to be checked. Figures 41 and 42 show the coefficients plotted against excitation amplitudes for cases when no other conditions were changed. The  $C_F$  and  $C_M$  plots on Figure 41 indicate a general trend toward linearity, but a slight reduction in the coefficient with increasing excitation in many cases. The  $C_p$  plots on Figure 42 show a more pronounced drop with increasing amplitude, the average reduction in  $C_p$  being 25 percent for a 100 percent increase in  $\theta_a$ .

Figure 41 Linearity of  $C_F$  and  $C_M$  with Oscillating Amplitude

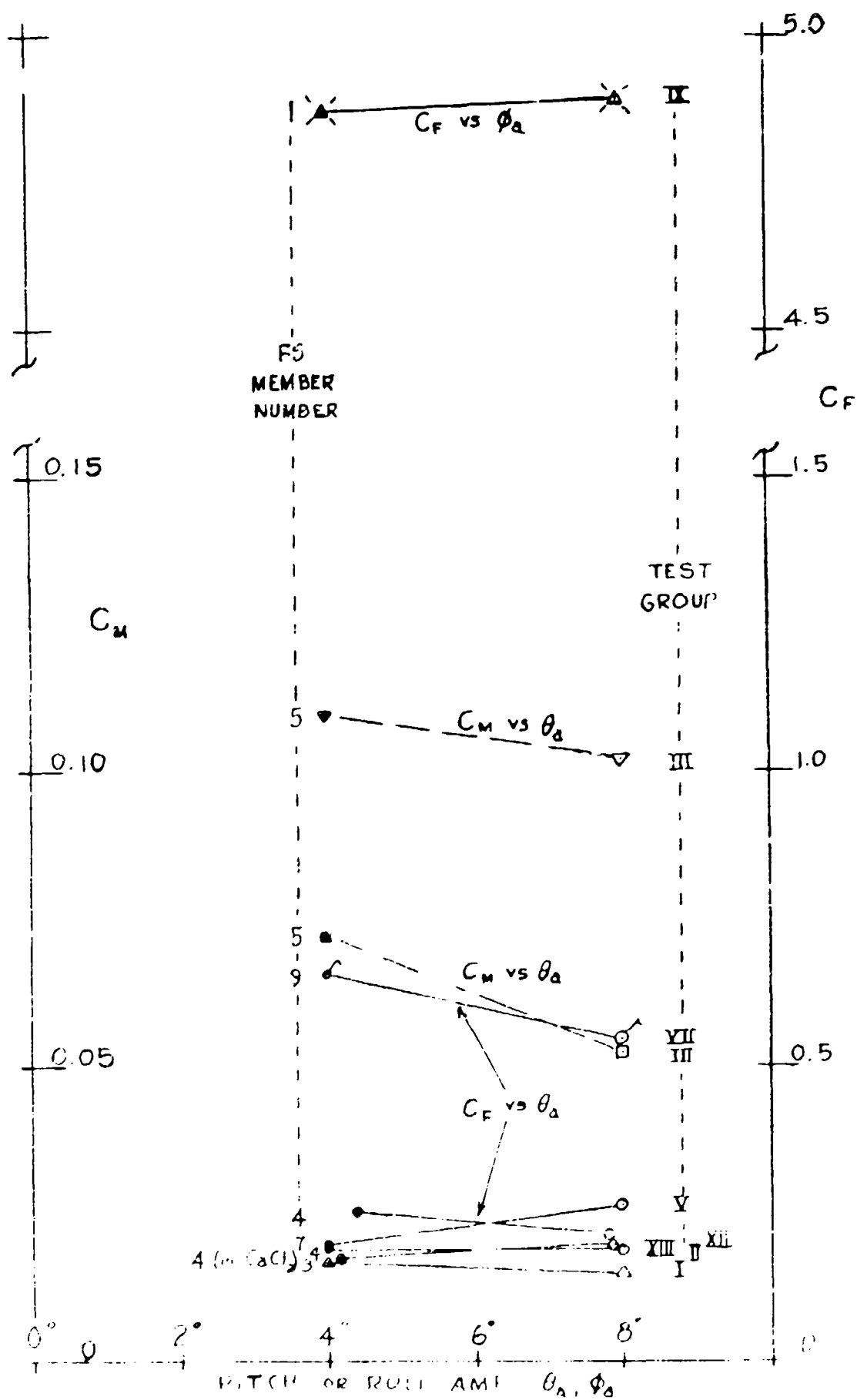
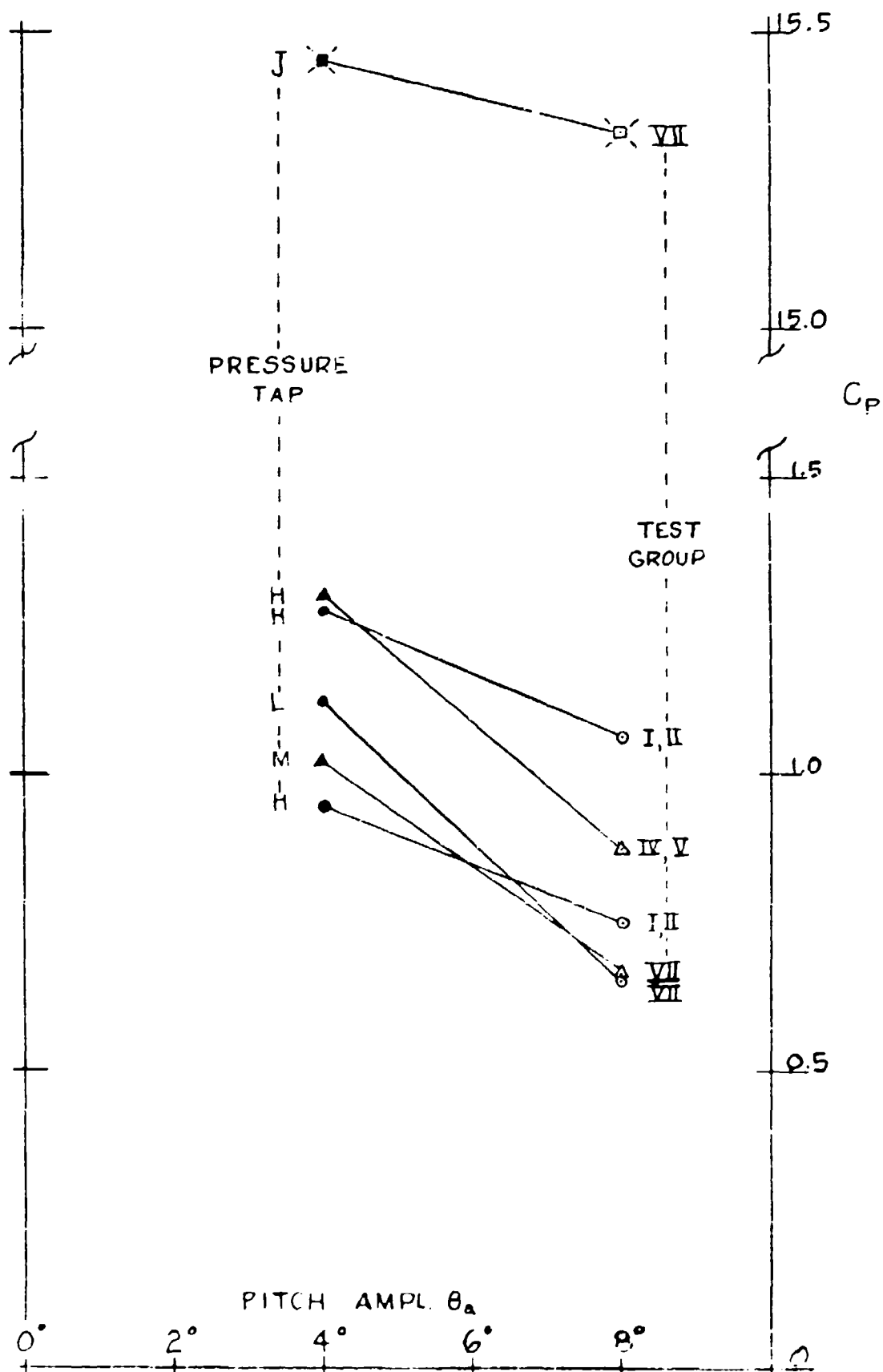


Figure 42 Linearity of  $C_p$  with Oscillating Amplitude



## XII. EXPERIMENTAL FORCES VERSUS THEORY

Dr. Jack Lou at Texas A&M University, in earlier and companion projects [Refs. (7), (12)], has developed theoretical methods of calculating by computer oscillating forces in a sloshing tank for idealized input parameters. As part of test group VII with a swash bulkhead at the middle of a tanker center tank, a run was made to confirm this calculation procedure. The end girders were removed from the tank and the face plate removed from the swash bulkhead, instrumented member FS-9. Thus, there was then no other structure in the tank. Experimentally measured  $C_F$  for this run -- made at 40 percent fill depth and with a pitch amplitude of 11.4 degrees,  $T_n/T = 0.47$  -- is shown as the starred spot on Figure 26.

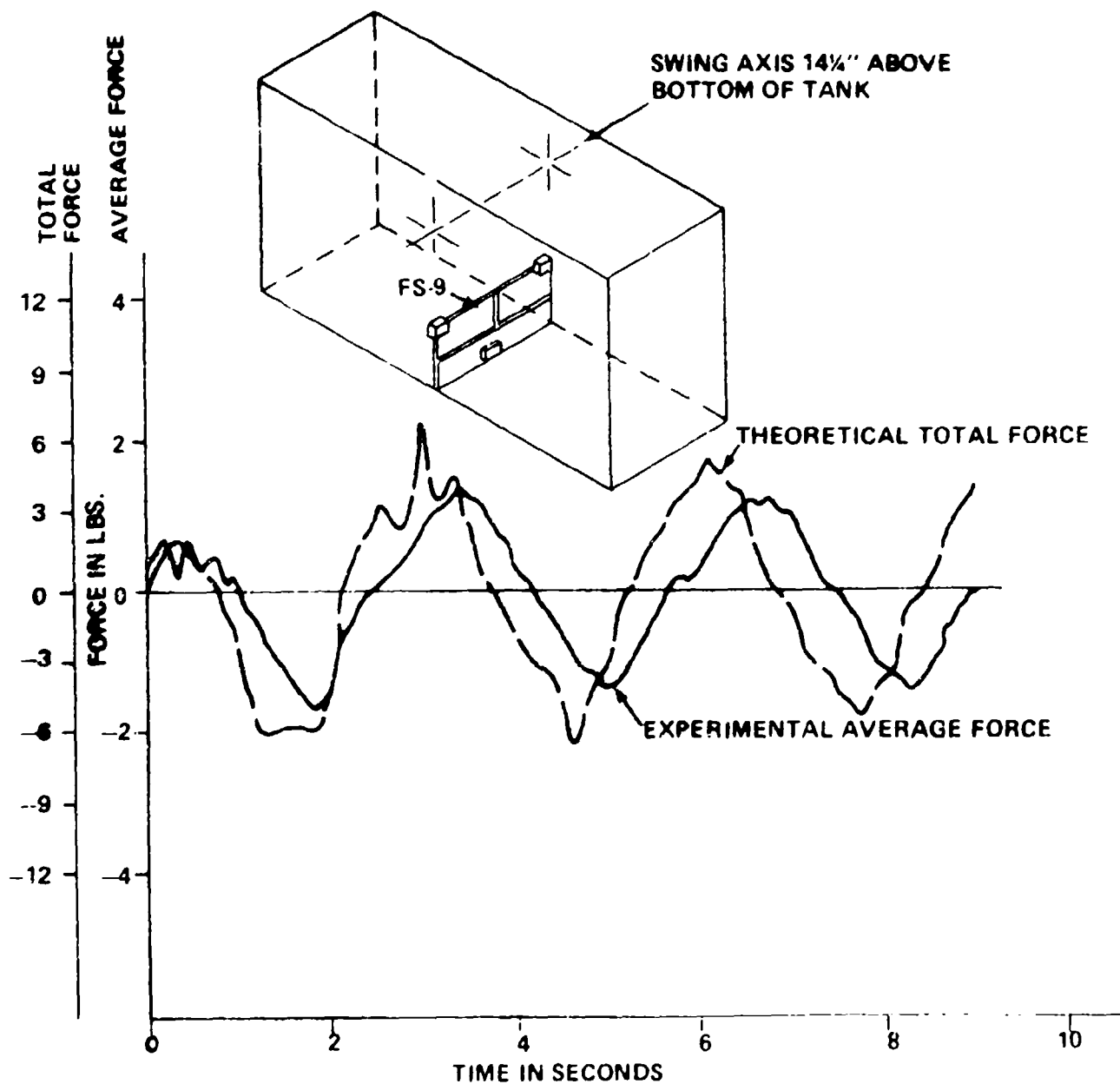
The theoretical calculations included a time history from when the tank first began to oscillate. The experiment, therefore, was arranged to record forces on the member as the tank was started and for the first 10 seconds thereafter. Figure 43 compares the two time histories, experimental and theoretical. The relatively later experimental force peaks compared with theory is the result of some lack of precision of the Vari Drive control and probably also some slippage of drive belts and inertia in moving parts as the test tank is started. It is seen that the experimental force time history is in good qualitative agreement with the theoretical record but the peak theoretical forces are about 25 percent higher than those measured. This difference may well be partly the result of three-dimensional effects and of some small flows which inevitably take place through the clearances provided between the instrumented experimental member and the tank walls -- about 1/8 inch on sides and bottom and more in the corners to accommodate the two space frames for attaching other structural members, which were not in place.

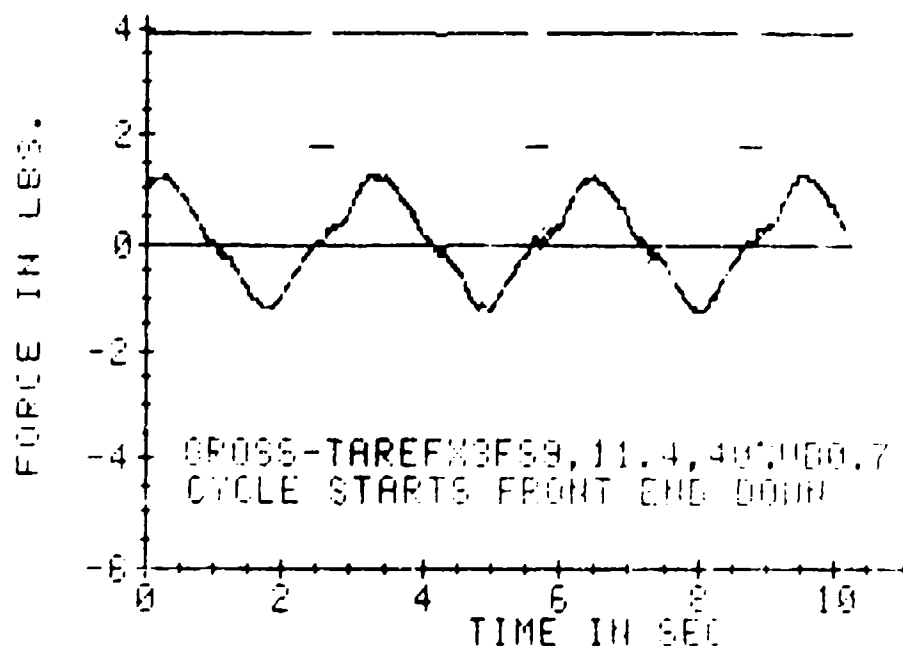
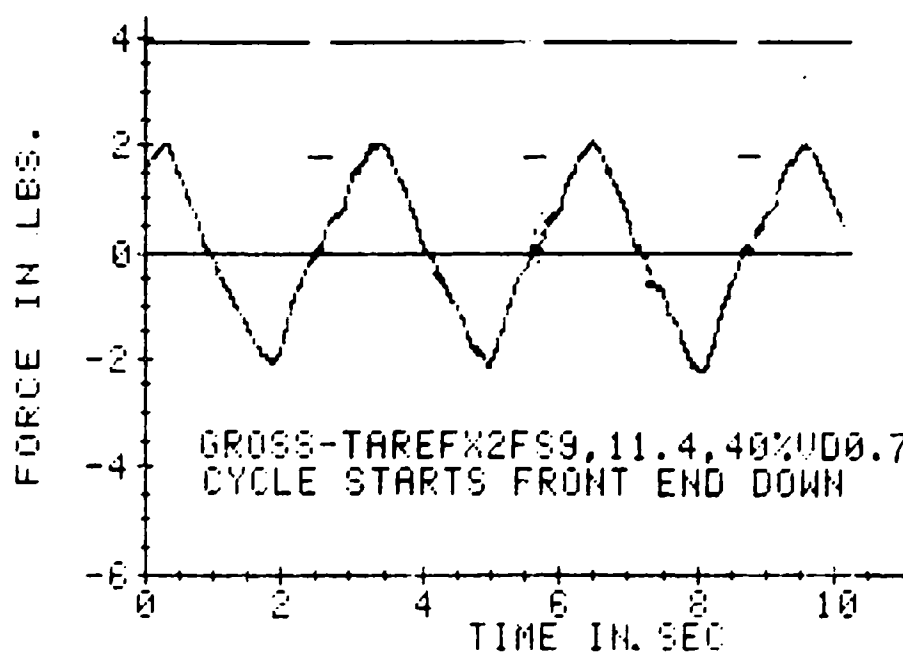
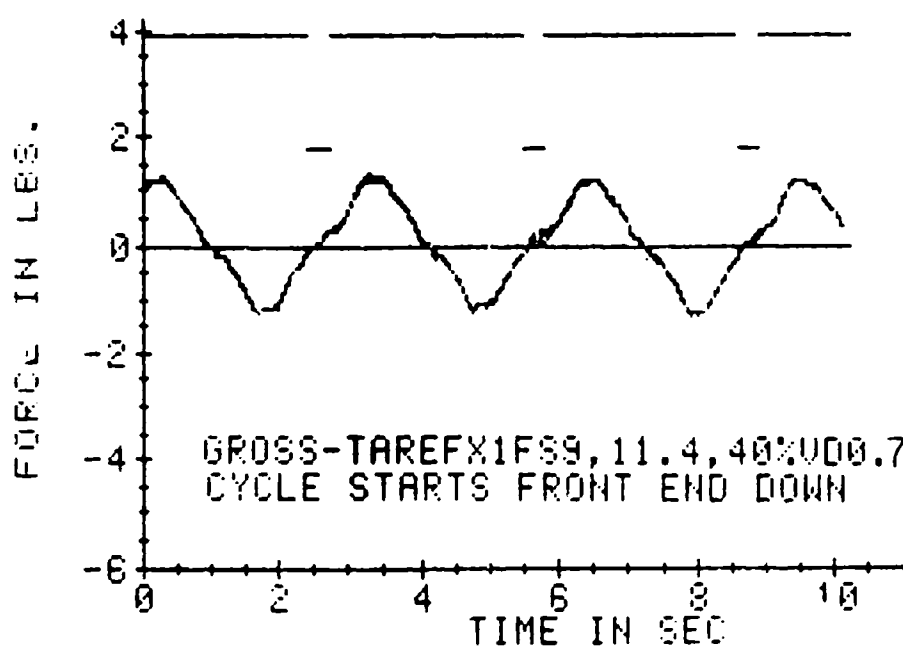
Figure 44 shows the gross minus tare forces recorded the three force gages as time histories after a steady state condition was achieved.

Figure 43

Time History of Theoretical and Measured Sloshing Force

GROSS-TARE, AUG. F88, 11.4, 40%VD0.7





Steady State Sloshing  
Forces at Three Ages

Member FS-9

Figure 44

Figure 44 Time History of Gross Minus Tare Sloshing Force

### XIII. APPLICATION TO DESIGN

In order to estimate full scale loads on a specific member in a specific tank of a specific ship, one must account for a number of factors. First are the ship variables including the draft and speed of the ship. Then, there are the environmental variables, that is, the seaway to be encountered (significant ocean wave height and period), whether the seaway is long crested or short crested (waves coming from a single direction or several directions), the ship to wave heading, and the shape of the wave spectrum curve. Finally, there are the tank variables, tank size and location on the ship including fill depth, density of liquid, other structural members in the tank and (perhaps) viscosity of liquid and presence of gas above the liquid.

The linear superposition example calculation below accounts for these effects and assumes the ship tank is geometrically similar to the model tanker wing tank for test group II. The following particulars are assumed:

Ship: Series 60 parent type,  $C_B = 0.75$ ,  $L = 720$  ft., Draft = 42.7 ft., Displacement = 70,300 tons, S.W. -- appropriate to a 50,000 DWT tanker.

Speed 13.5 knots;  $F_{\lambda} = 0.10$ .

Tank: Wing tank 102 ft. long, 54 ft. in depth with same proportions as model tank; scale factor ship to model = 34.

5 transverse webs on each side of tank of depth 6.7 ft., no other structure in tank. We seek the sloshing force on the middle web.

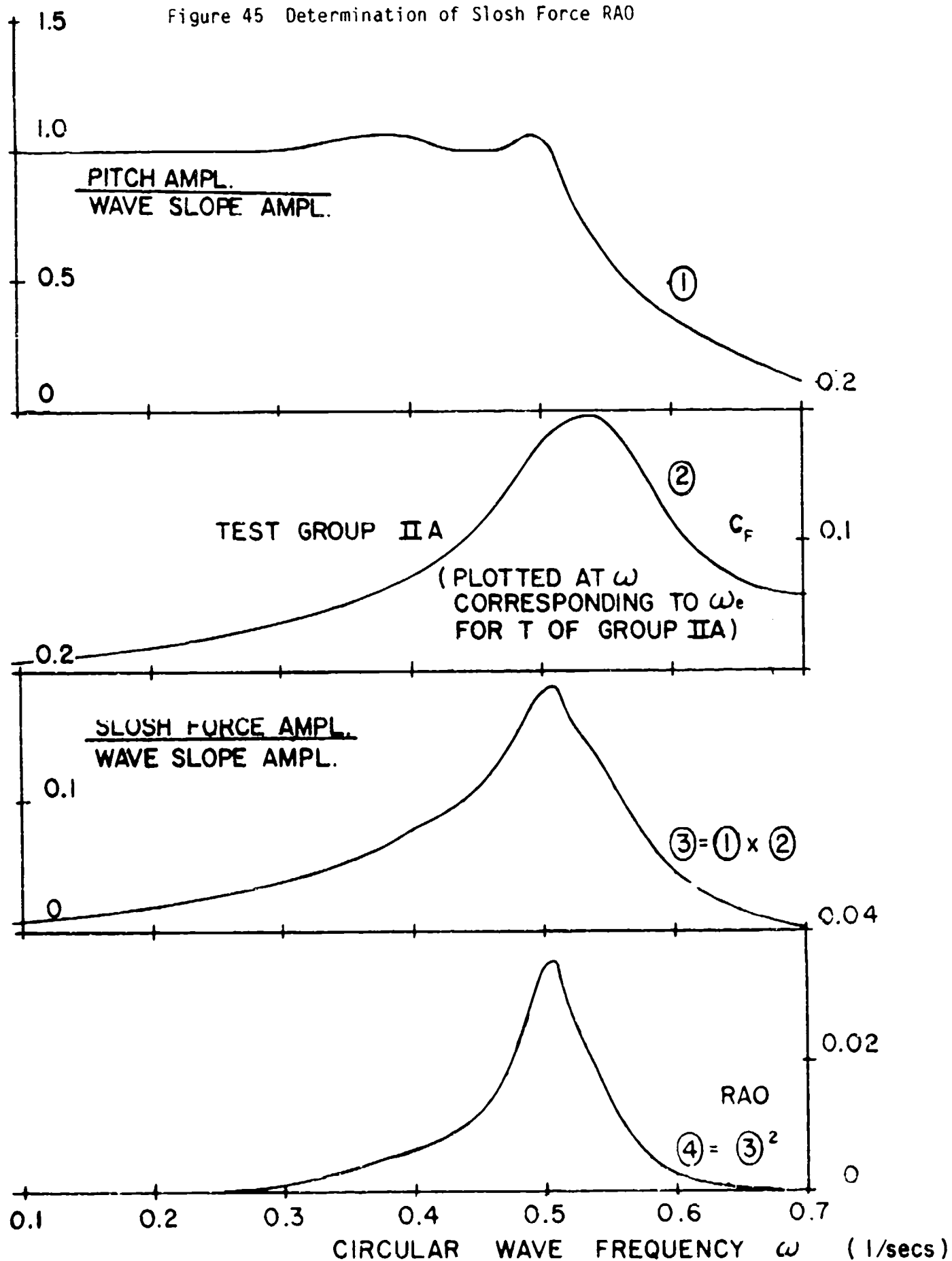
Tank 65% full of salt water ballast.

Seaway: ISSC spectrum, 20 ft. observed wave height, 12 seconds observed wave period, long crested, directly from ahead.

Dimensionless pitch response is determined from Ref. (4) giving curve ① in Figure 45.



Figure 45 Determination of Slosh Force RAO



It is now necessary to combine the dimensionless ship pitch with  $C_F$ , the dimensionless sloshing force coefficient, curve ② for the tank of interest, and then to find the response amplitude operator (RAO), curve ④. As shown in Figure 45, all curves are plotted against the common abscissa of circular wave frequency  $\omega$ . Curve ③ = curve ① multiplied by curve ②. Curve ④ is simply the square of curve ③. Thus, curve ④ may be thought of as

$$[ (\text{Pitch/Wave Slope}) \times (\text{Force Coefficient/Pitch}) ]^2 \\ = [ (\text{Force Coefficient}) / (\text{Wave Slope}) ]^2 = \text{RAO}$$

An important detail in this procedure is to plot curve ② at wave frequencies  $\omega$  which match the periods of tank excitation  $T$ . The  $\omega$  at which to plot  $C_F$  is found by first converting the dimensionless period  $T_n/T$  of Figure 19 to full-scale excitation period  $T$ , noting that  $T$  must now represent  $T_e$ , the period of encounter between ship and ocean wave. Then find  $\omega_e$  and  $\omega$  from the expression

$$\omega_e = \omega + \omega^2 (v/g)$$

where  $v$  is ship speed.

This expression is appropriate for head seas (ship to wave angle = 180 degrees) but must be modified for other ship to wave angles.

The ISSC wave spectrum formula is:

$$S_{\zeta}(\omega) = (171.5/\omega^5) \times (H_V^2/T_V^4) \times e^{L-690/(T_V^4 \omega^4)}$$

where:

$S_{\zeta}(\omega)$  = ordinate of wave elevation variance spectrum,  $\text{ft}^2 \times \text{sec}$

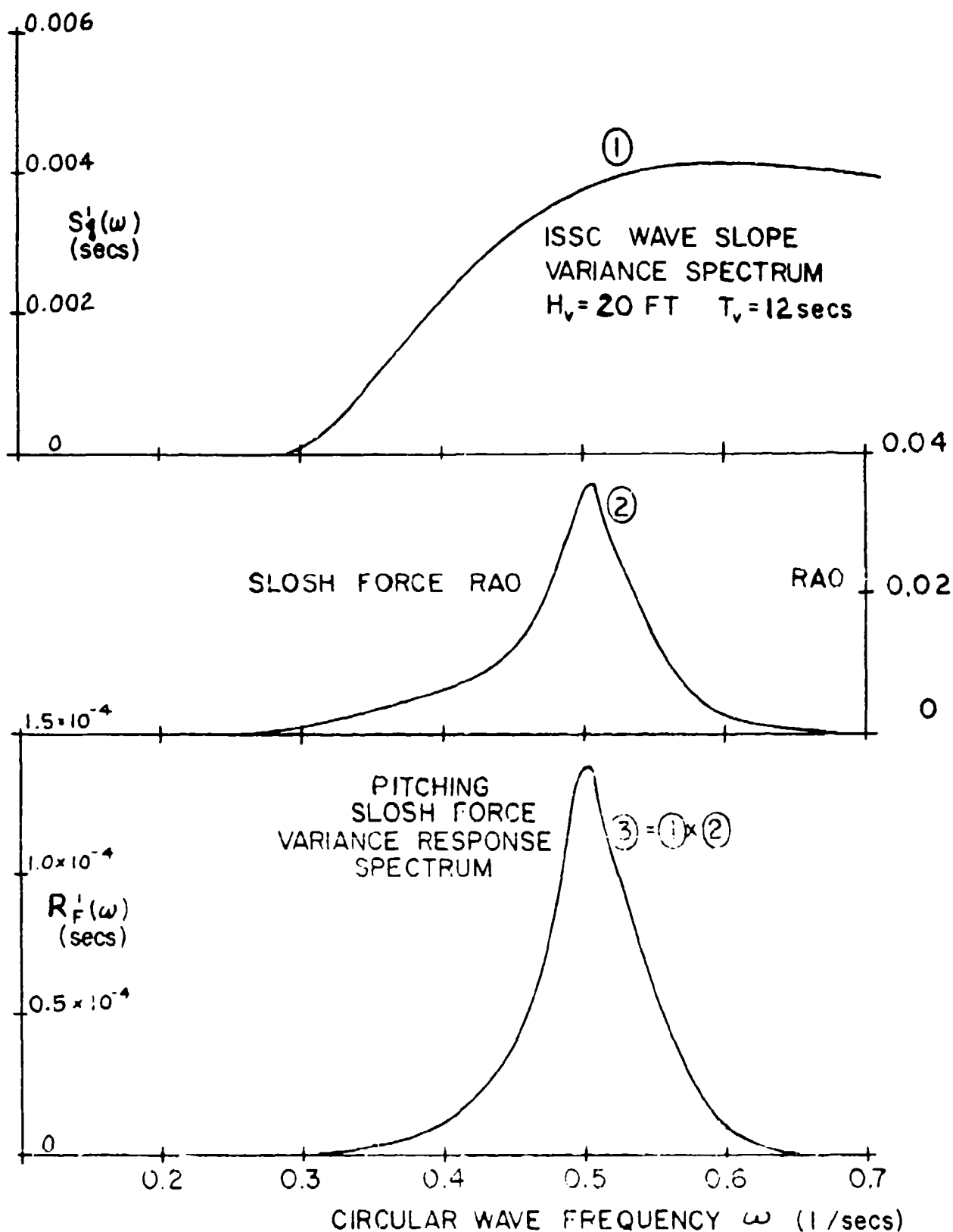
$\omega$  = circular wave component frequency, rad/sec

$H_V$  = observed or significant wave height, ft.

$T_V$  = observed wave period, secs.

In order to use the wave spectrum in a direct fashion,  $S_{\zeta}(\omega)$  is converted to a wave slope variance spectrum  $S'_{\zeta}(\omega)$  by multiplying  $S_{\zeta}(\omega)$  by  $\omega^4/g^2$  [Ref. (11), Chapter IX] giving curve ① of Figure 46. Thus, incremental areas under curve ① represent the variance of the wave surface slope for the frequency bandwidth considered.

Figure 46 Determination of Pitching Slosh Force Variance Response Spectrum;  
Transverse Web at Middle of Tanker Wing Tank



The three curves in Figure 46 are the typical ones used to demonstrate the application of the principle of linear superposition of ship motions, but as used here, are equally applicable to finding sloshing response in a ship mounted tank, provided we can assume that the motion of the liquid in the tank does not influence the motion of the ship. Curve ① is the wave spectrum. Curve ② is the RAO, which is the same as curve ④ from Figure 45. Curve ③ on Figure 46 represents the spectrum of dimensionless sloshing force response variance. The area under this curve represents the variance of the dimensionless sloshing force.

Numerically, the area under curve ③ =  $0.237 \times 10^{-4}$ . Then the variance of the sloshing force on the ship is given by  $\sigma^2(F)$ , where

$$\sigma^2(F) = 0.237 \times 10^{-4} [g A_L]^2 = 0.237 \times 10^{-4} [64 \times 347 \times 102]^2 = 1.216 \times 10^8 \text{ pounds}^2$$

The RMS of the sloshing force  $F_{RMS}$  is thus,

$$[\sigma^2(F)]^{1/2} = [1.216 \times 10^8]^{1/2} = 11,030 \text{ pounds} = F_{RMS}$$

Assuming the amplitudes of sloshing are Rayleigh distributed, then the significant sloshing force or average of the highest one third sloshing force amplitudes  $F_{1/3}$  in the seaway will be:

$$F_{1/3} = 2.002 \times F_{RMS} = 22,060 \text{ pounds}$$

In the event the sloshing forces were non-linear, it would be appropriate to calculate the RAO using amplitude of force of same order of magnitude as that of the desired response -- such as  $F_{1/3}$ .

Figure 45 shows that a strong factor in keeping the response spectrum at a low value is the limited response to the higher wave frequencies (shorter waves) of the Series 60 hull in pitch. This effectively prevents any excitation of sloshing in the second sloshing wave mode, making the RAO a peaked curve only extending over the period of fundamental sloshing response. Inasmuch as a shorter ship would show more pitch response at the higher frequencies, and a longer ship would show less, it is clear that tank length as a proportion of ship

length is an important parameter in determining whether sloshing is likely to be a problem. In the example shown, the ratio ship length/tank length =  $720/102 = 7.06$ . A shorter ship with the same tank would show a lower ratio. Correspondingly, more sloshing force response to the shorter waves, and hence a higher  $F_{RMS}$ , would be expected with the shorter ship.

#### XIV. SUMMARY OF MAJOR RESULTS OF TESTS

1. Sloshing force, moment and pressure coefficients determined by experiment for typical tank configurations are shown on the figures in the report. These show, in general, that sloshing is a resonant phenomenon with a peak at period ratios  $T_n/T$  between 0.80 and 1.00. An exception to this is the one rolling case tested with a bulk carrier hold model where resonance occurred at  $T_n/T$  slightly greater than 1.0.

The dimensionless sloshing force and pressure coefficients are applicable to any tank which has the same proportions as those tested. Clearly, the length to depth ratio is the more important parameter for cases in which sloshing occurs as a result of pitching -- that is, in a wing tank or a center tank of a typical two longitudinal bulkhead tanker.

In the case of a bulk carrier in which sloshing occurs as a result of rolling, the tank breadth to depth ratio will be the important parameter.

Proportions of the model tanks tested in this project are as follows:

	Tanker Wing <u>Tank</u>	Tanker Center <u>Tank</u>	Bulk Carrier <u>Hold</u>
Length/Depth	1.89	1.89	1.25
Breadth/Depth	0.63	0.63	1.89

2. The highest sloshing force coefficients found in pitching tests with tanker model tanks were developed on horizontal end girders located on a transverse bulkhead when impacts occurred as the tank wave surface rose from below ( $C_F = 1.7$ ), when the fill depth was 65 percent. However, a  $C_F$  value of 4.8 was found to develop from sloshing wave impacts on the under side of a hold-side longitudinal of an upper sloping bulkhead in a bulk carrier hold when rolling.

3. The highest  $C_p$  values were measured on the top of tanker model tanks at the ends when impacts were experienced from the rising wave below. Generally, pressures in the corners exceeded those measured at the ends midway across the tank, although these pressures are strongly influenced by the tank internal structure, both top and bottom. The highest  $C_p$  value -- 18.8 -- was measured when the only structure in the tank was a swash bulkhead at tank midlength and three end girders, and the fill depth was 90 percent.
4. In general, the presence of a face plate on the instrumented member increased the sloshing force on it. At the same time, the presence of a face plate generally led to some slight reduction of sloshing pressures.
5. In general, increasing the structure in a tank provides additional damping which tends to reduce sloshing forces on any particular member and sloshing pressures on the tank boundary.
6. The dimensionless slosh induced force  $C_F$  was generally linear with increasing amplitude of excitation, but showed a slight reduction in many cases. Dimensionless slosh induced pressure  $C_p$  showed a more pronounced drop, the average reduction being 25 percent when the excitation amplitude was doubled.
7. Sloshing forces from pitching experienced by a tanker transverse web generally increased slightly as the tank was moved longitudinally away from the pitch axis. However, for one case, the sloshing force was reduced.
8. The theory of linear superposition of sloshing forces from separate excitations (pitch and surge) was generally confirmed by the tests in that the resulting force curves for combined pitch and surge were very similar to synthesized curves made up by combining the separately measured forces from pure pitching and from pure surging.

9. For one case in which measured sloshing forces could be compared with sloshing forces determined by theory -- furnished by a separate investigator -- the comparison was favorable, although the peak theoretical force was about 25 percent higher than that measured.



## **XV. RECOMMENDATIONS**

### **A. Design**

1. In order to minimize sloshing in a slack tank with minimum structure -- such as a bulk carrier hold with a liquid cargo or water ballast -- tank boundaries should be provided with structural roughness to maximize the development of turbulence as sloshing waves pass back and forth through the tank. An example of such roughness is vertical corrugations parallel to the direction of the more troublesome sloshing. Generation of the desired turbulence and associated damping will then take place less abruptly than if the only source of damping is the impact of sloshing waves on horizontal surfaces at the ends of the tank.
2. The lower boundaries of upper corner tanks in bulk carrier holds which are to carry liquids should be strongly constructed if a horizontal shelf or flat is located at that elevation. It seems obvious that a more sloping bottom boundary of these tanks would reduce the occurrence of high sloshing pressures.
3. Horizontal end girders in tanker center tanks have been shown to be subjected to high impact sloshing loads directed upward from below. Consideration should be given to redesign of these girders to minimize such loads, perhaps by the use of sloping plates on the underside of the girders.
4. The upper wing tanks in bulk carrier holds should be stiffened internally as is the usual practice rather than on the hold side of the sloping bulkhead if liquids are to be carried in the hold.
5. The longitudinal bulkheads of tankers with long center tanks should be stiffened on the center tank side, rather than the wing tank side, if the center tank is to be slack in operation. Vertical stiffening such as transverse webs appears to provide effective damping for such tanks.

6. Studies should be made of the effect of tank size on sloshing forces on critical structure of new ship designs using the procedure demonstrated in Section XIII.

## **B. Additional Testing**

1. Measure the upward sloshing force on a model hatch cover fitted on a bulk carrier hold with the hold nearly filled with water, using several periods of oscillation, amplitudes of roll and fill depths.
2. Measure the sloshing force on a pitching tanker wing tank strut connecting a web frame on the longitudinal bulkhead with the corresponding shell web frame. This is suggested in consideration of a structural failure on a tanker strut which came to light after the present program was finalized.
3. Devise variations to the geometry of horizontal tanker end girders and test them to determine a reduction in impact sloshing forces compared with those measured in the present program (test groups IV and V).
4. Develop a test program to measure the sloshing force on a portion of a full scale tanker ballast tank internal structure, including separating a portion of this structure to allow suspension by force gages, reinforcing the structure so modified and calibrating the force suspension system. At the same time, the ship's basic motions of pitch and surge -- and perhaps roll and sway -- should be measured.
5. Make further linear superposition calculations of sloshing forces on a typical tanker structural member, such as the horizontal end girder in test group IV using an available ship motion computer program and RAO's from the present project. Also, modify the oscillating table drive system to allow oscillating the model tank with an irregular excitation; compare the theoretical predictions with those from the test.
6. Consider additional model tests to further investigate the effect of temperature, viscosity and density of liquid on sloshing forces.

### C. Adaptations to Model Test Instrumentation

1. Increase the capacity of the data acquisition system. The present system requires reloading of programs each time a measuring run is to be made owing to the limited memory of the Apple computer. This requires a prolonged period -- of the order of 10 minutes -- between successive pairs of runs.
2. Provide a potentiometer to measure the rotation of the swinging table of the test facility, thereby avoiding the need both to check the amplitude of swing visually and to have the swinging table close a switch at the end of the swing.
3. Replace the present mechanical drive from the speed reducer, which oscillates the swinging table in pitch, by two hydraulic rotational inducers. The additional equipment needed to accomplish this appears to be moderate. Such a change should eliminate much of the lost motion which occurs with the present system. If further tests using the existing system are to be run, the speed reducer should be overhauled to minimize its lost motion.
4. Redesign the attachment housing of the force gages in order to reduce their weight and volume and simplify their connection to the instrumented structural members.
5. Provide drains in the force gage support housing to allow draining when located in the tank bottom and so minimize possible corrosion of the assembly after the tank has been emptied.
6. Develop a computer-based control system in order to eliminate the use of a rotating command potentiometer and to allow generating irregular pitch and surge motions.

## XVI. CONCLUDING REMARKS

1. Additional test conditions were intended during the planning phases of the project but could not be accomplished because of time, cost and equipment limitations. However, it is believed their absence does not seriously limit the usefulness of the data that have been obtained.
2. Use of the sloshing force and pressure coefficients  $C_F$  and  $C_P$  given in the report should provide helpful guidance to those who must design tanks which will experience sloshing. No evidence came to light during the project to suggest that the coefficients are unrealistically high. If anything, based upon the one theory-to-experiment comparison available, and general consideration of model test extrapolation, the coefficients may be slightly low for typical ship sizes.
3. The generally well known principals for avoidance of sloshing are not altered by this report. These include:
  - (a) Reduce the size of the tank in relation to the size of the ship. This will reduce the resonant tank sloshing period to a point where little ship response to the seaway is expected.
  - (b) If such size limitations are not feasible, operate the ship with the tank pressed up or with a low fill depth.
  - (c) Do not minimize the amount of structure within the tank without due consideration of the degree of tank damping which will also be reduced.
  - (d) In the event (a), (b) and (c) are not acceptable, provide adequate strength in the structural members and tank boundaries to withstand sloshing forces and pressures such as may be estimated from the present report, or similar sources.

(THIS PAGE INTENTIONALLY LEFT BLANK)

## XVIII. REFERENCES AND BIBLIOGRAPHY

[References (1) through (12) are referred to in the report]

1. The Record of the American Bureau of Shipping, 1983 and 1963.
2. "Slosh Loads on Partially Filled Tanks with Internal Structure -- Industry Survey", Report Prepared for the Center for Maritime Studies, Webb Institute of Naval Architecture, By M. Rosenblatt and Son, Inc., May 27, 1983.
3. "Seminar on Liquid Sloshing", Det Norske Veritas, May 20-21, 1976.
4. "Experiments with Series 60 Models in Waves", Vossers, Swaan and Rijken, SNAME Transactions, 1960.
5. "Study on Partial Fillings in Ship Holds", Guidance Note By Bureau Veritas, Paris, August 1976.
6. "Calcium Chloride Properties and Forms Handbook", Dow Chemical Company, 1974.
7. "A Non-Linear Analysis of Liquid Sloshing in Rigid Containers", By Su, Lou, Flipse and Bridges, Dept. of Civil Engineering, Texas A&M University, DOT-RC-92037, October 1981.
8. "CRC Handbook of Chemistry and Physics", Chemical Rubber Company Press, Inc., 1982.
9. "The Design and Construction of the Liquid Sulphur Carrier S.S. LOUISIANA BRIMSTONE", By C.W. Coward and E.B. Foster, Chesapeake and Hampton Roads Section, SNAME, December 1, 1965.
10. "Ship Motions Prediction in Realistic Short-Crested Seas", By Z.G. Wachnik and E.E. Zarnick, SNAME Transactions, 1965.

11. "Principles of Naval Architecture -- Chapter IX, The Motion of Ships in Waves", By E.V. Lewis (Edited by Comstock), SNAME 1967.
12. "A Numerical Analysis of Large Amplitude Liquid Sloshing in Baffled Containers", By Su, Lou, Flipse and Bridges, Maritime Administration Report No. MA-RD-940-82046 March 1982.
13. "A Method for Estimating the Strength of Ship Hulls Against Sloshing Loads", By Hagiwara, Tozawa, Suka and Hashimoto, Mitsubishi Heavy Industries Technical Review, No. 3, 1982.
14. "Recommendations Concerning Safety in OBO's; The Avoidance of Slack Holds in Ballast", Proceedings of the Marine Safety Council, U.S. Coast Guard, February 1983.
15. "On the Motion of Cargo Oil in Long Tanks", Akita, Maeda, Furuta and Kitamura, Journal of the Society of Naval Architects of Japan, Volume 123, June 1968, P. 130-143 (in Japanese).
16. "Dynamic Pressure of Cargo Oil Due to Pitching and Effectiveness of Swash Bulkhead in Long Tanks", Shipbuilding Research Association of Japan, SR-74 Report, 1974.
17. "Results of Model Sloshing Experiments in Two Bulk Carrier Shaped Tanks Due to Rolling", Lloyds Register Development Unit Report No. 50, By C.A. Blixell, January 1974.
18. "Sloshing on Horizontal Girder in Tanks (Report for SSF Project 5609 - Laterally Loaded Plates)", Lloyds Register Development Unit Report No. 99, By W.D. Morris, October 1974.
19. "Results of Model Sloshing Experiment for Two Rectangular Tanks with Internal Bottom Stiffening", Lloyds Register Development Unit Report No. 49, By C.A. Blixell, January 1974.

20. "Calculation of Wall Pressures in a Smooth Rectangular Tank Due to Movement of Liquids", Lloyds Register R & T AS Report No. 5108, By A. Blixell (undated).
21. "Liquid Sloshing in Tanks with Internal Structures", Swedish Ship Research Foundation Summary Report SSF Project 5609, M. Huther, H. Olssen and O. Thomsson, 1977.
22. "Evaluation of Sloshing Conditions, Pressure Loads and Corresponding Intact Stability for COMBO CLASS CARRIER", Det Norske Veritas Technical Note, Distributed By K. Rigg Johnsen, December 1980.
23. "Measurement of Dynamic Forces Caused By Water on Long Tanks of Ships", By J. Hagiwara, Journal of the Society of Naval Architects in Japan, June 1967 (in Japanese).
24. "Behavior of Liquids in a Rectangular Tank in Motion", By G. Sears and E. Brizzolara, International Shipbuilding Progress, October 1970.
25. "Pressures in a Tank Due to Sloshing", By W.D.M. Morris and R.F. Allen, Shipping World and Shipbuilder, February 1974.
26. "Effect of Sloshing on the Internal Structural Members and Tanks", By M. Huther, Bulletin Technique du Paris Veritas.
27. "Statistical Distributions of Local Impact Pressures in Liquid Sloshing", By S. Gran, Norwegian Maritime Research, Volume 9, No. 2, 1981.
28. "Non-Linear Oscillations of Fluid in a Container", By J.H.G. Verhagen and L. Van Wijngaarden, Journal of Fluid Mechanics, Volume 22, Part 4, 1965.
29. "Dynamic SLOSH Induced Loads on Liquid Cargo Tank Bulkheads", SNAME T&R Research Report R-19, 1975.



30. "Model Studies on the Movement of Liquid in Tanks", By M. Huther, M. Dubois and J.M. Planeix, Marine Engineers Review, January 1973.
31. "Tank Size and Dynamic Loads on Bulkheads in Tankers", E. Abrahamsen, European Shipbuilding No. 1, Volume XI, 1962.
32. "The Movement of Liquids in Cargo Tanks", Shipping World and Shipbuilder, September 1971.
33. "Dynamic Loads on Slack Ballast Tanks -- An Exposition and Some Effects", The Motor Ship, February 1971.
34. "Danger of Standing Waves on Oil Tanker", By J.R.O. Francis and G. Kempson, Engineering, December 28, 1962.
35. "Sloshing Loads Due to Random Pitch Motion", By J. Mathisen, Norwegian Maritime Research, No. 3, Volume 4, 1976.
36. "Two Tanks for Sloshing Tests, Design and Instrumentation", By T. Didriksen, Det Norske Veritas Technical Report 75-269, November 1975.
37. "Experimental Study on the Sloshing Pressure of Rectangular Tanks - Third Report", By M. Sawayanagi and Y. Matsumoto, Mitsui Technical Review, No. 101, BSRA No. 49.402, 1978 (in Japanese).
38. "A Numerical Non-Linear Method of Sloshing in Tanks with Two-Dimensional Flow", By O. Faltinsen, Journal of Ship Research, September 1978.
39. "Resonant Surface Waves", By J. Ockendon and H. Ockendon, Journal of Fluid Mechanics, Volume 59, Part 2, 1973.
40. "Sloshing of Fluids in Closed Container at High Fill Levels", By J. Narickas and J. C. Peck, McDonnell Douglas Astronautics, Company - West.

41. "Sloshing in Partially Filled Liquid Tanks and Its Effect on Ship Motions: Numerical Simulation and Experimental Verification", Mikelis, Moller and Taylor, The Naval Architect, October 1984.
42. "Liquid Sloshing in Slack Ship Tanks - Theory, Observations, and Experiments", Hamlin, Lou, Maclean, Seibold, and Chandras, SNAME Annual Meeting, November 1986.

## APPENDIX A

Title:        Dynamic Force Measurement Device for Structural Members in a Scaled-  
              Down Model of a Ship Tank

Prepared by: John L. Mathieson  
              Professor of Engineering, SUNY Maritime College

Date:         September 1983

Contents:     Introduction  
              Measurement Technique  
              Description of Force Measurement Device  
              Operating Characteristics  
              Sketches

## Introduction

A force measurement device was designed to measure dynamic normal forces on selected structural members mounted at different locations in a scale model of a ship tank. A preliminary estimate of the dynamic forces indicated that the total normal force on the members would vary between one and eleven pounds and the frequency of the force was approximately one hertz. It was decided to design a device which when attached at three different locations on a member would measure the total normal force on the member. An electronic device is to be used for signal conditioning and summing the three signals. This electronic device is described in a separate section of the project report. The subject of this section is to describe the force measurement device.

## Measurement Technique

The measurement technique is to measure the strain on the top and bottom surface of a cantilever beam when a normal force is applied to the beam at a specified distance from the point of measurement on the beam. The normal force exerted on the beam by the structural member results in a tensile strain on one surface and a compressive strain on the other surface of the beam. Strain gages will be attached to the cantilever beam to measure the strain, calibrate the device and determine the dynamic forces on the model structural member. A normal force on the axis of the beam should result in only an axial strain along the axis of the beam. It is this axial strain that will be used to determine the dynamic forces. Since the lateral strain at the point of measurement should be zero on the top and bottom surface, it will be used by the electronic device for temperature compensation. Therefore, two signals from each of two strain gages will be used to determine the force at each of three points on the member. The signals from the strain gage on the top and bottom surface will be subtracted from each other to effectively average and magnify the measurement. The magnification results from subtracting two signals having opposite signs (ie, one is a tensile and the other is a compressive strain). Since the strain is proportional to the

### Measurement Technique (cont'd)

applied normal force, a calibration procedure will be used to determine the relationship between the applied force and resulting strain signals. The electronic device will be used to sum the signals from three strain measurement devices on the member and determine the temperature compensated dynamic normal force spectrum for a specified interval of time. The interval of time will be selected to include several cycles of force variation.

### Description of Force Measurement Device

The force measurement device is made up of three sub-assemblies. The sub-assemblies are called the support housing, cantilever beam and base and attachment housing. The support housing is attached to the outside of the tank by four screws. The cantilever base is attached to the support housing with six screws so that the cantilever can extend into the tank. A force button is threaded into the cantilever at a specified distance, on the top and bottom surface, from strain gages located near the base of the cantilever. Therefore, the strain gages are located in the fluid that fills the support housing and the force button is located in the fluid in the tank itself. The attachment housing is attached to the structural member being tested by four screws which will be used to obtain the proper alignment of the device with the structural member and the tank surface. The cantilever and attachment housing are fitted with several threaded fittings for alignment, motion constraint and the transfer of the normal force from the member to the cantilever. Three force measurement devices are to be attached to the member so that they measure the total normal force on the member and limit the motion of the member in the two other mutually perpendicular directions. The conductors carrying the signals from the strain gages on both surfaces of the cantilever beam will be lead out to the electronic device through watertight holes in the cantilever base.

### Operating Characteristics

The dimensions of the cantilever beam were selected to obtain values of strain which would be larger than the "noise level" of the electronic

### Operating Characteristics cont'd

device and therefore permit signal conditioning and summation of the signals. This design resulted in the natural frequency of the force measurement device being several times larger than the frequency of the applied dynamic forces. Satisfying both of these factors was considered essential to the design. The force range was estimated to be between one third of a pound and three and one half pounds on the measurement device. The signals from the strain gages for these forces will be between thirty-three and three hundred and fifty micro-inches per inch. The "noise level" of the external electronic device is expected to be between fifteen and thirty micro-inches per inch. From this, it appears that the "worst case" will be that no absolute value can be determined at the lowest force level of the expected force range and only a qualitative statement can be made (ie; "minimum" or "negligible" forces exist). This was considered an acceptable conclusion for this test program.

The estimate of the lowest natural frequency of the force measurement device with attached mass of member and entrained water was estimated to be 25 hertz. This would occur when testing the shortest and deepest member (12 inches x 4.8 inches). Since the frequency of the dynamic forces was considered to be between one and two hertz no vibration problems are anticipated.

Aluminum and stainless steel are the two materials used in the force measurement device. Stainless steel is used where surface contact and wear might occur. This combination of materials should yield a sturdy device which can be reused for the different structural members included in the test program.

Calibration will probably have to be accomplished with all three devices attached to the structural member and the electronic device used to sum the signals from each device. The summation of the strain signals for several known values of applied normal force will yield the data to calibrate a particular structural member with the three force measurement devices attached.

\* Assumes member is rigid and that entire member and added mass is carried by one force measurement device.

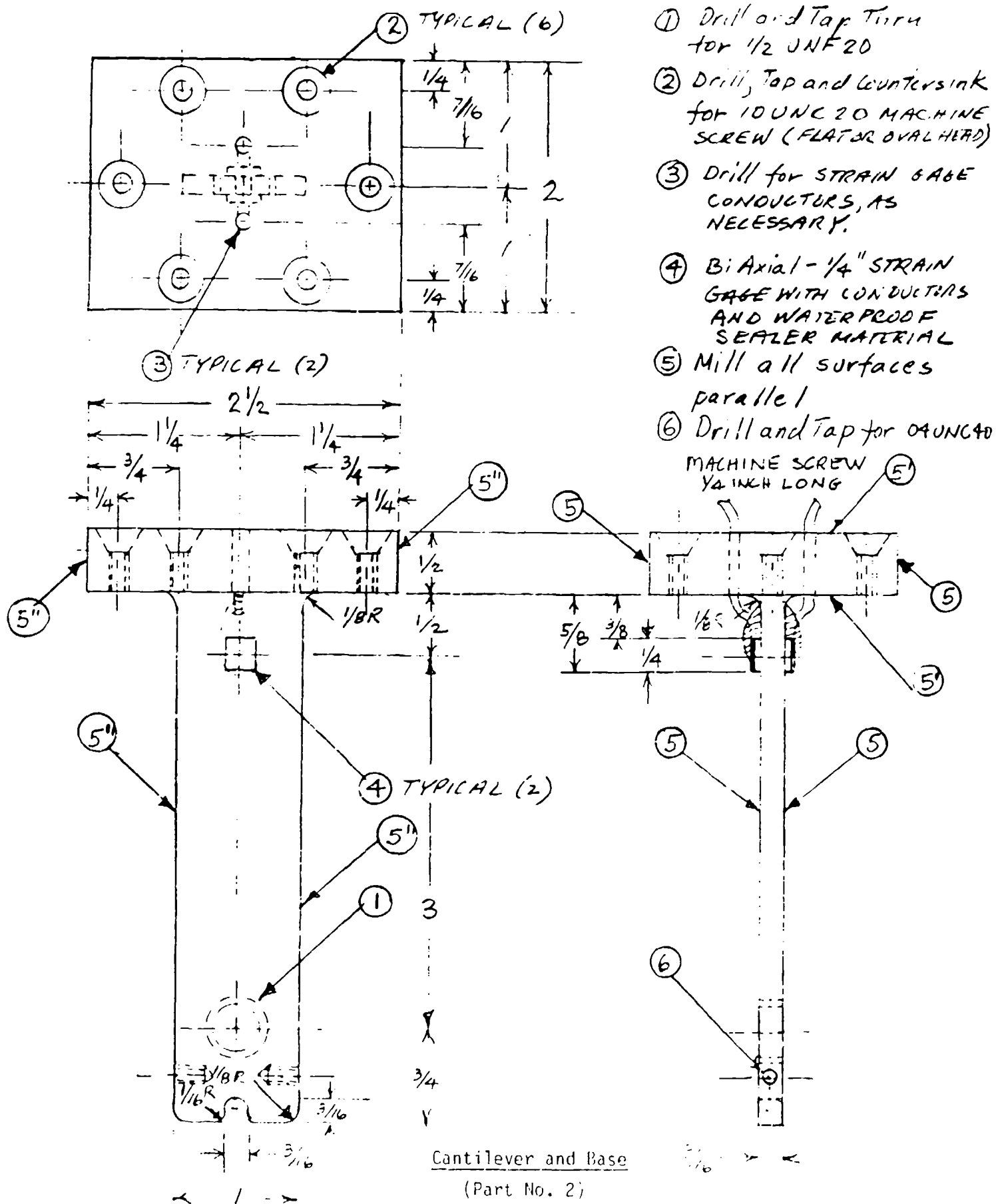


Figure A1: Force Gage Cantilever

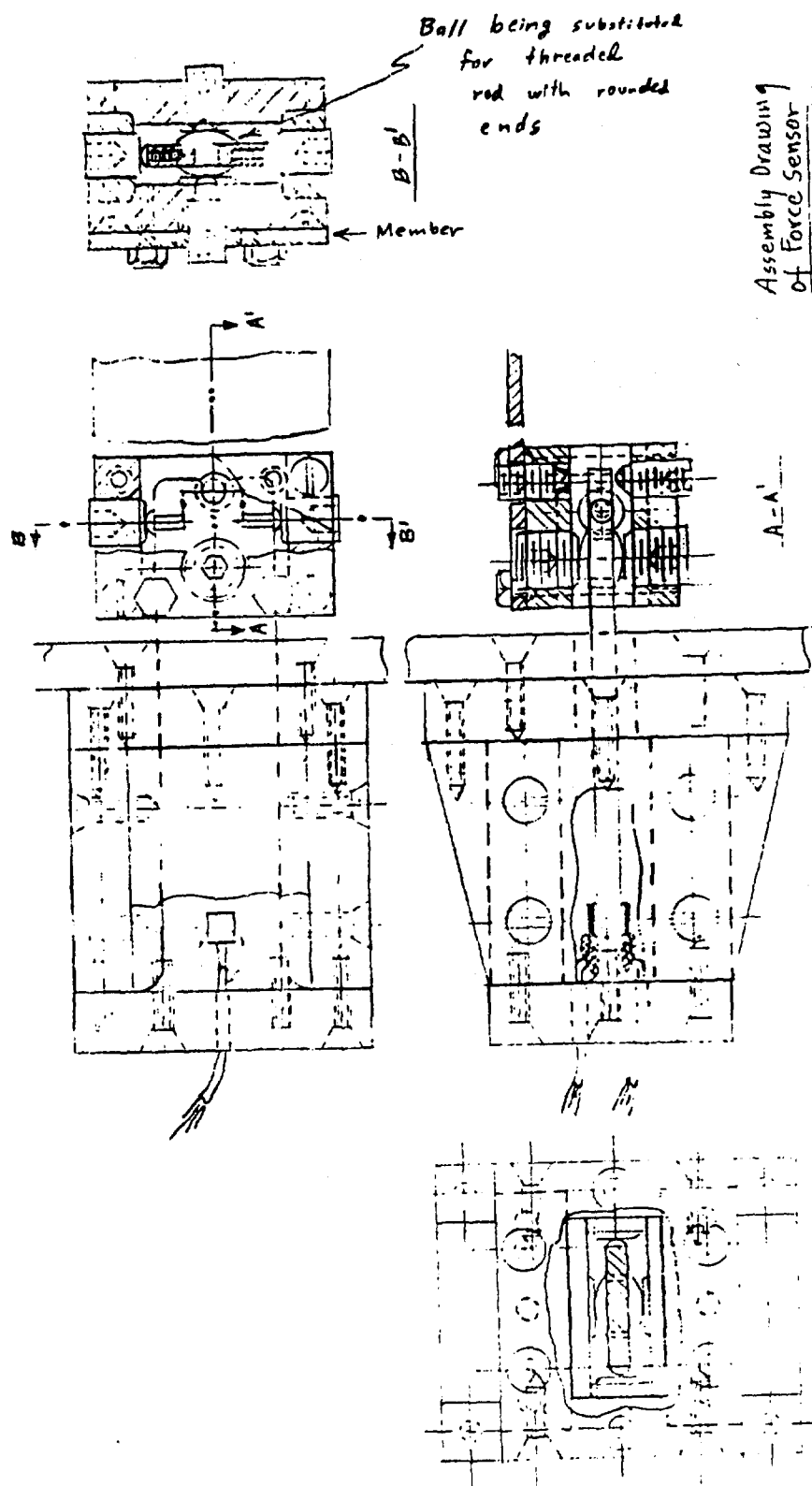


Figure A2: Assembly Drawing of Force Gage Support Housing,  
Cantilever and Attachment Housing

Best Available Copy



APPENDIX B  
TANK DRIVE SYSTEM

The Webb Oscillating Table Facility uses a separate mechanical drive system for oscillating the table in rotation -- i.e. pitch or roll. This is accomplished by a controllable eccentric which drives a crank arm through a connecting rod. This induces a cyclic rotation of the swing table varying nearly as a sinusoid. The eccentric is driven by a speed reducer which, in turn, is driven by a 2 HP electric motor with "Vari Drive" control. The range of oscillating periods desired for this project fell well within the available band-- 0.7 seconds to 4.5 seconds. Amplitudes of rotation up to and beyond 30 degrees are available by increasing the eccentric setting.

In order to produce translation of the carriage -- surge for this project -- an hydraulic power pack driven by a 7.5 HP motor furnishes high pressure oil to a servo valve which directs the oil to an hydraulic cylinder thereby driving the carriage horizontally. An extra return hydraulic line is provided from the servo valve to the power pack tank.

Control of surge is provided by a rotating ~~comm~~and potentiometer which is driven at the same RPM as the output shaft of the speed reducer. This produces a sinusoidally varying voltage at the ~~same~~ period as the period of oscillation of the eccentric. Another potentiometer is rotated by the translation of the carriage, thus providing a feedback signal. This latter signal is compared with the command signal; the difference in signals, after amplification, is used to drive the servo valve causing it to open one way or the other and directing greater or lesser amounts of oil to the appropriate end of the cylinder. An amplitude potentiometer on the amplifier is used to control surge amplitude.

For generating combined pitch and surge motion, the toothed chain to the command potentiometer may be slipped an integral number of teeth and the eccentric setting may be changed. Experience with this control system shows quite reasonable combined motions when the phase difference, surge from pitch, is either 0 degrees or 180 degrees.

Other runs made in this project included testing in combined pitch and surge with phase angles of  $\pm 90$  degrees. From these runs, the combined motion had the desired amplitudes and period, but the motion itself was somewhat erratic, partly because of the limitations of the crank connecting rod approximation to a sinusoid and because of lost motion in the various members and the speed reducer. It would be relatively simple to procure and install an additional hydraulic swing inducer (one is already on hand) and connect these directly to the swing table shafts driving them by the hydraulic power pack and an existing servo valve. This would eliminate the mechanical/hydraulic combined drive limitations. This step is included as a recommendation in the report.

Figure B1 is an isometric sketch of the oscillating table drive system.

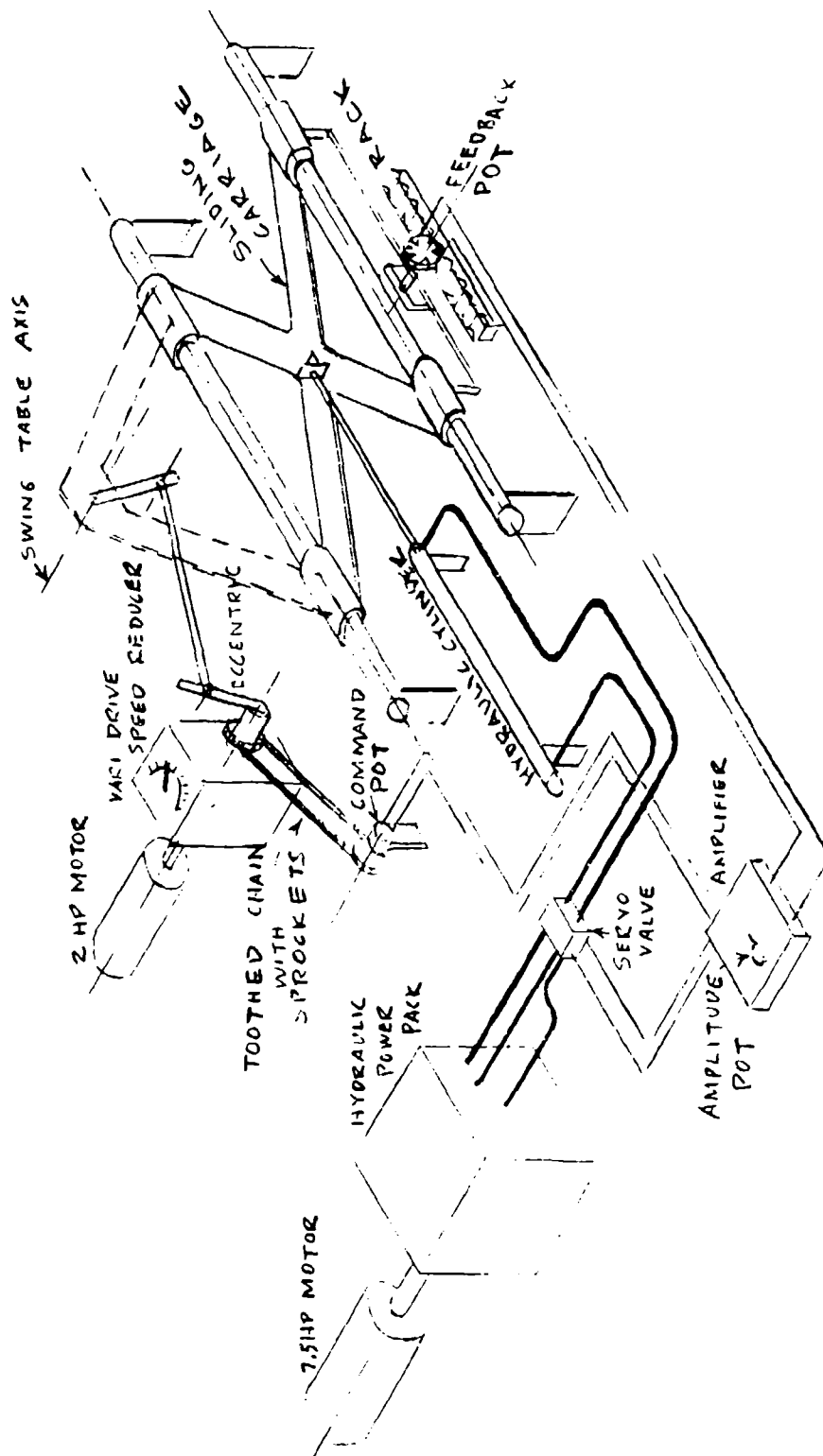


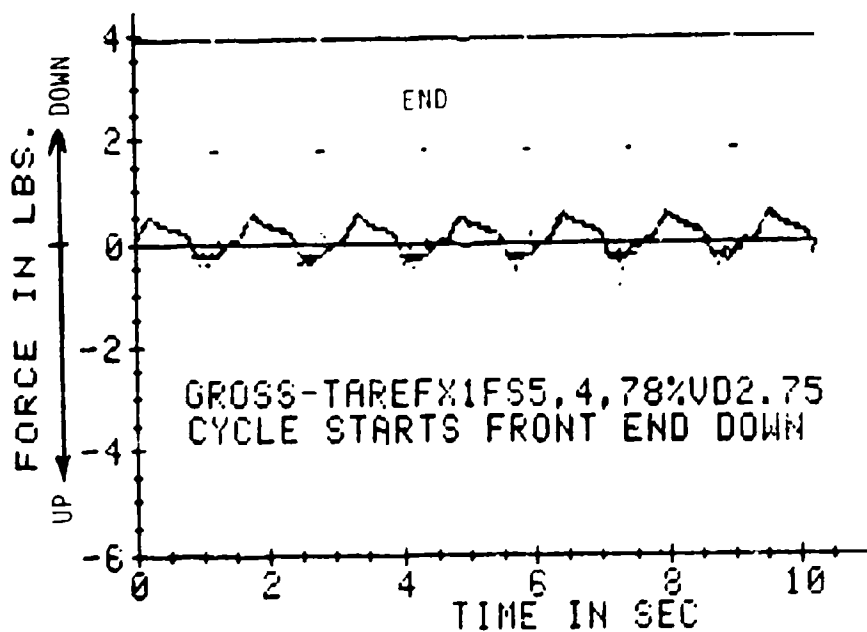
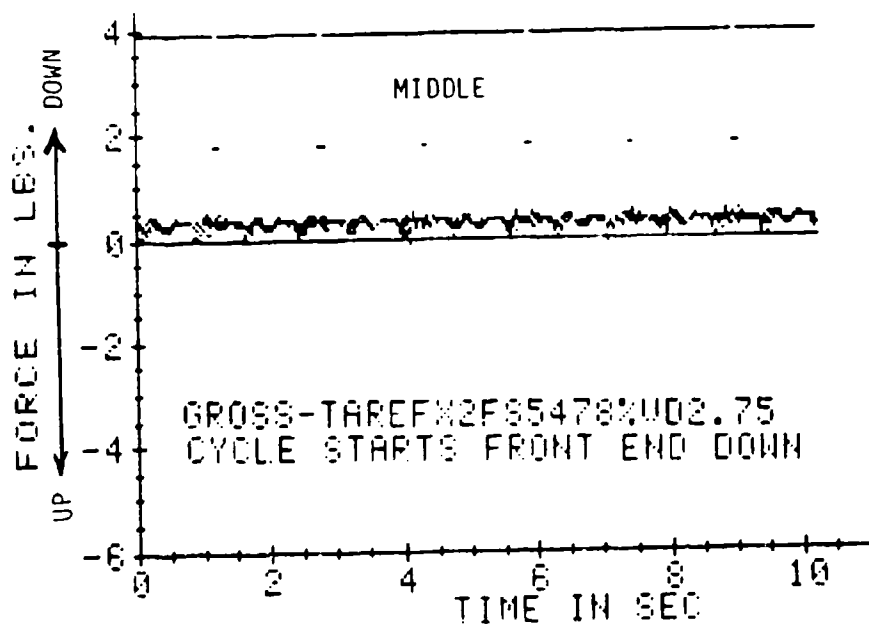
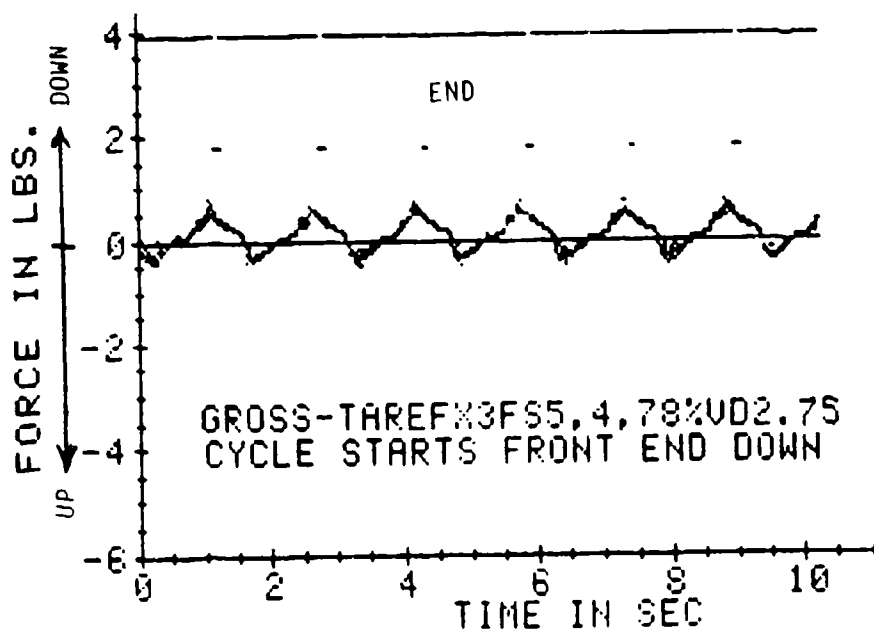
Figure B1: Oscillating Table Mechanical and Hydraulic Drive System

APPENDIX C  
REPRESENTATIVE SLOSHING FORCE GRAPHS

Several representative graphs of the time history of sloshing forces as recorded by the computer during test runs and subsequently printed are shown. The basic test run conditions are noted. An example of a run when a large impact occurred is included.

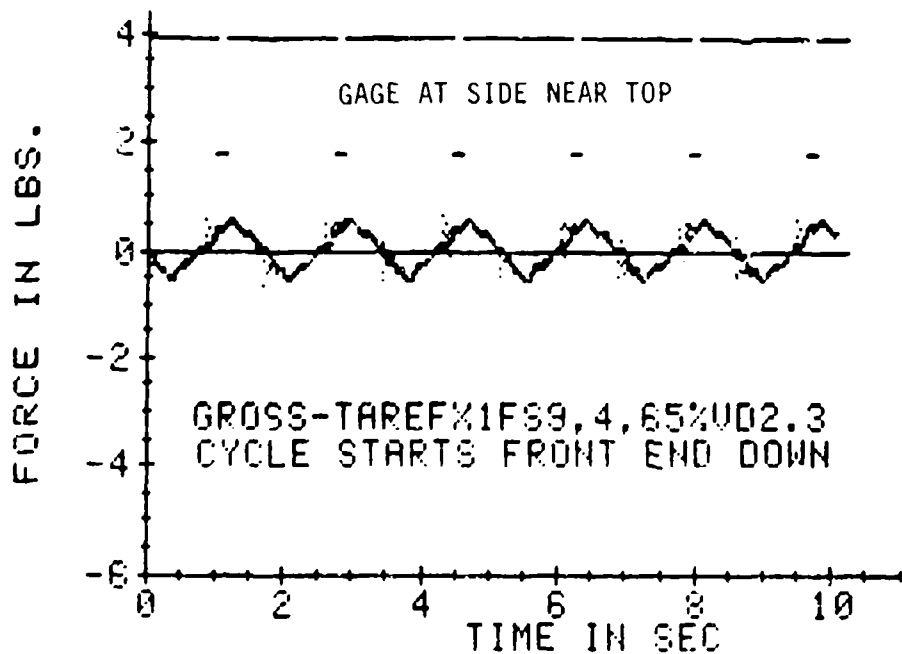
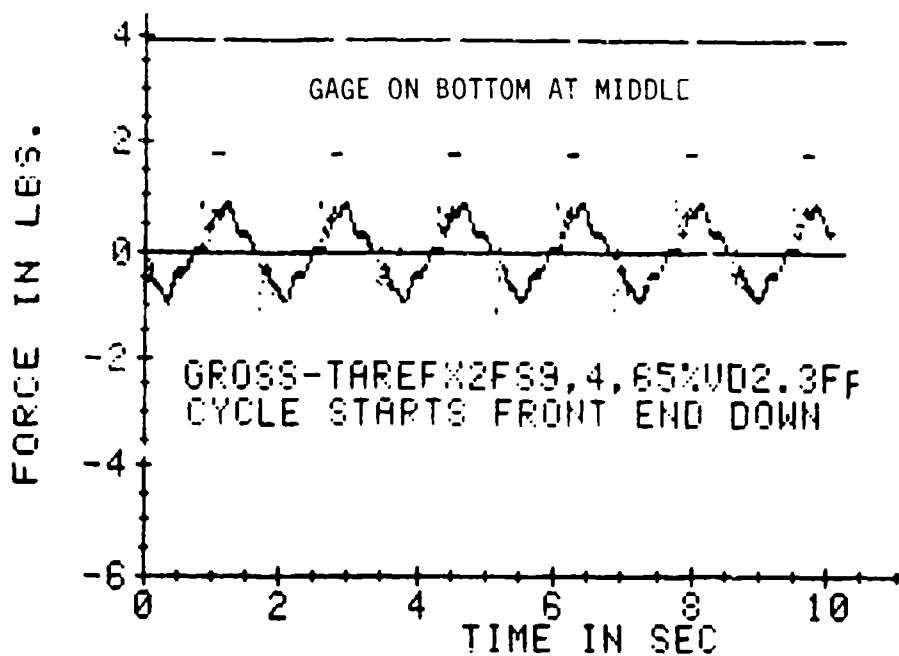
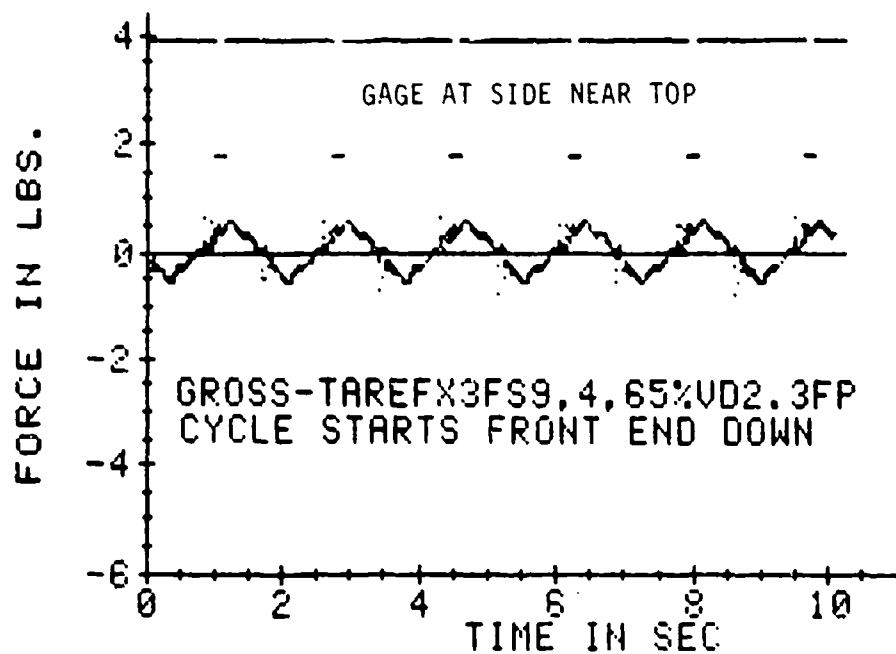
The run identification data shown on each graph includes the following information:

Type of force (gross, tare, or gross minus tare); force gage number; member number; amplitude (of pitch) in degrees; percent fill; vari-drive setting.



Sloshing Force  
at 3 Gages.  
Member FS-5  
Shell Longitudinal

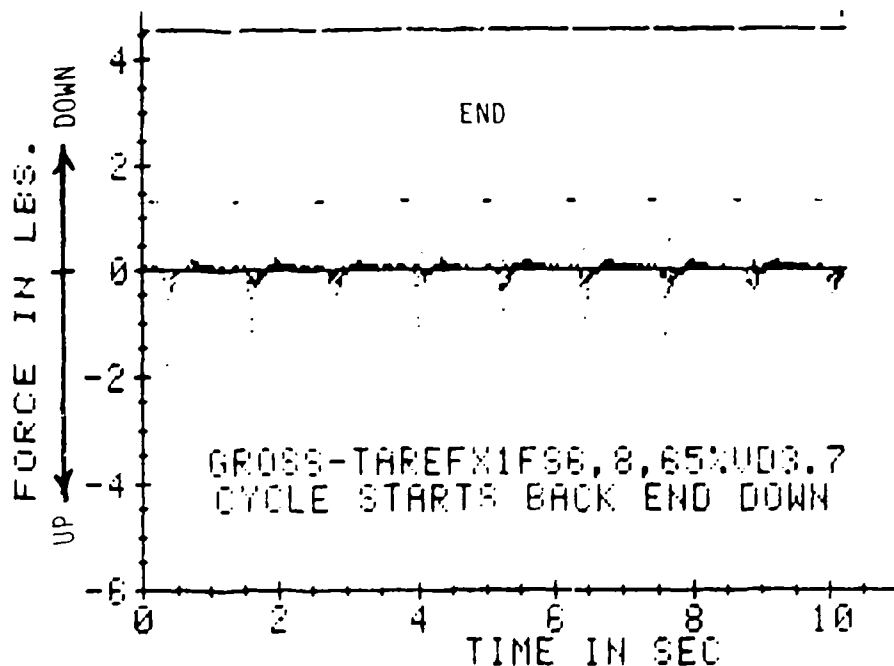
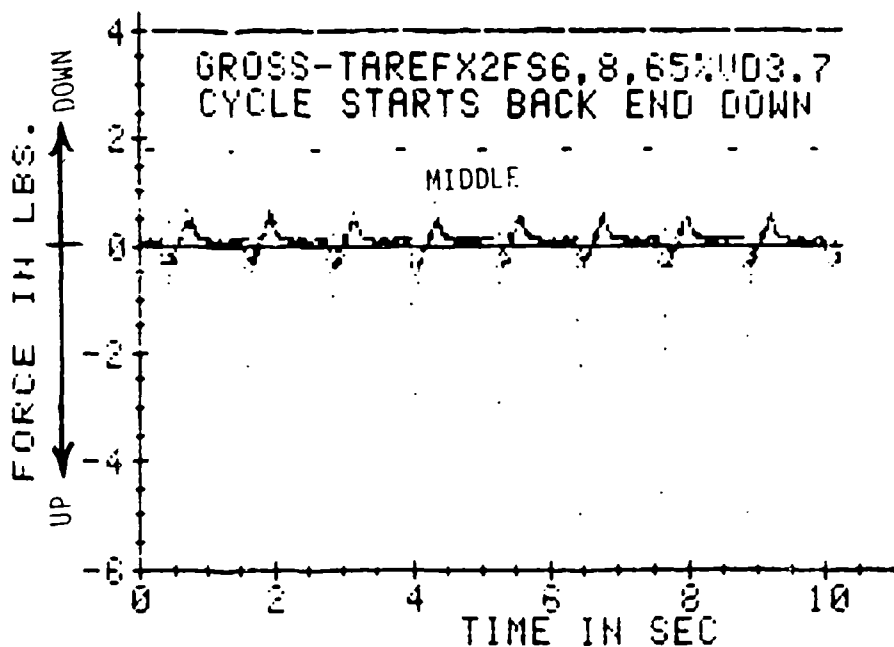
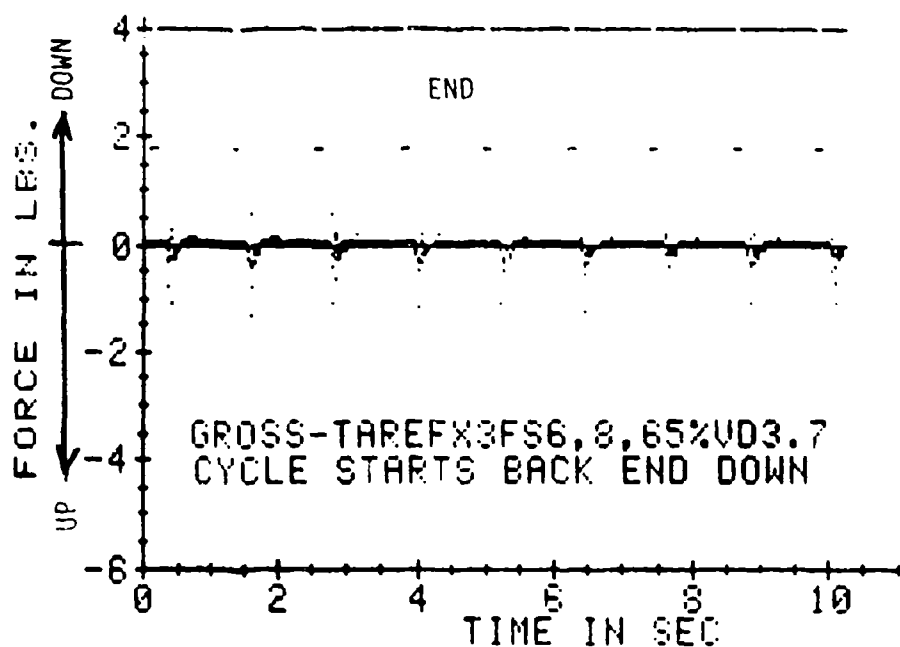
Figure C1



Sloshing Force  
at 3 Gages.  
Member FS-9  
Swash Bulkhead  
with Face Plate  
at Mid Length  
Bottom

Figure C2





Sloshing Force  
at 3 Gages,  
Member FS-6  
Horizontal Girder  
on Transverse Bulkhead,  
Top Location.

Impacts Recorded  
at all Gages.  
Measuring Limit  
Exceeded at  
Middle Gage

Figure C3

## COMMITTEE ON MARINE STRUCTURES

Commission on Engineering and Technical Systems

National Academy of Sciences - National Research Council

The COMMITTEE ON MARINE STRUCTURES has technical cognizance over the interagency Ship Structure Committee's research program.

Stanley G. Stiansen (Chairman), Riverhead, NY  
Mark Y. Berman, Amoco Production Company, Tulsa, OK  
Peter A. Gale, Webb Institute of Naval Architecture, Glen Cove, NY  
Rolf D. Glasfeld, General Dynamics Corporation, Groton, CT  
William H. Hartt, Florida Atlantic University, Boca Raton, FL  
Paul H. Wirsching, University of Arizona, Tucson, AZ  
Alexander B. Stavovy, National Research Council, Washington, DC  
Michael K. Parmelee, Secretary, Ship Structure Committee,  
Washington, DC

### LOADS WORK GROUP

Paul H. Wirsching (Chairman), University of Arizona, Tucson, AZ  
Subrata K. Chakrabarti, Chicago Bridge and Iron Company, Plainfield, IL  
Keith D. Hjelmstad, University of Illinois, Urbana, IL  
Hsien Yun Jan, Martech Incorporated, Neshanic Station, NJ  
Jack Y. K. Lou, Texas A & M University, College Station, TX  
Naresh Maniar, M. Rosenblatt & Son, Incorporated, New York, NY  
Soloman C. S. Yim, Oregon State University, Corvallis, OR

### MATERIALS WORK GROUP

William H. Hartt, Florida Atlantic University, Boca Raton, FL  
Fereshteh Ebrahimi, University of Florida, Gainesville, FL  
Santiago Ibarra, Jr., Amoco Corporation, Naperville, IL  
Paul A. Lagace, Massachusetts Institute of Technology, Cambridge, MA  
John Landes, University of Tennessee, Knoxville, TN  
Mamdouh M. Salama, Conoco Incorporated, Ponca City, OK  
James M. Sawhill, Jr., Newport News Shipbuilding, Newport News, VA

## SHIP STRUCTURE COMMITTEE PUBLICATIONS

- SSC-324 Analytical Techniques for Predicting Grounded Ship Response by J. D. Porricelli and J. H. Boyd, 1984
- SSC-325 Correlation of Theoretical and Measured Hydrodynamic Pressures for the SL-7 Containership and the Great Lakes Bulk Carrier S. J. Cort by H. H. Chen, Y. S. Shin & I. S. Aulakh, 1984
- SSC-326 Long-Term Corrosion Fatigue of Welded Marine Steels by O. H. Burnside, S. J. Hudak, E. Oelkers, K. B. Chan, and R. J. Dexter, 1984
- SSC-327 Investigation of Steels for Improved Weldability in Ship Construction by L. J. Cuddy, J. S. Lally and L. F. Porter 1985
- SSC-328 Fracture Control for Fixed Offshore Structures by P. M. Besuner, K. Ortiz, J. M. Thomas and S. D. Adams 1985
- SSC-329 Ice Loads and Ship Response to Ice by J. W. St. John, C. Daley, and H. Blount, 1985
- SSC-330 Practical Guide for Shipboard Vibration Control by E. F. Noonan, G. P. Antonides and W. A. Woods, 1985
- SSC-331 Design Guide for Ship Structural Details by C. R. Jordan and R. P. Krumpen, Jr., 1985
- SSC-332 Guide for Ship Structural Inspections by Nedret S. Basar & Victor W. Jovino, 1985
- SSC-333 Advance Methods for Ship Motion and Wave Load Prediction by William J. Walsh, Brian N. Leis, and J. Y. Yung, 1989
- SSC-334 Influence of Weld Porosity on the Integrity of Marine Structures by William J. Walsh, Brian N. Leis, and J. Y. Yung, 1989
- SSC-335 Performance of Underwater Weldments by R. J. Dexter, E. B. Norris, W. R. Schick, P. D. Watson, 1986
- SSC-336 Liquid Slosh Loading in Slack Ship Tanks; Forces on Internal Structures & Pressures by N. A. Hamlin, 1986
- None Ship Structure Committee Publications - A Special Bibliography, AD-A140339